

Quantum phase transitions in condensed matter

The 8th Asian Winter School on
“Strings, Particles, and Cosmology”,
Puri, India
January 11-18, 2014

Subir Sachdev

Talk online: sachdev.physics.harvard.edu



Outline

I. The simplest models without quasiparticles

A. Superfluid-insulator transition

of ultracold bosons in an optical lattice

*B. Conformal field theories in $2+1$ dimensions and
the AdS/CFT correspondence*

2. Metals without quasiparticles

A. Review of Fermi liquid theory

*B. A “non-Fermi” liquid: the Ising-nematic
quantum critical point*

C. The holographic view: charged black-branes

Outline

I. The simplest models without quasiparticles

A. Superfluid-insulator transition

of ultracold bosons in an optical lattice

B. Conformal field theories in $2+1$ dimensions and the AdS/CFT correspondence

2. Metals without quasiparticles

A. Review of Fermi liquid theory

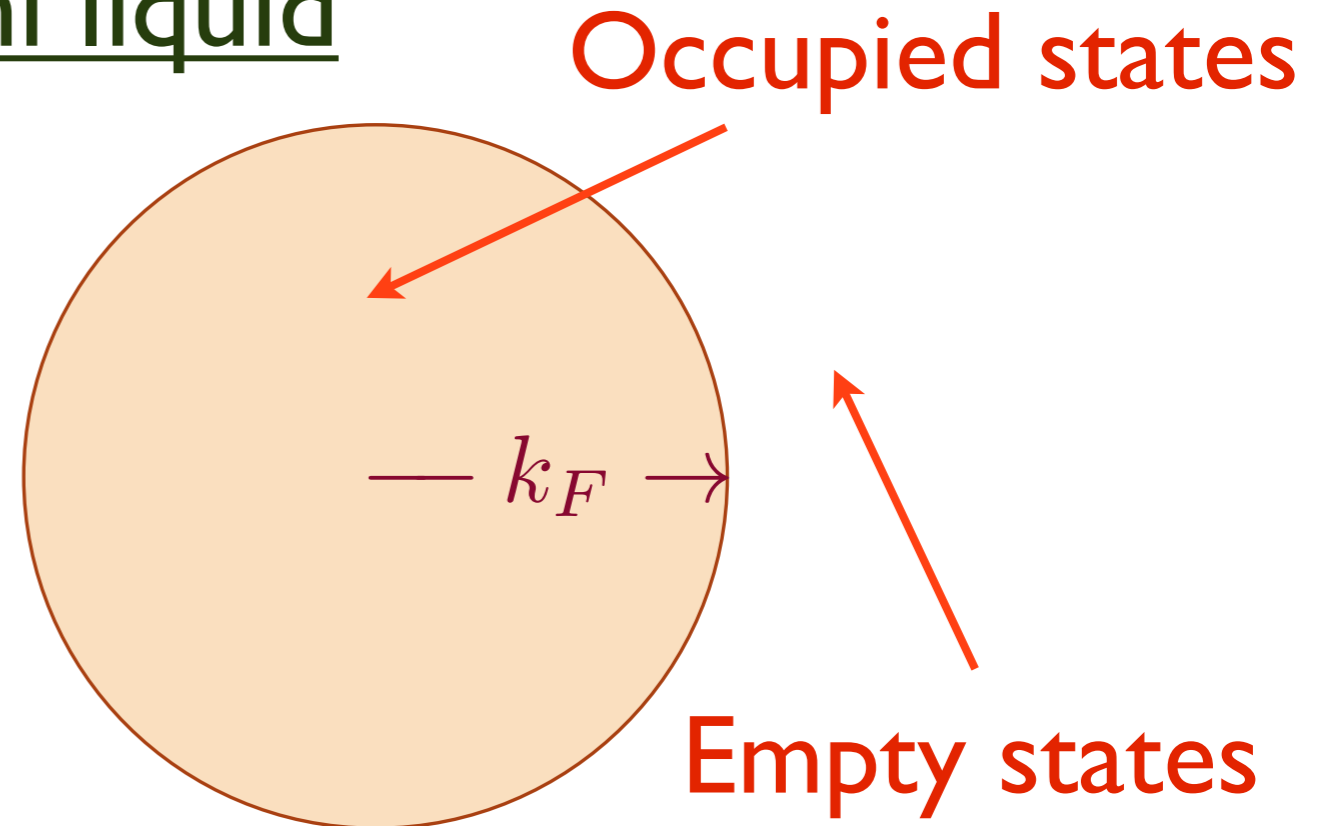
B. A “non-Fermi” liquid: the Ising-nematic quantum critical point

C. The holographic view: charged black-branes

The Fermi liquid

$$\mathcal{L} = f^\dagger \left(\partial_\tau - \frac{\nabla^2}{2m} - \mu \right) f$$

+ 4 Fermi terms



- Fermi wavevector obeys the Luttinger relation $k_F^d \sim Q$, the fermion density

FERMI LIQUIDS, AND THEIR PHASE TRANSITIONS
From Chapter 18 of
Quantum Phase Transitions, Second Edition
Cambridge University Press

Subir Sachdev

Department of Physics, Harvard University, Cambridge MA 02138

The Fermi liquid is perhaps the most familiar quantum many-body state of solid state physics. It is the generic state of fermions at non-zero density, and is found in all metals. Its basic characteristics can already be understood in a simple free fermion picture. Non-interacting fermions occupy the lowest energy single particle states, consistent with the exclusion principle. This leads to the fundamental concept of the Fermi surface: a surface in momentum space separating the occupied and empty single fermion states. The lowest energy excitations then consist of quasi-particle excitations which are particle-like outside the Fermi surface, and hole-like inside the Fermi surface. Landau's Fermi liquid theory is a careful justification for the stability of this simple picture in the presence of interactions between fermions.

The purpose of this chapter is to describe two paradigms of symmetry breaking quantum transitions in Fermi liquids. In the first class, studied in Section II,

the broken symmetry is related to the point-group symmetry of the crystal, while translational symmetry is preserved; consequently the order parameter resides at zero wavevector. In the second class, studied in Section III, the order parameter is at a finite wavevector, and so translational symmetry is also broken. We will find that these transitions have distinct effects on the Fermi surface, and so lead to very different critical theories. We will study both critical theories using a simple example in each class, both motivated by the physics of the cuprate superconductors. For the first class we will consider the case of Ising nematic ordering, while in the second class we will consider the onset of spin density wave order.

Among our aims is to understand the possible breakdown of Landau's Fermi liquid theory in Fermi gases. The most prominent example of this breakdown is in spatial dimension $d = 1$, where we generically obtain (not necessarily near any quantum phase transitions) a different quantum state known as the Tomonaga-Luttinger liquid. We will meet examples of Fermi liquid breakdown in $d \geq 2$ in the present chapter.

A comprehensive theoretical treatment of symmetry breaking transitions in a Fermi liquid was given by Hertz [1], although many important points were anticipated in earlier work [2–5]. We will review this treatment here, adapted to our field-theoretic approach. A key step in Hertz's work is to completely integrate out the fermionic excitations near the Fermi surface, resulting in an effective action for the order parameter characterizing the symmetry breaking alone. Such an approach seems natural from the perspective of the classical phase transitions, in which we

need only pay attention to the low energy fluctuations of the order parameter. However, here we also have the low energy quasiparticles near the Fermi surface: they are not associated directly with the broken symmetry, but their existence is protected by the requirement of the presence of a Fermi surface. It seems dangerous to integrate them out, and it would be preferable to make them active participants in the critical theory. This is a subtle question which we will address carefully in the present chapter. The main conclusion will be that the Hertz's strategy remains largely correct in $d \geq 3$, but that it fails badly in the important case of $d = 2$. This conclusion applies to both classes of symmetry breaking transitions in a Fermi liquid: with order parameters at zero and non-zero momentum.

I. FERMI LIQUID THEORY

Let us begin with a review of some basic ideas from the Fermi liquid theory of interacting fermions in d dimensions. We consider spin-1/2 fermions c_{ka} with momentum k and spin $a = \uparrow, \downarrow$ and dispersion ε_k . Thus the non-interacting fermions are described by the action

$$\mathcal{S}_c = \int d\tau \int \frac{d^d k}{(2\pi)^d} c_{ka}^\dagger \left(\frac{\partial}{\partial \tau} + \varepsilon_k \right) c_{ka}, \quad (1)$$

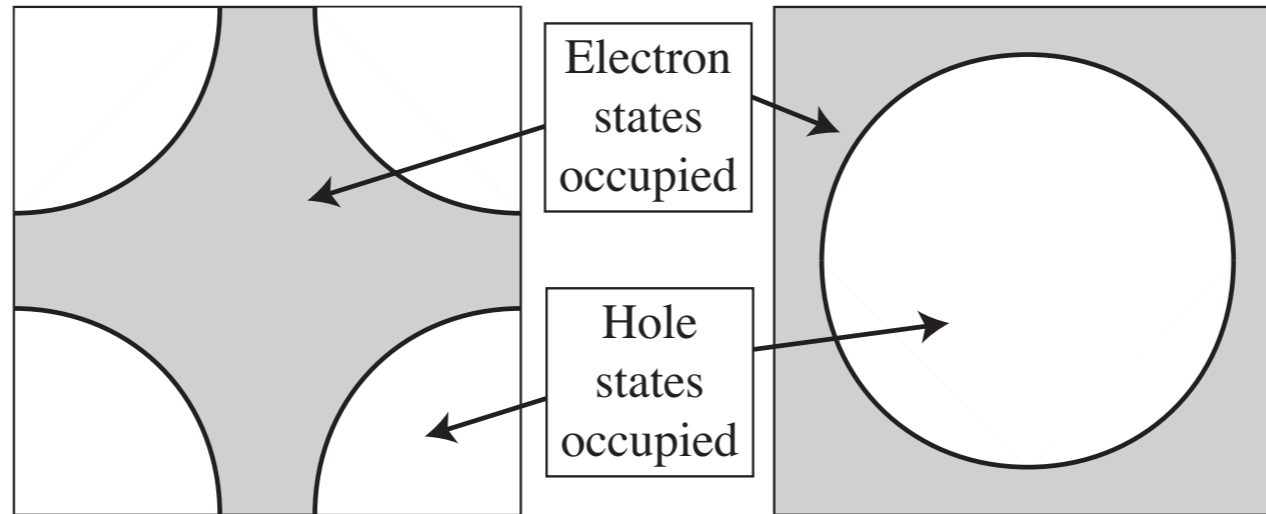


FIG. 1: Two views of the Fermi surface of the cuprate superconductors (hole and electron doped). The chemical potential is included in the dispersion ε_k , and so the Fermi surface is determined by $\varepsilon_k = 0$. The left panel has the momentum $k = (0, 0)$ (the “ Γ point”) in the center of the square Brillouin zone, while the right panel has the Γ point at the left edge. The momenta with both up and down electron states occupied are shaded gray.

As an example it is useful to keep in mind the dispersion ε_k appropriate for the cuprate superconductors, which is shown in Fig. 1. The fermion Green’s function under the free fermion action \mathcal{S}_c has the simple form

$$G_0(k, \omega_n) = \frac{1}{-i\omega_n + \varepsilon_k} \quad (2)$$

After analytically continuing to real frequencies, we observe that this Green’s function has a pole at energy ε_k with residue 1. Thus there are quasiparticle excitations

with residue $\mathcal{A} = 1$, much like those found in the strong or weak coupling expansions of the quantum Ising model. However, unlike those excitations, these quasiparticles can have both positive and negative energies, as ε_k can have either sign; the Fermi surface is the locus of points where ε_k changes sign. The positive energy quasiparticles are electron-like, while those with negative energy are hole-like *i.e.* they correspond to the absence of an electron. Note that the existence of negative energy quasiparticles is not an indication of the instability of the ground state. All true excitation energies are positive: the excitations are electron-like on one side of the Fermi surface, and hole-like on the other side. It is just convenient to combine the electron and hole quasiparticles within a single Green's function, by identifying hole-like quasiparticles with negative energy electron-quasiparticles.

We now wish to examine the stability of quasiparticles to interactions between them. In keeping with the strategy followed in this book, this should be preceded by an effective action for the low energy quasiparticles. The latter is usually done by a gradient expansion, leading to an effective field theory. However, here we face a unique difficulty: there are zero energy quasiparticles along a $d - 1$ dimensional Fermi surface identified by $\varepsilon_k = 0$. It would therefore seem that we should expand about all points on the Fermi surface. This is indeed the strategy followed in textbook treatments of Fermi liquid theory: we measure momenta, k_\perp , from the Fermi surface, choose a cutoff so that $|k_\perp| < \Lambda$, and then perform an RG which reduces the value of Λ [6]. This procedure is illustrated in Fig. 2. Formally, for each direction

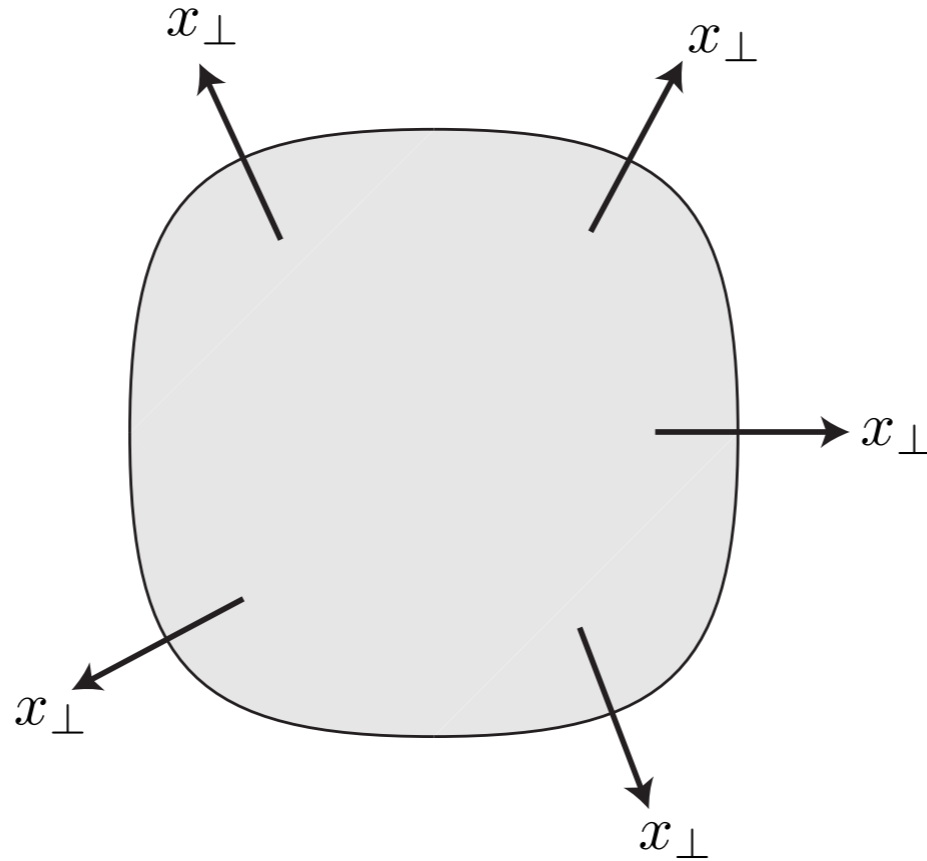


FIG. 2: Traditional low energy limit of Fermi liquid theory. The Fermi surface has one dimensional chiral fermions on every point, moving along the direction x_{\perp} . There fermions are present for momenta $|k_{\perp}| < \Lambda$; *i.e.* in a momentum shell of width 2Λ around the Fermi surface.

\hat{n} , we define the position of the Fermi surface by the wavevector $\vec{k}_F(\hat{n})$, so that $\hat{n} = \vec{k}_F(\hat{n})/|\vec{k}_F(\hat{n})|$. Then we identify wavevectors near the Fermi surface by

$$\vec{k} = \vec{k}_F(\hat{n}) + k_{\perp} \hat{n} \quad (3)$$

Now we should expand in small momenta k_{\perp} . For this, we define the infinite set of

fields $\psi_{\hat{n}a}(k_{\perp})$, which are labeled by the spin a and the direction \hat{n} , related to the fermions c by

$$c_{\vec{k}a} = \frac{1}{\sqrt{S_F}} \psi_{\hat{n}a}(k_{\perp}), \quad (4)$$

where \vec{k} and k_{\perp} are related by (3), and S_F is the area of the Fermi surface. Inserting (4) into (1), expanding in k_{\perp} , and Fourier transforming to real space x_{\perp} , we obtain the low energy theory

$$\mathcal{S}_{\text{FL}} = \int d\Omega_{\hat{n}} \int dx_{\perp} \psi_{\hat{n}a}^{\dagger}(x_{\perp}) \left(\frac{\partial}{\partial \tau} - i v_F(\hat{n}) \frac{\partial}{\partial x_{\perp}} \right) \psi_{\hat{n}a}(x_{\perp}), \quad (5)$$

where the Fermi velocity is energy gradient on the Fermi surface $v_F(\hat{n}) = |\nabla_k \varepsilon_{\vec{k}_F(\hat{n})}|$. For each \hat{n} , (5) describes fermions moving along the single dimension x_{\perp} with the Fermi velocity: this is a one-dimensional chiral fermion; the ‘chiral’ refers to the fact that the fermion only moves in the positive x_{\perp} direction, and not the negative x_{\perp} direction. In other words, the low energy theory of the Fermi liquid is an infinite set of one-dimensional chiral fermions, one chiral fermion for each point on the Fermi surface.

Apart from the free Fermi term in (5), Landau’s Fermi liquid theory also allows for contact interactions between chiral fermions along different directions [6]. These

are labeled by the Landau parameters, and lead only to shifts in the quasiparticle energies which depend upon the densities of the other quasiparticles. Such shifts are important when computing the response of the Fermi liquid to external density or spin perturbations. However, the resulting fixed-point action of Fermi liquid theory does not offer a route to computing the decay of quasiparticles: the stability of the quasiparticles is implicitly assumed in the fixed point theory. Our primary purpose here is to verify the stability of the quasiparticles, so that we will be prepared for the breakdown of Fermi liquid theory at quantum critical points. So we refer the reader to the many textbook treatments of the traditional formulation of Landau's Fermi liquid theory, and turn to an alternative analysis below.

A shortcoming of the effective action (5) is that it only includes the dispersion of the fermions transverse to the Fermi surface. Thus, if we discretize the directions \hat{n} , and pick a given point on the Fermi surface, the Fermi surface is effectively *flat* at that point. We will shortly see that the curvature of the Fermi surface is important in understanding the decay and breakdown of quasiparticles. Thus we have to take the continuum scaling limit in a manner which keeps the curvature of the Fermi surface fixed, and does not scale it to zero. For this, as shown in Fig. 3, we focus attention on a single arc of the Fermi surface in the vicinity of any chosen point \vec{k}_0 . We will show in Section I A that the results are independent of the choice of \vec{k}_0 on the Fermi surface, but we defer that issue for now. Then we will choose our cutoff Λ to scale towards the single point k_0 (the cutoff will be defined more carefully

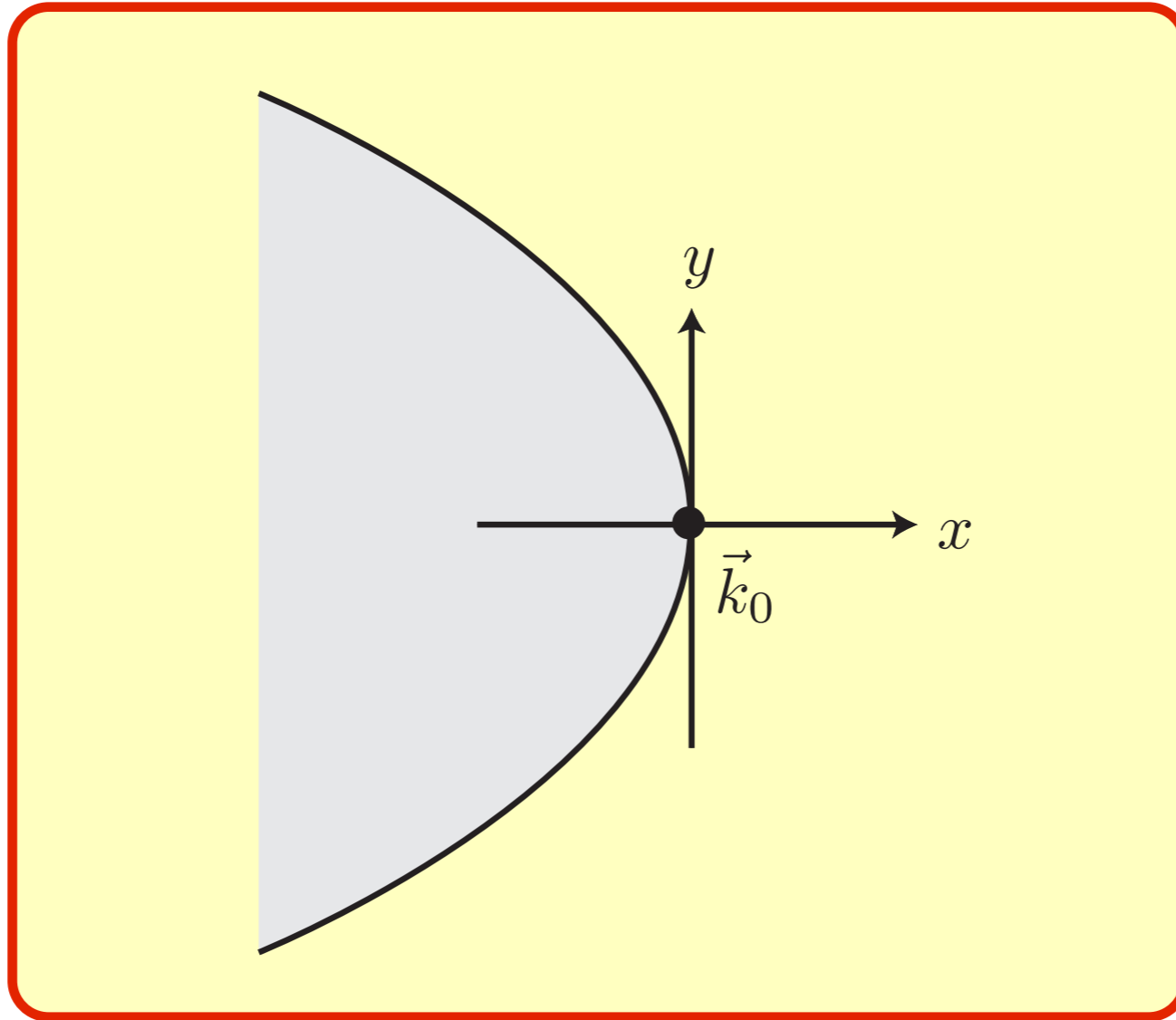


FIG. 3: Alternative low energy formulation of Fermi liquid theory. We focus on an extended patch of the Fermi surface, and expand in momenta about the point \vec{k}_0 on the Fermi surface. This yields a theory of d -dimensional fermions ψ in (7), with dispersion (14). The co-ordinate y represents the $d - 1$ dimensions parallel to the Fermi surface.

below), rather than scaling to all points on the Fermi surface, as we did for (5).

With \vec{k}_0 chosen as Fig. 3, let us now define our low energy theory and scaling limit [7]. Unlike the one-dimensional chiral fermions which appeared in (5), we

will now use a d dimensional fermion $\psi_a(x, y)$. Here x is the one dimensional coordinate orthogonal to the Fermi surface, and \vec{y} represents the $(d - 1)$ -dimensional transverse co-ordinates. After Fourier transformations, this fermion is related to the underlying fermions c_{k_a} simply by

$$\psi_a(\vec{k}) = c_{\vec{k}_0 + \vec{k}, a} \quad (6)$$

In other words, we only shift the origin of momentum space from $\vec{k} = 0$ to $\vec{k} = \vec{k}_0$. Inserting (6) in (1), and expanding the dispersion in the vicinity of \vec{k}_0 (contrast to the expansion away from all points on the Fermi surface in (5)), we obtain the low energy theory

$$\mathcal{S}_0 = \int d\tau \int dx \int d^{d-1}y \psi_a^\dagger \left(\zeta \frac{\partial}{\partial \tau} - i v_F \frac{\partial}{\partial x} - \frac{\kappa}{2} \nabla_y^2 \right) \psi_a. \quad (7)$$

We have added a co-efficient ζ to the temporal gradient term for future convenience: we are interested in $\zeta = 1$, but will see later that in non-Fermi liquid states it is convenient to allow ζ to renormalize. Notice the additional second-order gradients in y which were missing from (5): the co-efficient κ is proportional to the curvature of the Fermi surface at \vec{k}_0 . Also, as we have already noted, the fermion field in (7) is d -dimensional, while that in (5) is one-dimensional. One benefit of (7) is now

immediately evident: it has zero energy excitations when

$$v_F k_x + \kappa \frac{k_y^2}{2} = 0, \quad (8)$$

and so (8) defines the position of the Fermi surface, which is then part of the low energy theory including its curvature. Note that (7) now includes an extended portion of the Fermi surface; contrast that with (5), where the one-dimensional chiral fermion theory for each \hat{n} describes only a single point on the Fermi surface.

The gradient terms in (7) define a natural momentum space cutoff, and associated scaling limit. We will take such a limit at *fixed* ζ , v_F and κ . Notice that momenta in the x direction scale as the square of the momenta in the y direction, and so we can choose $v_F^2 k_x^2 + \kappa^2 k_y^4 < \Lambda^4$. Notice that as we reduce Λ , we scale towards the single point \vec{k}_0 on the Fermi surface, as we required above.

It now a simple matter to apply the RG analysis to the fermion theory in (7). At fixed ζ , v_F and κ , the action (7) is invariant under the following rescalings of spacetime:

$$x' = x e^{-2\ell}, \quad y' = y e^{-\ell}, \quad \tau' = \tau e^{-2\ell} \quad (9)$$

Note that we have chosen the directions parallel to the Fermi surface as the ones defining the primary length scale, with $\dim[y] = -1$, and the transverse direction

has $\dim[x] = -2$. The temporal direction rescaling implies that we have the dynamic exponent $z = 2$ when measured relative to the y spatial directions. The RG invariance of (7) also requires the field rescaling

$$\psi' = \psi e^{(d+1)\ell/2}. \quad (10)$$

We now have the tools needed to determine the role of fermion interactions. The simplest contact interaction has the form

$$\mathcal{S}_1 = u_0 \int d\tau \int dx \int d^{d-1}y \Psi_a^\dagger \Psi_b^\dagger \Psi_b \Psi_a. \quad (11)$$

Apply the RG rescalings in (10) we find

$$u'_0 = u_0 e^{(1-d)\ell}. \quad (12)$$

In other words, the interaction between the fermions u_0 is irrelevant in all dimension $d > 1$. This strongly suggests that the Fermi liquid picture of non-interacting fermions is indeed RG stable.

Let us understand the stability of Fermi liquid theory a bit better by computing corrections to the fermion Green's function in (2). Let us write the interaction corrected Green's function as

$$G(k, \omega) = \frac{1}{-\zeta\omega + \varepsilon_k - \Sigma(k, \omega)}, \quad (13)$$

where now

$$\varepsilon_k = v_F k_x + \kappa \frac{k_y^2}{2}. \quad (14)$$

To first order in u_0 , the fermion self energy is real (for real frequencies), and so only modifies the quasiparticle dispersion and residue, \mathcal{A} , but does not destabilize the existence of the quasiparticle pole.

So let us move to second order in u_0 . First, we use an RG argument. We are interested in the imaginary part of the self energy, and let us assume for now at small ω

$$\text{Im}\Sigma(k=0, \omega) \sim u_0^2 \omega^p. \quad (15)$$

We determine p by scaling arguments. From (13) we know that $\dim[\Sigma] = z = 2$, and so conclude from matching dimensions in (15) that $p = d$. However, there is a subtlety here: scaling arguments only yield the powerlaws of singular corrections, and do not say anything about analytic backgrounds that may be allowed from the structure of the theory. Here, a term with $p = 2$ is permitted because $\text{Im}\Sigma$ is an even function of ω . So the proper conclusion is

$$p = \min(d, 2). \quad (16)$$

The above scaling argument is fine as it stands, but cannot substitute for the insight gained by an explicit computation. The Feynman diagram contributing to

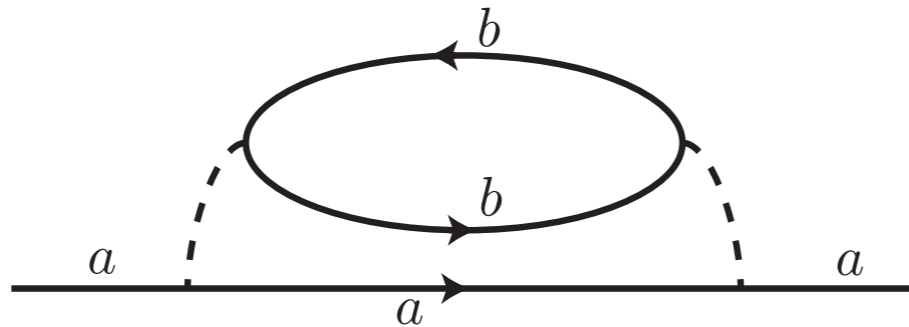


FIG. 4: Feynman diagram for the decay of quasiparticles at order u_0^2 . The dashed line is the interaction u_0 , and a, b are spin labels.

the quasiparticle decay at order u_0^2 is indicated in Fig. 4. We evaluate it in two stages. First we evaluate the fermion loop of the fermions with spin label b ; this gives us the fermion polarizability

$$\Pi(q, \omega_n) = \int \frac{d^d k}{(2\pi)^d} \int \frac{d\epsilon_n}{2\pi} G_0(k + q, \epsilon_n + \omega_n) G_0(k, \epsilon_n). \quad (17)$$

This enters the self-energy by

$$\Sigma(k, \epsilon_n) = u_0^2 \int \frac{d^d q}{(2\pi)^d} \int \frac{d\omega_n}{2\pi} \Pi(q, \omega_n) G_0(k + q, \epsilon_n + \omega_n). \quad (18)$$

We first explicitly evaluate $\Pi(q, \omega_n)$. We will only be interested in terms that are singular in q and ω_n , and will drop regular contributions from regions of high

momentum and frequency. In this case, it is permissible to reverse the conventional order of integrating over frequency first in (17), and to first integrate over k_x . It is a simple matter to perform the integration over k_x in using the method of residues to yield

$$\begin{aligned}\Pi(q, \omega_n) &= \frac{1}{2v_F} \int \frac{d^{d-1}k_y}{(2\pi)^{d-1}} \int \frac{d\epsilon_n}{2\pi} \frac{\text{sgn}(\epsilon_n + \omega_n) - \text{sgn}(\epsilon_n)}{\left(\zeta\omega_n + iv_Fq_x + i\kappa q_y^2/2 + i\kappa\vec{q}_y \cdot \vec{k}_y\right)} \\ &= \frac{|\omega_n|}{2\pi v_F} \int \frac{d^{d-1}k_y}{(2\pi)^{d-1}} \frac{1}{\left(\zeta\omega_n + iv_Fq_x + i\kappa q_y^2/2 + i\kappa\vec{q}_y \cdot \vec{k}_y\right)}.\end{aligned}\quad (19)$$

We now integrate along the component of \vec{k}_y parallel to the direction of \vec{q}_y to obtain

$$\begin{aligned}\Pi(q, \omega_n) &= \frac{|\omega_n|}{2\pi v_F \kappa |q_y|} \int \frac{d^{d-2}k_y}{(2\pi)^{d-2}} \\ &= \frac{|\omega_n|}{2\pi v_F \kappa |q_y|} \Lambda^{d-2}\end{aligned}\quad (20)$$

Note that in $d = 2$ the last non-universal factor is not present, and the result for Π is universal with $\Lambda^{d-2} = 1$. Note also that ζ has dropped out of the result Π : this will be important in our subsequent treatment of quantum critical points.

Now we insert (20) into (18). After evaluating the integral over q_x we obtain

$$\begin{aligned}
 \Sigma(k, \omega_n) &= i \frac{u_0^2}{2\pi v_F^2 \kappa} \int \frac{d^{d-1} q_y}{(2\pi)^{d-1}} \int \frac{d\epsilon_n}{2\pi} \frac{\text{sgn}(\epsilon_n + \omega_n) |\epsilon_n|}{|q_y|} \\
 &= i \text{sgn}(\omega_n) \omega_n^2 \frac{u_0^2}{4\pi v_F^2 \kappa} \int \frac{d^{d-1} q_y}{(2\pi)^{d-1}} \frac{1}{|q_y|} \\
 &= i \text{sgn}(\omega_n) \omega_n^2 \frac{u_0^2}{4\pi v_F^2 \kappa} \Lambda^{d-2}, \quad d > 2.
 \end{aligned} \tag{21}$$

Again, ζ has dropped out. This result is in perfect accord with the scaling arguments in (15) and (16).

Let us consider the important case $d = 2$. There is an infrared divergence in the q_y integral in (21) at small q_y . This is only cutoff after we include a self-consistent damping of the quasiparticle propagators in the Feynman diagram of Fig. 4, rather than the bare propagators we have used above. After including this damping, we expect that (15) will be modified to

$$\text{Im}\Sigma(k, \omega) \sim u_0^2 \omega^2 \log \left(\frac{\Lambda}{u_0 |\omega|} \right), \quad d = 2; \tag{22}$$

thus the scaling result is modified by a logarithm in $d = 2$.

With $\text{Im}\Sigma \sim u_0^2\omega^2$ (up to logarithms), we can now easily examine the fate of the quasiparticles from (13). From (13), we see that the quasiparticle pole is always broadened: the width of the quasiparticle peak is $\sim u_0^2\varepsilon_k^2$ for a quasiparticle with energy $\omega = \varepsilon_k$. Thus the quasiparticle width vanishes as the square of the distance from the Fermi surface. Asymptotically close to the Fermi surface, the quasiparticle width is much smaller than the quasiparticle energy: this is sufficient to regard the quasiparticle as a sharp excitation, and confirm the validity of Landau's Fermi liquid theory.

An important and frequently used diagnostic of the stability of the quasiparticle is the discontinuity in the fermion momentum distribution function $n(k) = \langle c_{ka}^\dagger c_{ka} \rangle$. This can be computed from the real frequency Green's function $G(k, \omega)$ by (here we set $\zeta = 1$)

$$n(k) = \int_{-\infty}^0 \frac{d\omega}{(2\pi)} \text{Im}G(k, \omega). \quad (23)$$

Assuming a pole in the Green's function of the form

$$G(k, \omega) = \frac{A}{-\omega + \varepsilon_k + ic\omega^2} + \dots \quad (24)$$

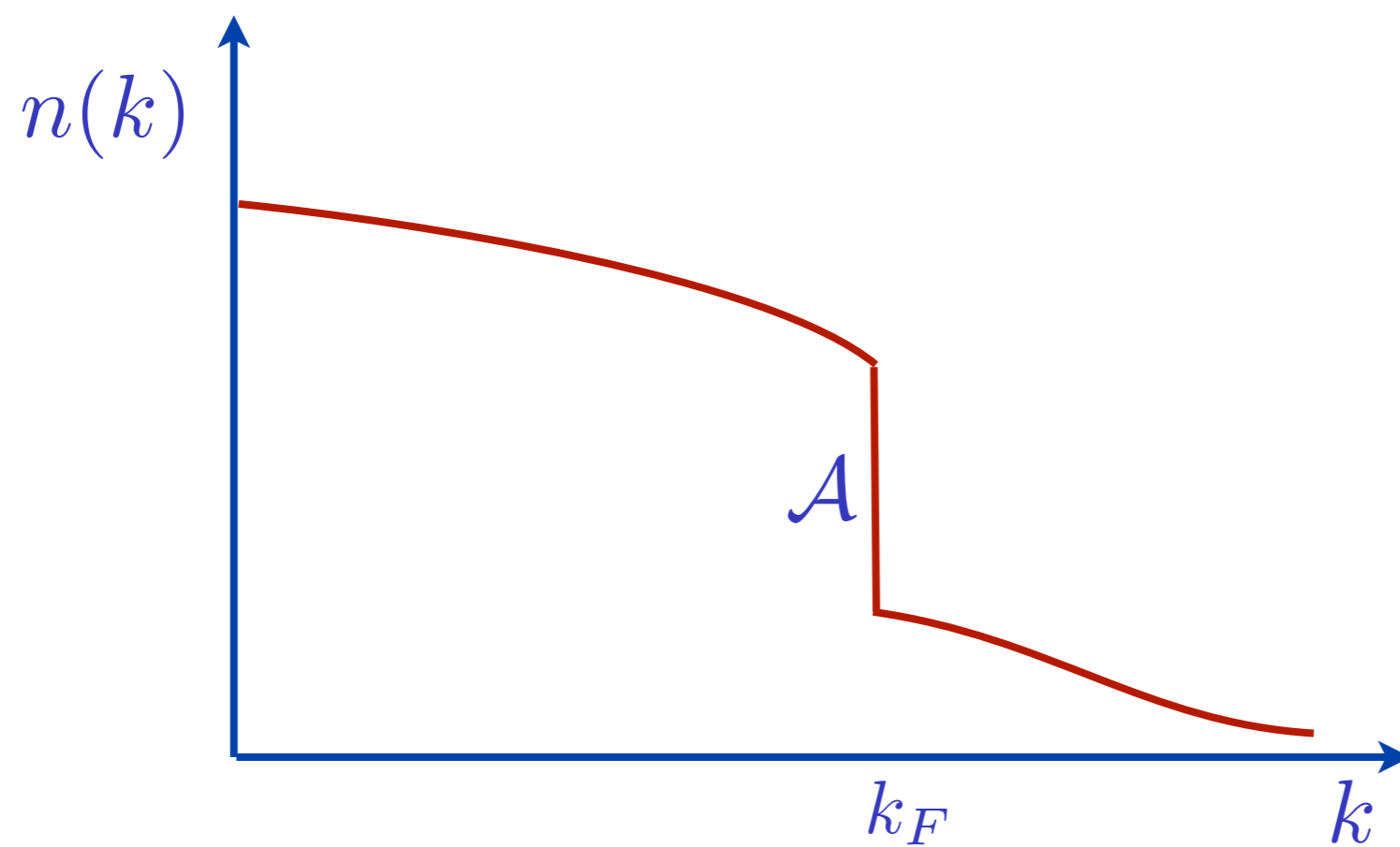
we find a step discontinuity in the momentum distribution function at the Fermi

surface

$$n(k) = \mathcal{A}\theta(-\varepsilon_k) + \dots$$

(25)

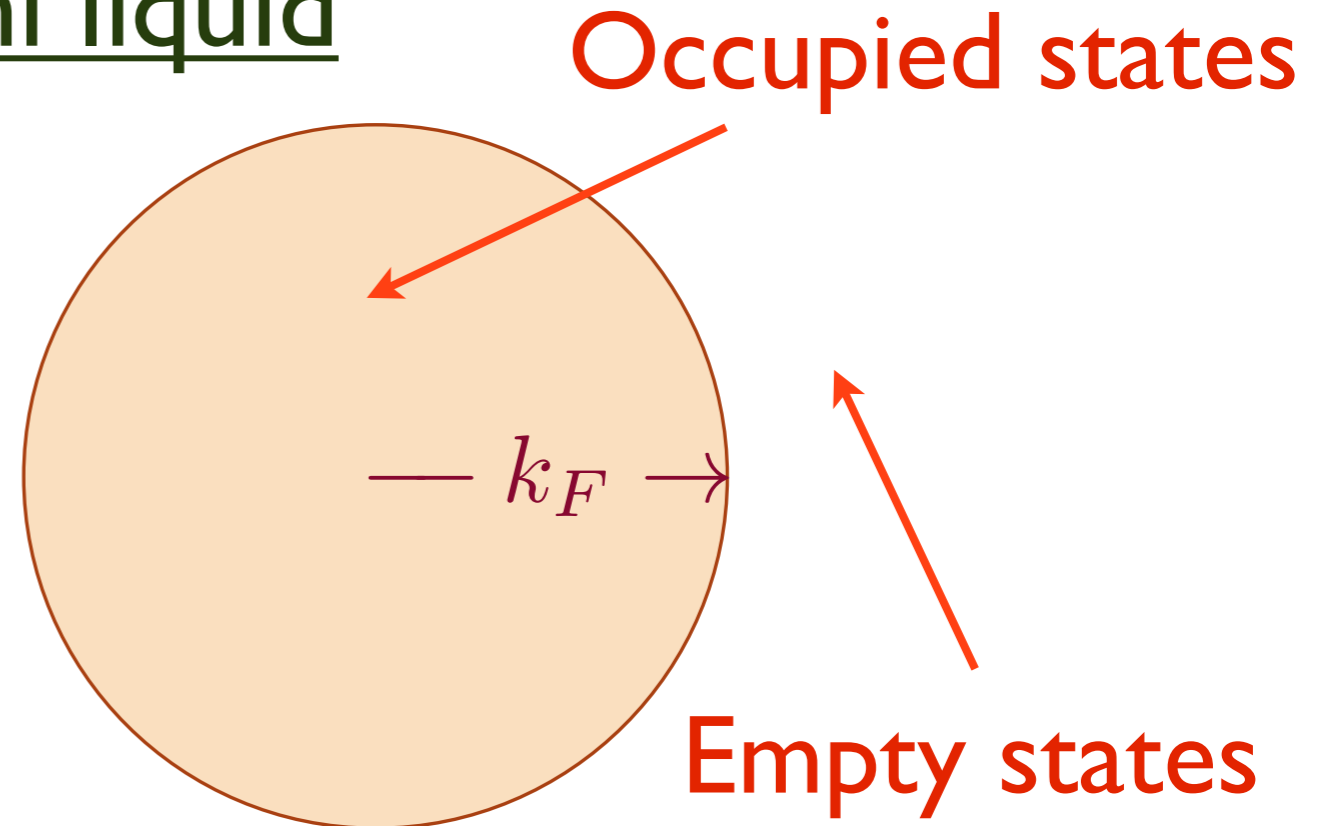
of strength \mathcal{A} .



The Fermi liquid

$$\mathcal{L} = f^\dagger \left(\partial_\tau - \frac{\nabla^2}{2m} - \mu \right) f$$

+ 4 Fermi terms

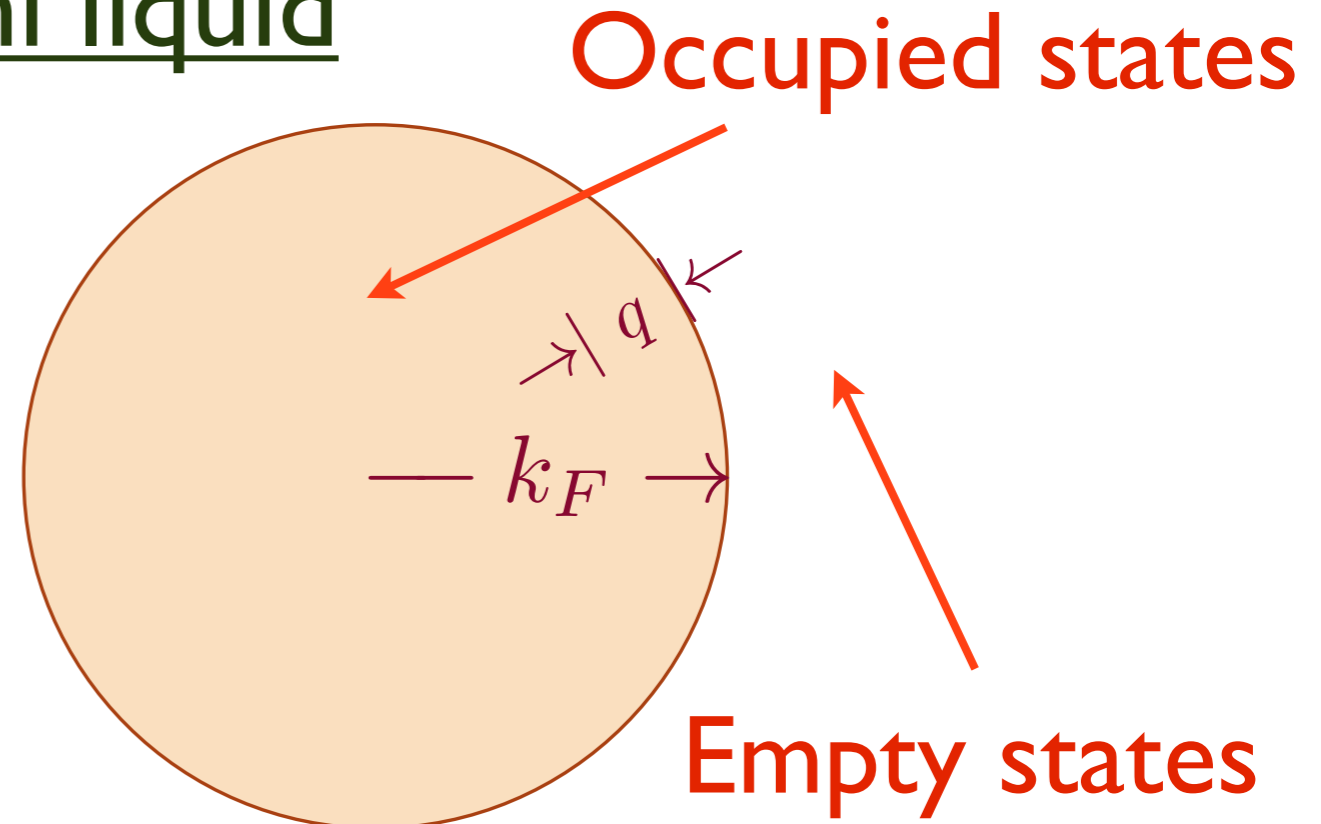


- Fermi wavevector obeys the Luttinger relation $k_F^d \sim Q$, the fermion density

The Fermi liquid

$$\mathcal{L} = f^\dagger \left(\partial_\tau - \frac{\nabla^2}{2m} - \mu \right) f$$

+ 4 Fermi terms

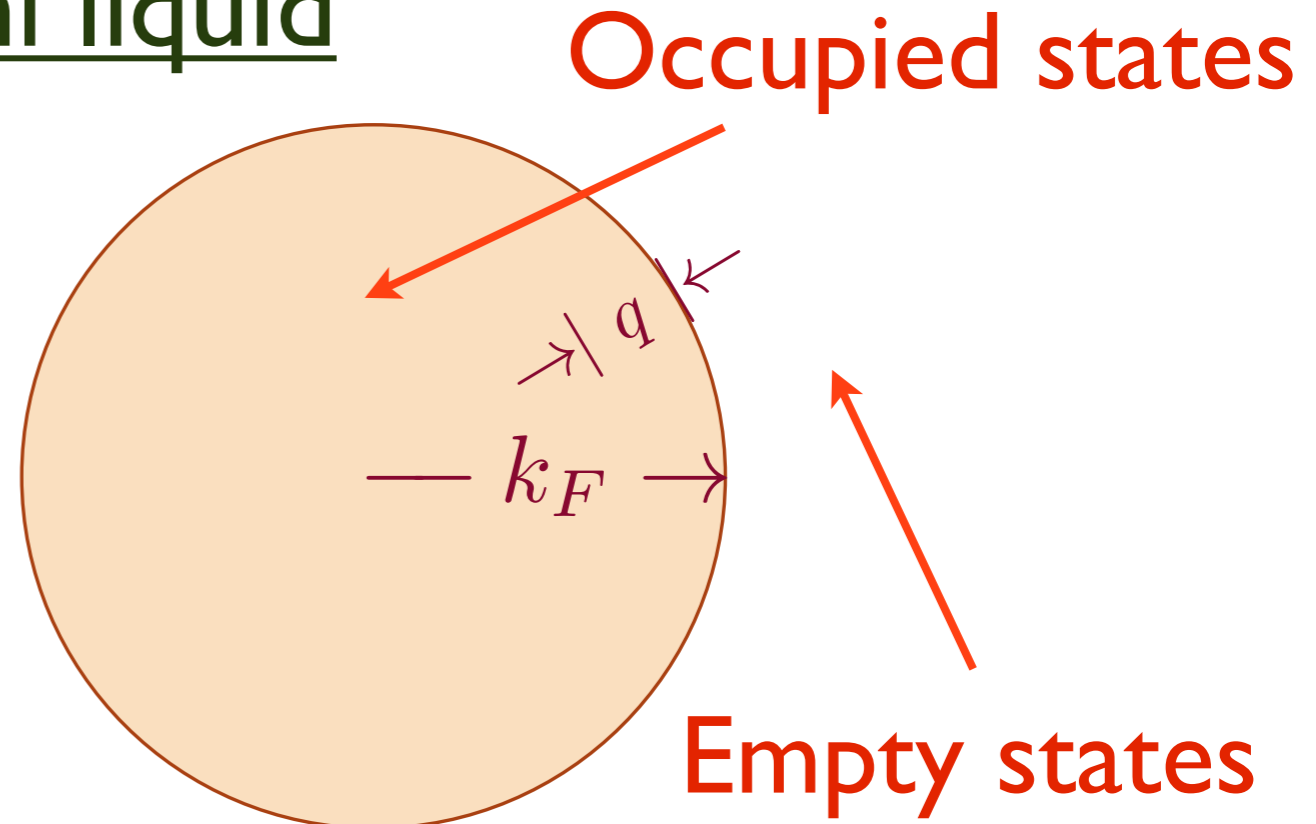


- Fermi wavevector obeys the Luttinger relation $k_F^d \sim Q$, the fermion density
- Sharp particle and hole of excitations near the Fermi surface with energy $\omega \sim |q|^z$, with dynamic exponent $z = 1$.

The Fermi liquid

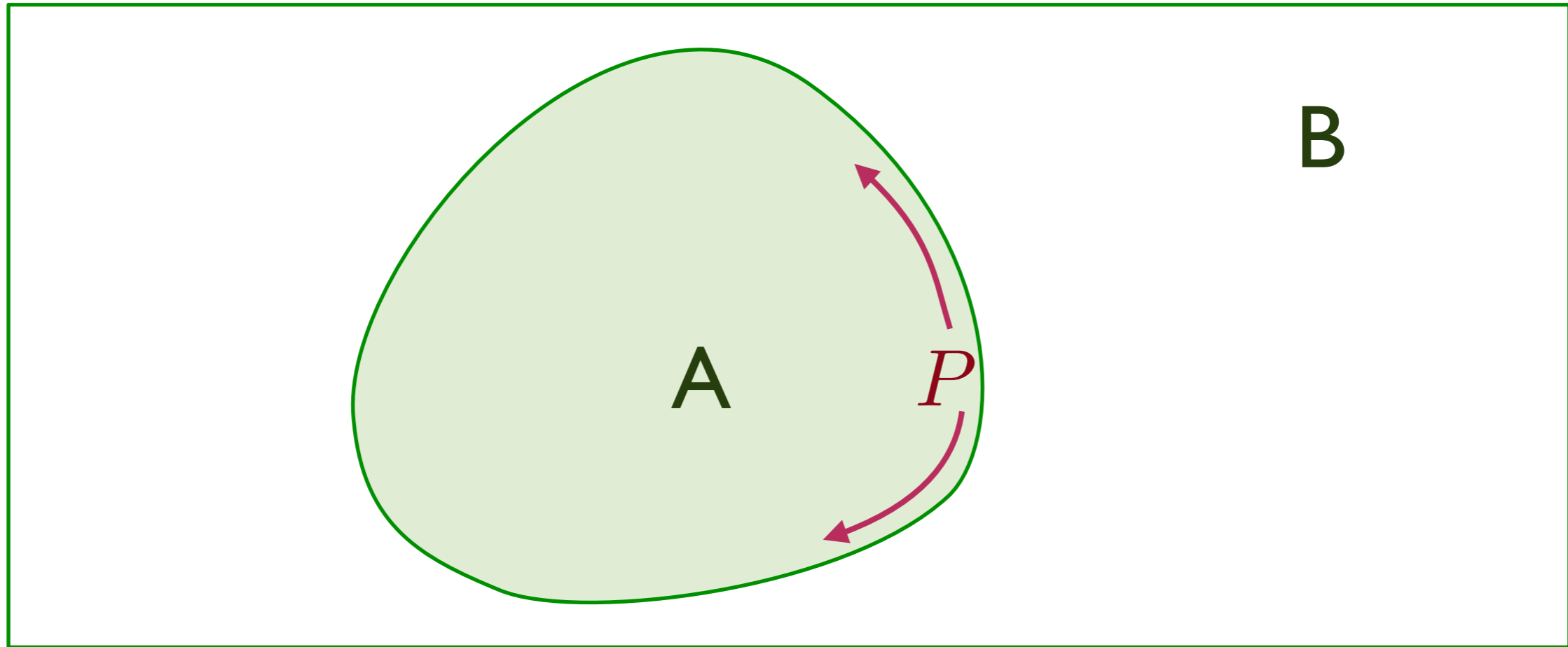
$$\mathcal{L} = f^\dagger \left(\partial_\tau - \frac{\nabla^2}{2m} - \mu \right) f$$

+ 4 Fermi terms



- Fermi wavevector obeys the Luttinger relation $k_F^d \sim Q$, the fermion density
- Sharp particle and hole of excitations near the Fermi surface with energy $\omega \sim |q|^z$, with dynamic exponent $z = 1$.
- The phase space density of fermions is effectively one-dimensional, so the entropy density $S \sim T$. It is useful to write this as $S \sim T^{(d-\theta)/z}$, with violation of hyperscaling exponent $\theta = d - 1$.

Entanglement entropy of the Fermi liquid



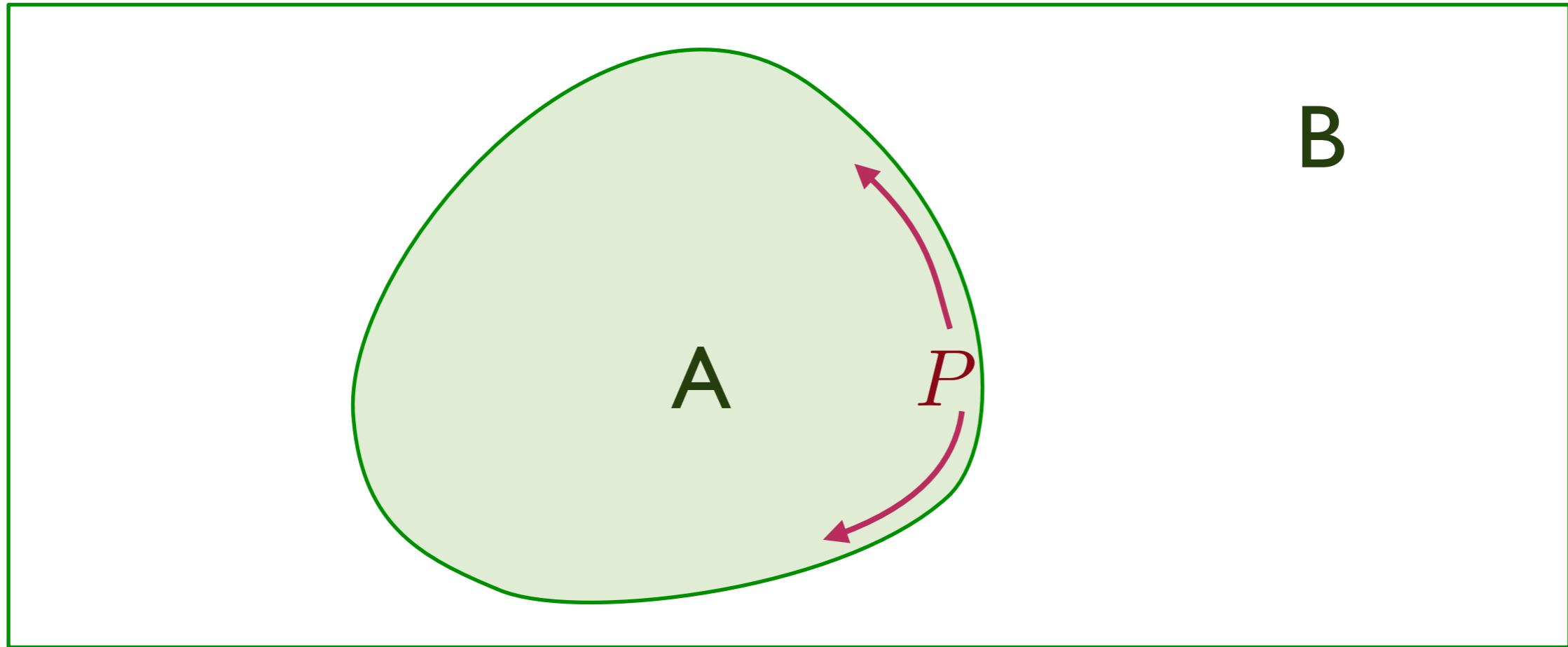
Logarithmic violation of “area law”: $S_E = \frac{1}{12} (k_F P) \ln(k_F P)$

for a circular Fermi surface with Fermi momentum k_F , where P is the perimeter of region A with an arbitrary smooth shape.

D. Gioev and I. Klich, *Physical Review Letters* **96**, 100503 (2006)

B. Swingle, *Physical Review Letters* **105**, 050502 (2010)

Entanglement entropy of the Fermi liquid



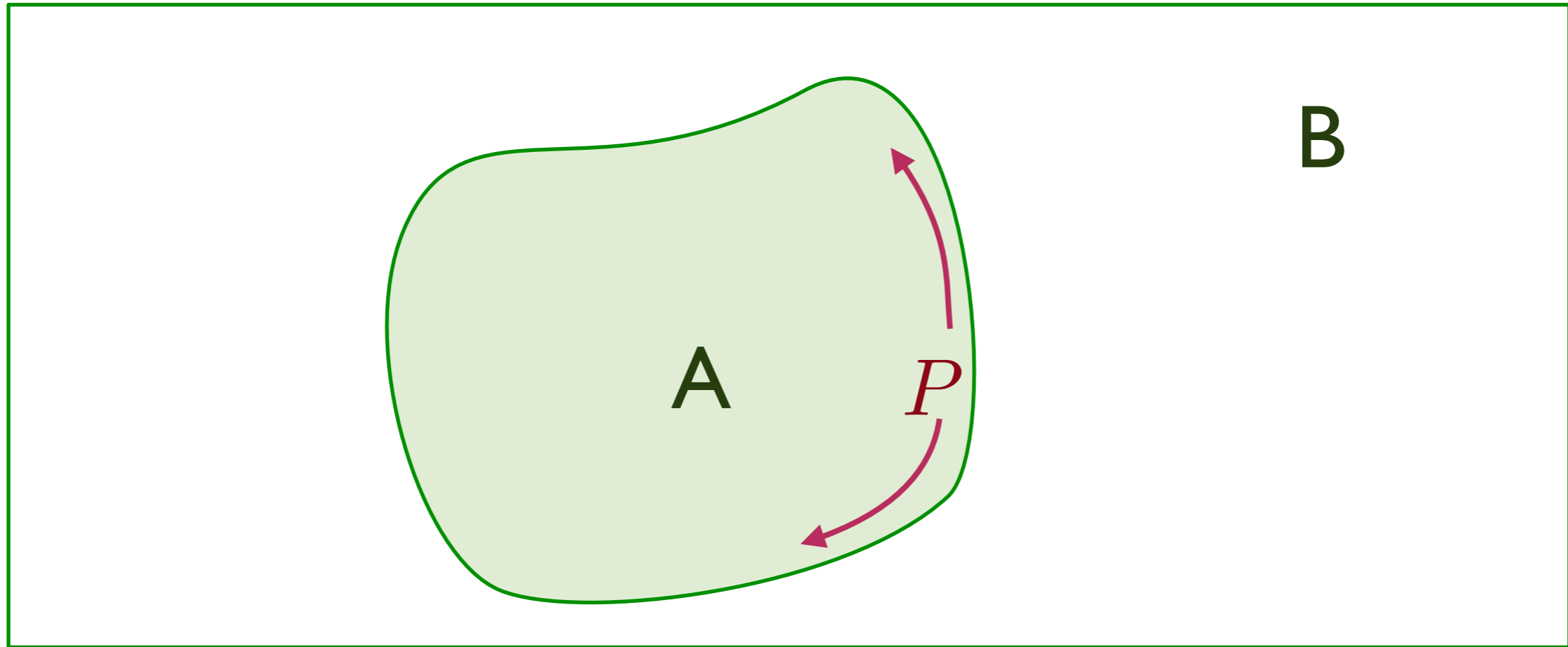
Logarithmic violation of “area law”: $S_E = \frac{1}{12} (k_F P) \ln(k_F P)$

for a circular Fermi surface with Fermi momentum k_F , where P is the perimeter of region A with an arbitrary smooth shape. The prefactor $1/12$ is *universal*: it is independent of the shape of the entangling region, and of the strength of the interactions.

D. Gioev and I. Klich, *Physical Review Letters* **96**, 100503 (2006)

B. Swingle, *Physical Review Letters* **105**, 050502 (2010)

Entanglement entropy of the Fermi liquid



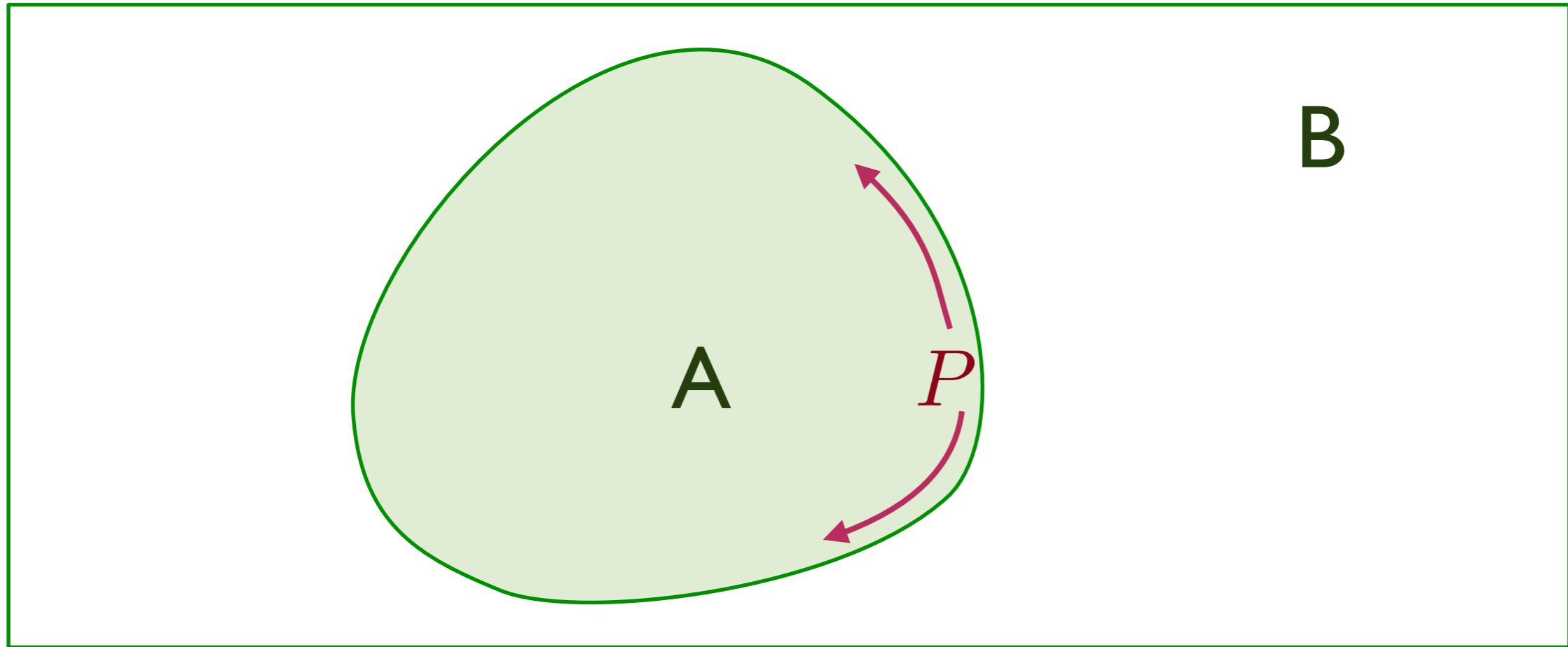
Logarithmic violation of “area law”: $S_E = \frac{1}{12} (k_F P) \ln(k_F P)$

for a circular Fermi surface with Fermi momentum k_F , where P is the perimeter of region A with an arbitrary smooth shape. The prefactor $1/12$ is *universal*: it is independent of the shape of the entangling region, and of the strength of the interactions.

D. Gioev and I. Klich, *Physical Review Letters* **96**, 100503 (2006)

B. Swingle, *Physical Review Letters* **105**, 050502 (2010)

Entanglement entropy of the Fermi liquid



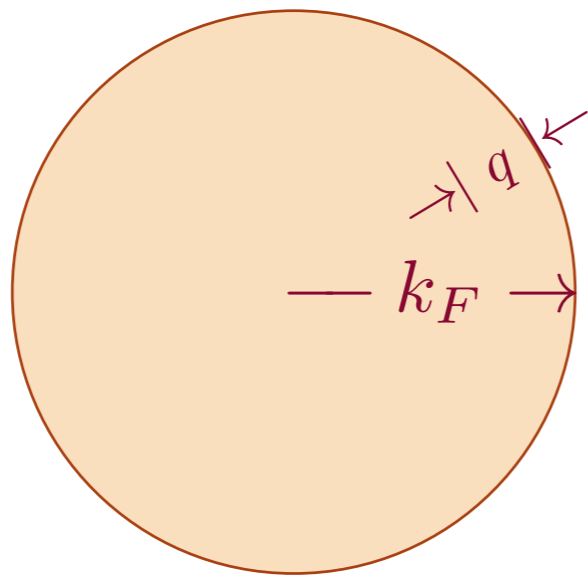
Logarithmic violation of “area law”: $S_E = \frac{1}{12} (k_F P) \ln(k_F P)$

for a circular Fermi surface with Fermi momentum k_F , where P is the perimeter of region A with an arbitrary smooth shape. The prefactor $1/12$ is *universal*: it is independent of the shape of the entangling region, and of the strength of the interactions.

D. Gioev and I. Klich, *Physical Review Letters* **96**, 100503 (2006)

B. Swingle, *Physical Review Letters* **105**, 050502 (2010)

FL Fermi liquid



- $k_F^d \sim Q$, the fermion density
- Sharp fermionic excitations near Fermi surface with $\omega \sim |q|^z$, and $z = 1$.
- Entropy density $S \sim T^{(d-\theta)/z}$ with violation of hyperscaling exponent $\theta = d - 1$.
- Entanglement entropy $S_E \sim k_F^{d-1} P \ln P$.

Outline

1. The simplest models without quasiparticles

A. Superfluid-insulator transition

of ultracold bosons in an optical lattice

*B. Conformal field theories in $2+1$ dimensions and
the AdS/CFT correspondence*

2. Metals without quasiparticles

A. Review of Fermi liquid theory

*B. A “non-Fermi” liquid: the Ising-nematic
quantum critical point*

C. The holographic view: charged black-branes

Outline

I. The simplest models without quasiparticles

A. Superfluid-insulator transition

of ultracold bosons in an optical lattice

B. Conformal field theories in $2+1$ dimensions and the AdS/CFT correspondence

2. Metals without quasiparticles

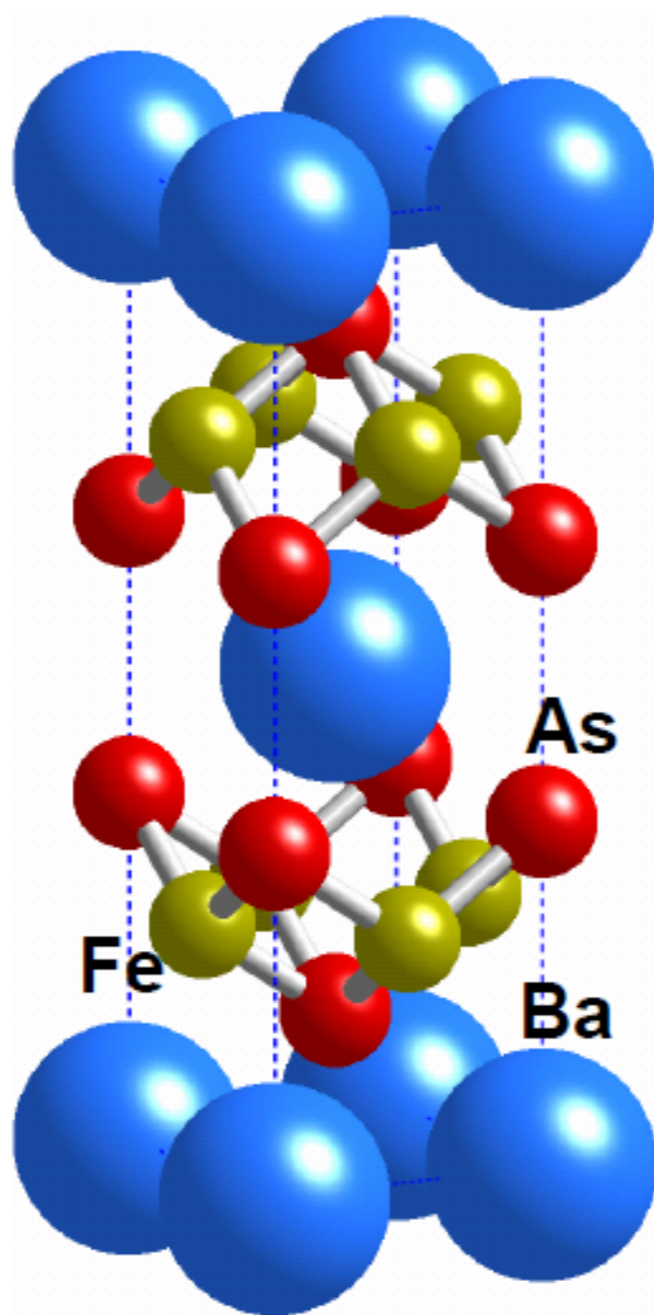
A. Review of Fermi liquid theory

B. A “non-Fermi” liquid: the Ising-nematic quantum critical point

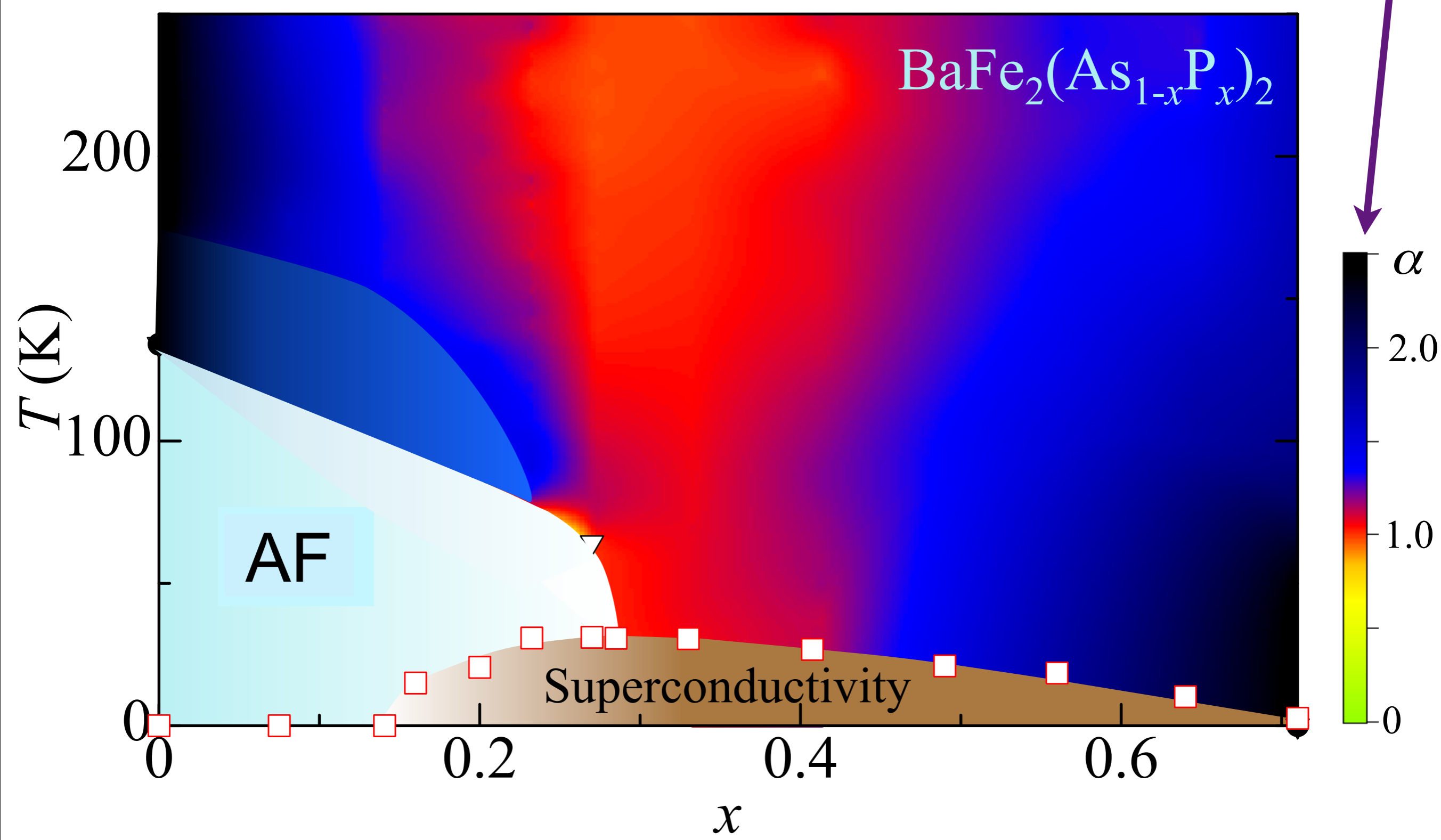
C. The holographic view: charged black-branes

Iron pnictides:

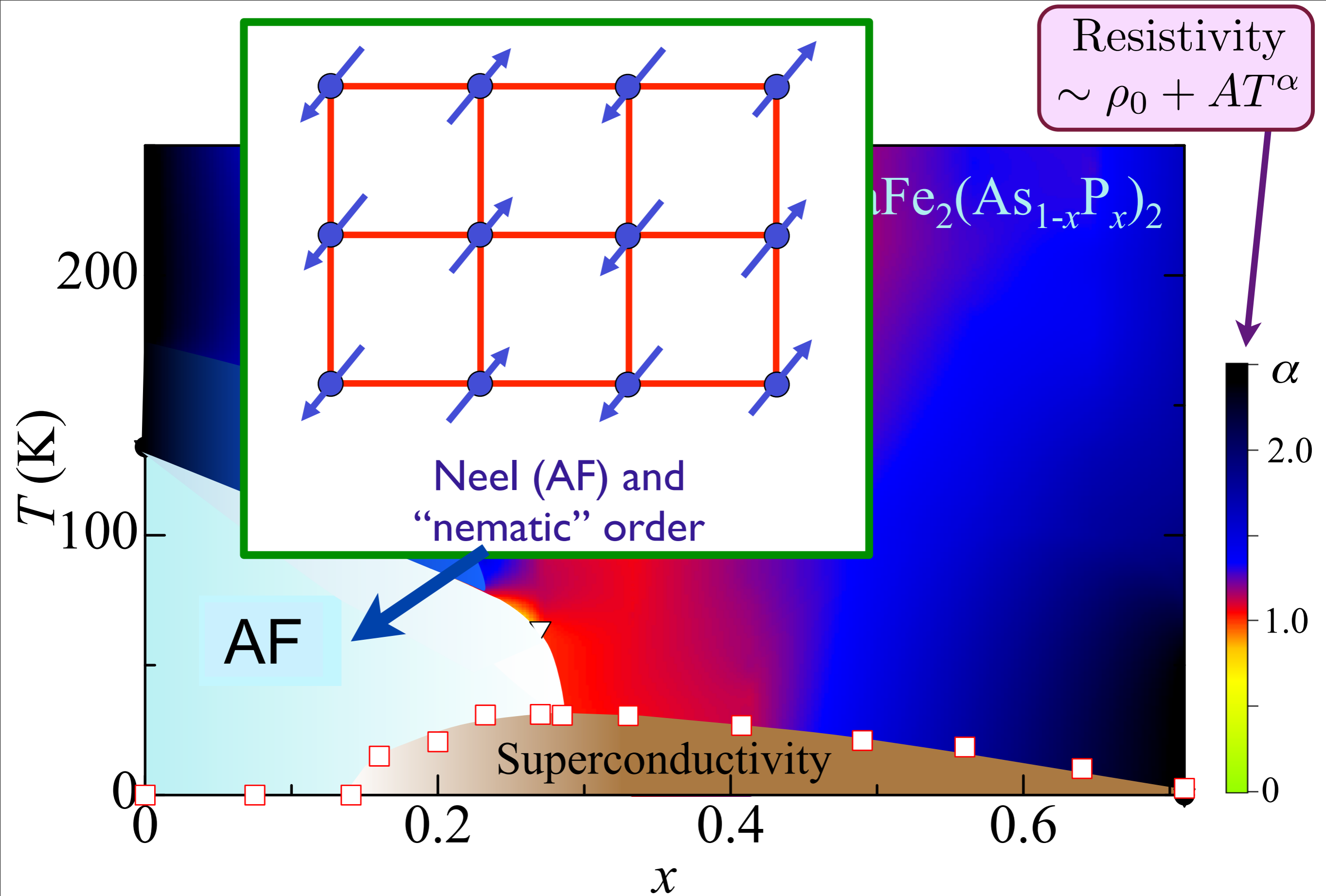
a new class of high temperature superconductors



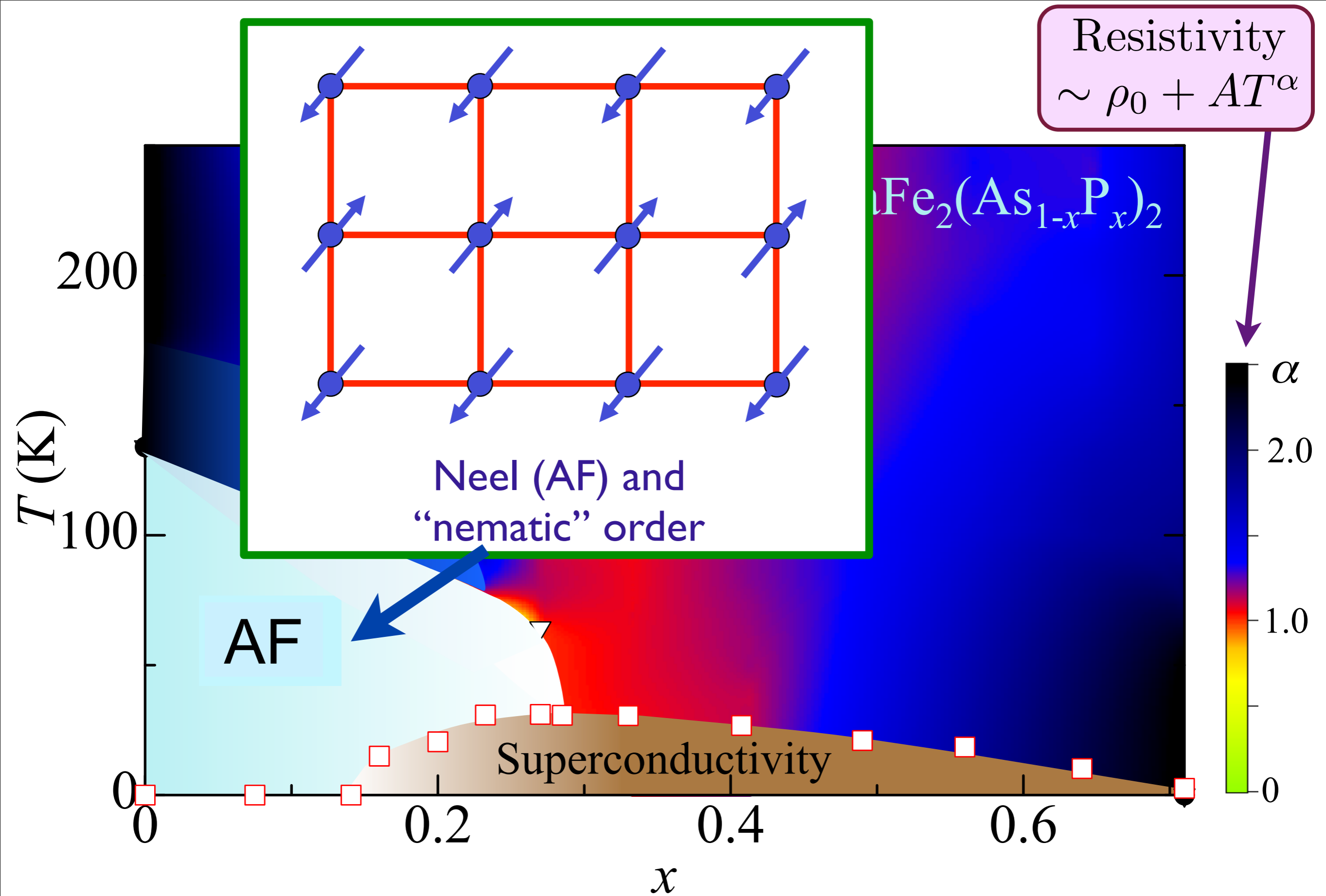
Resistivity
 $\sim \rho_0 + AT^\alpha$



S. Kasahara, T. Shibauchi, K. Hashimoto, K. Ikada, S. Tonegawa, R. Okazaki, H. Shishido, H. Ikeda, H. Takeya, K. Hirata, T. Terashima, and Y. Matsuda, *Physical Review B* **81**, 184519 (2010)

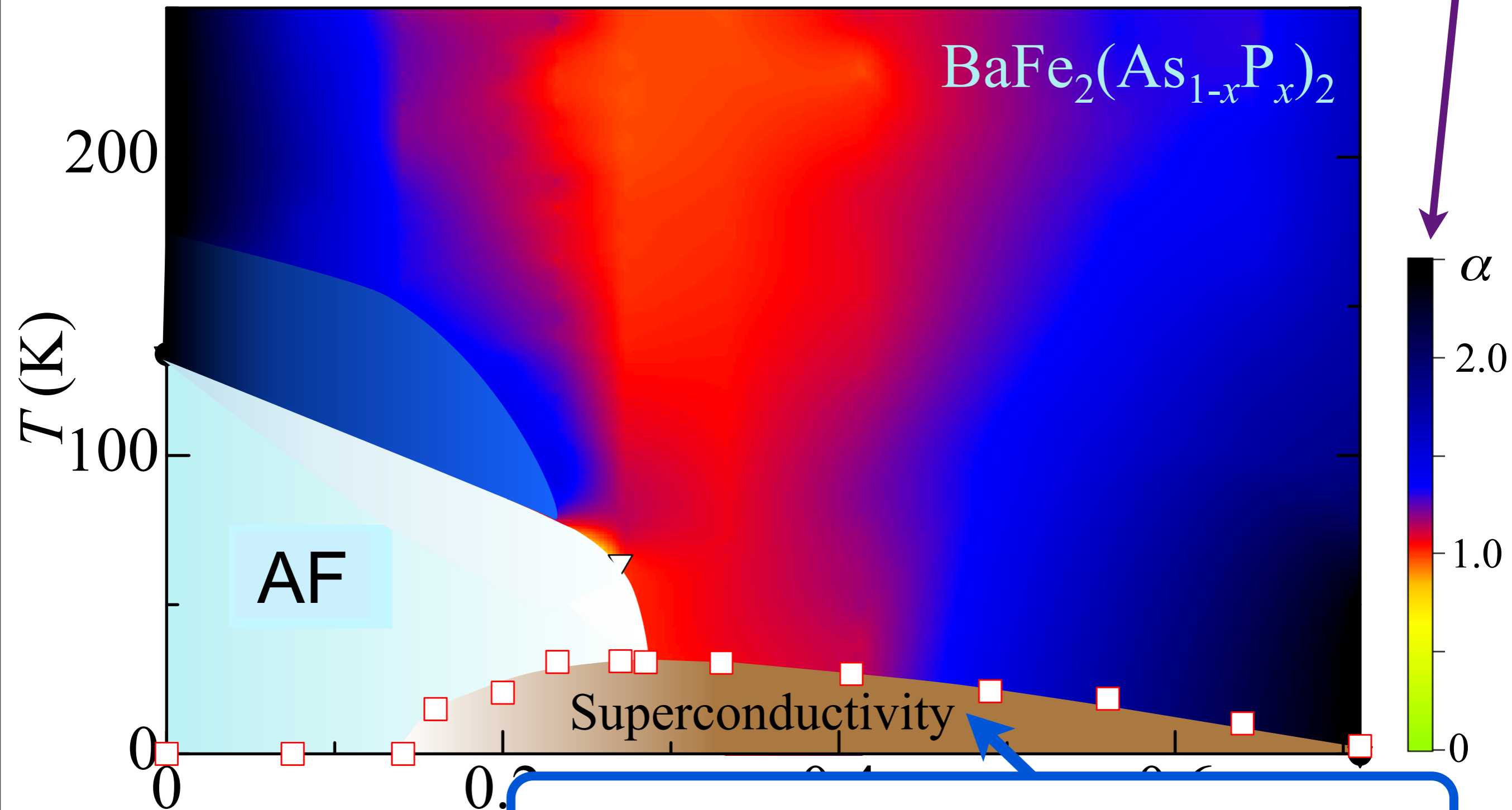


S. Kasahara, T. Shibauchi, K. Hashimoto, K. Ikada, S. Tonegawa, R. Okazaki, H. Shishido,
 H. Ikeda, H. Takeya, K. Hirata, T. Terashima, and Y. Matsuda,
Physical Review B **81**, 184519 (2010)



S. Kasahara, T. Shibauchi, K. Hashimoto, K. Ikada, S. Tonegawa, R. Okazaki, H. Shishido,
 H. Ikeda, H. Takeya, K. Hirata, T. Terashima, and Y. Matsuda,
Physical Review B **81**, 184519 (2010)

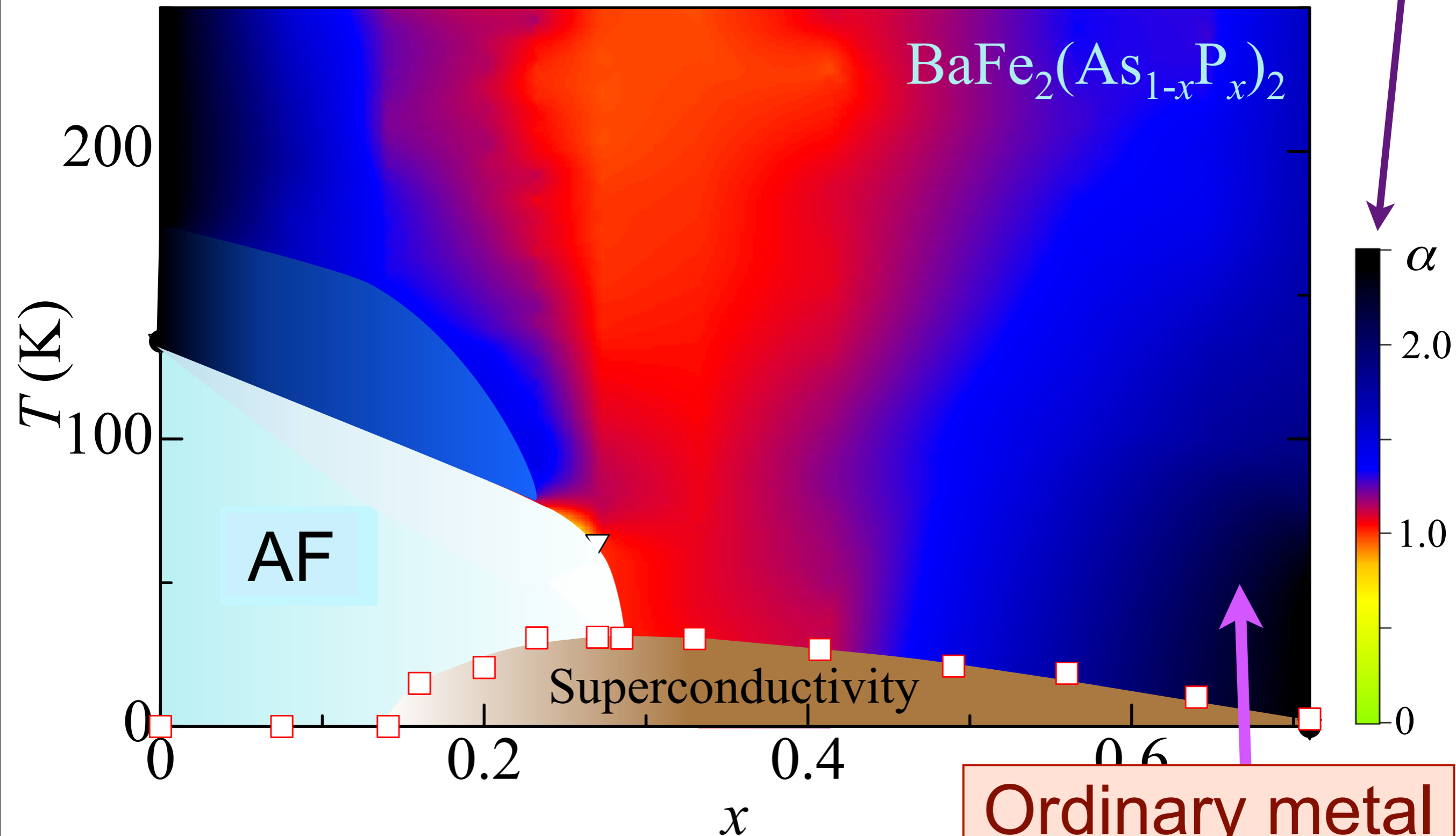
Resistivity
 $\sim \rho_0 + AT^\alpha$



Superconductor
Bose condensate of pairs of electrons

S. Kasahara, T. Shiba
H. Ike

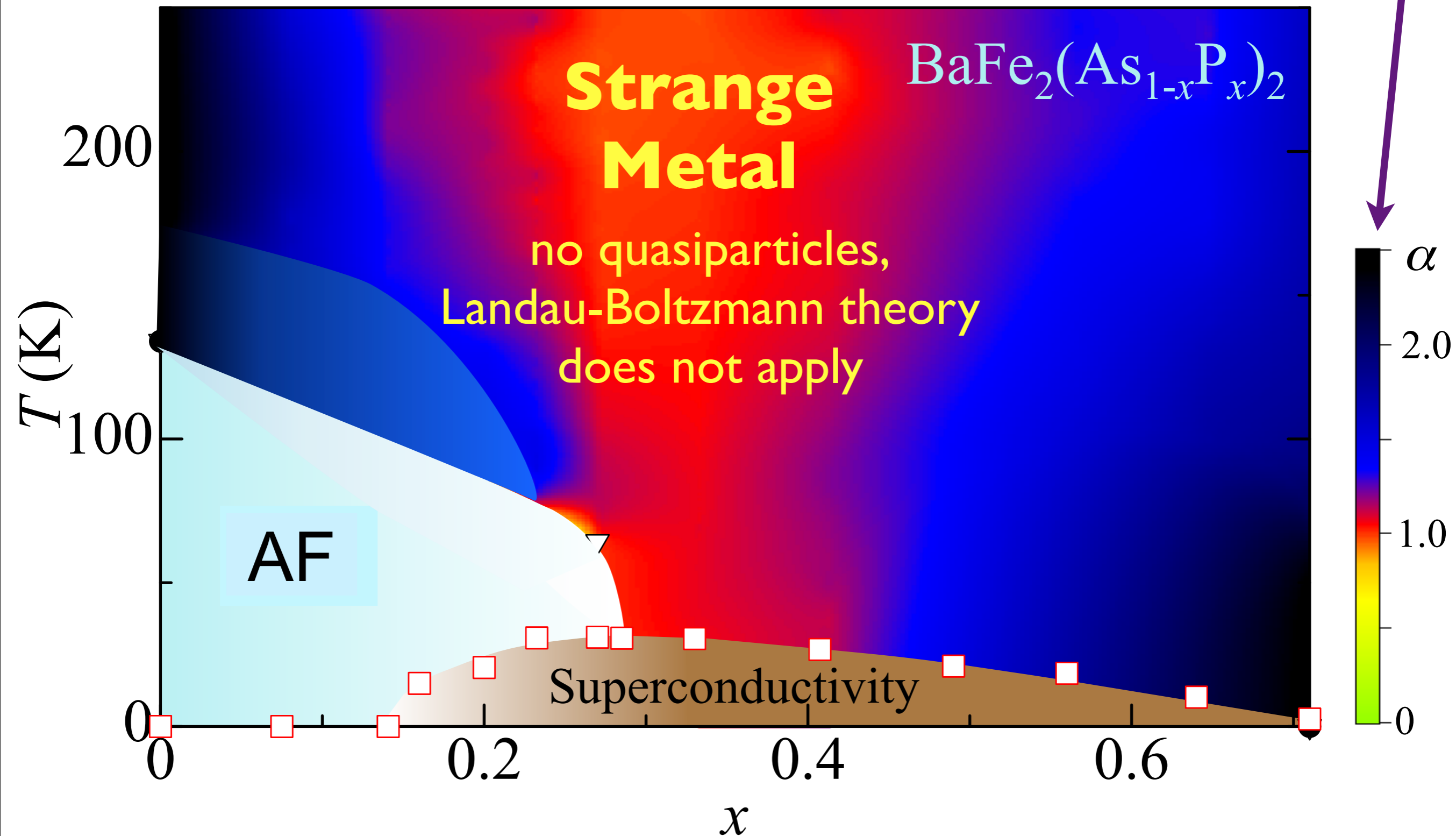
Resistivity
 $\sim \rho_0 + AT^\alpha$



S. Kasahara, T. Shibauchi, K. Hashimoto, K. Ikada, S. Tonegawa, R. O.
H. Ikeda, H. Takeya, K. Hirata, T. Terashima, and Y. Ma
Physical Review B **81**, 184519 (2010)

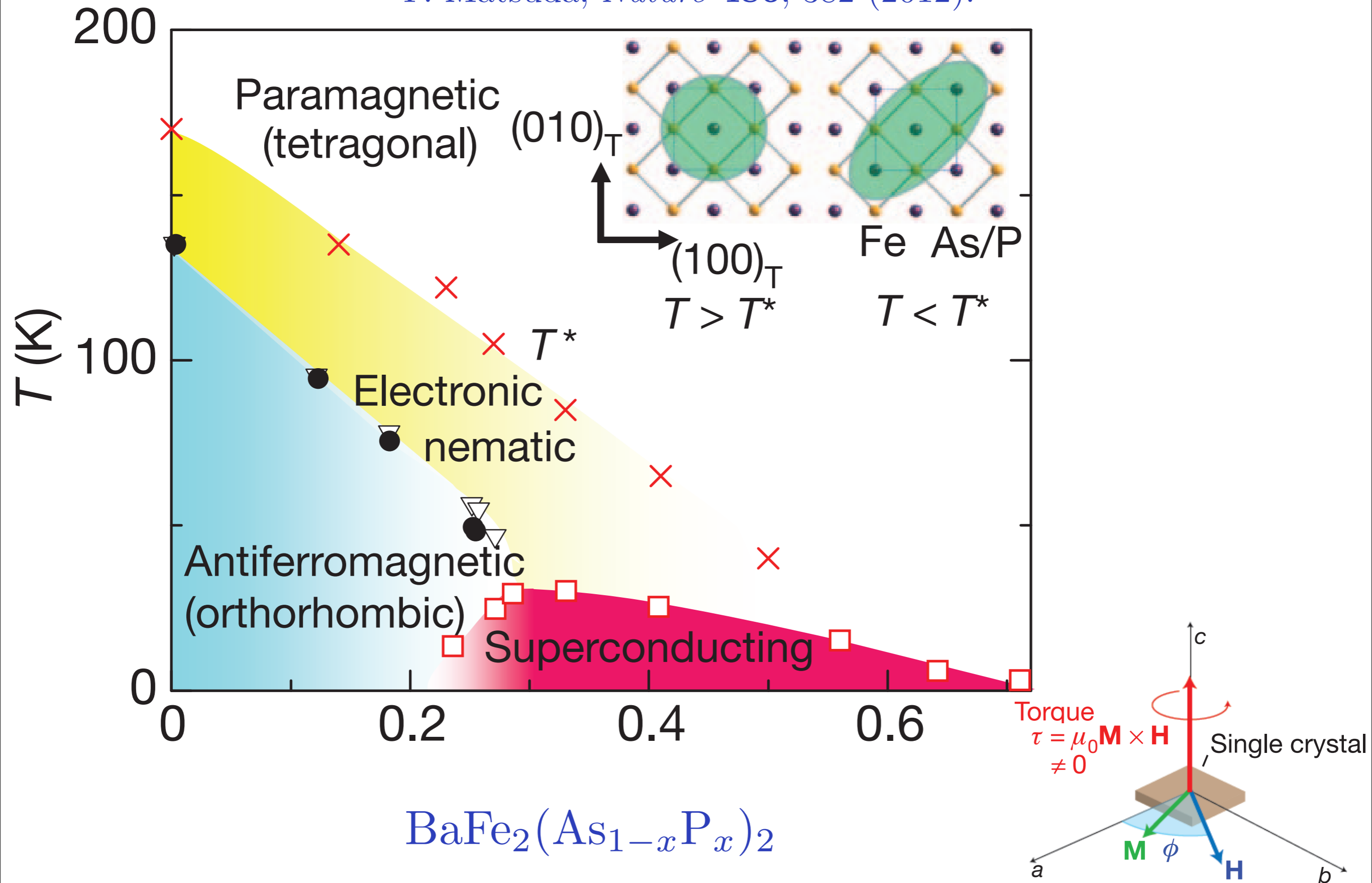
Ordinary metal
(Fermi liquid)

Resistivity
 $\sim \rho_0 + AT^\alpha$

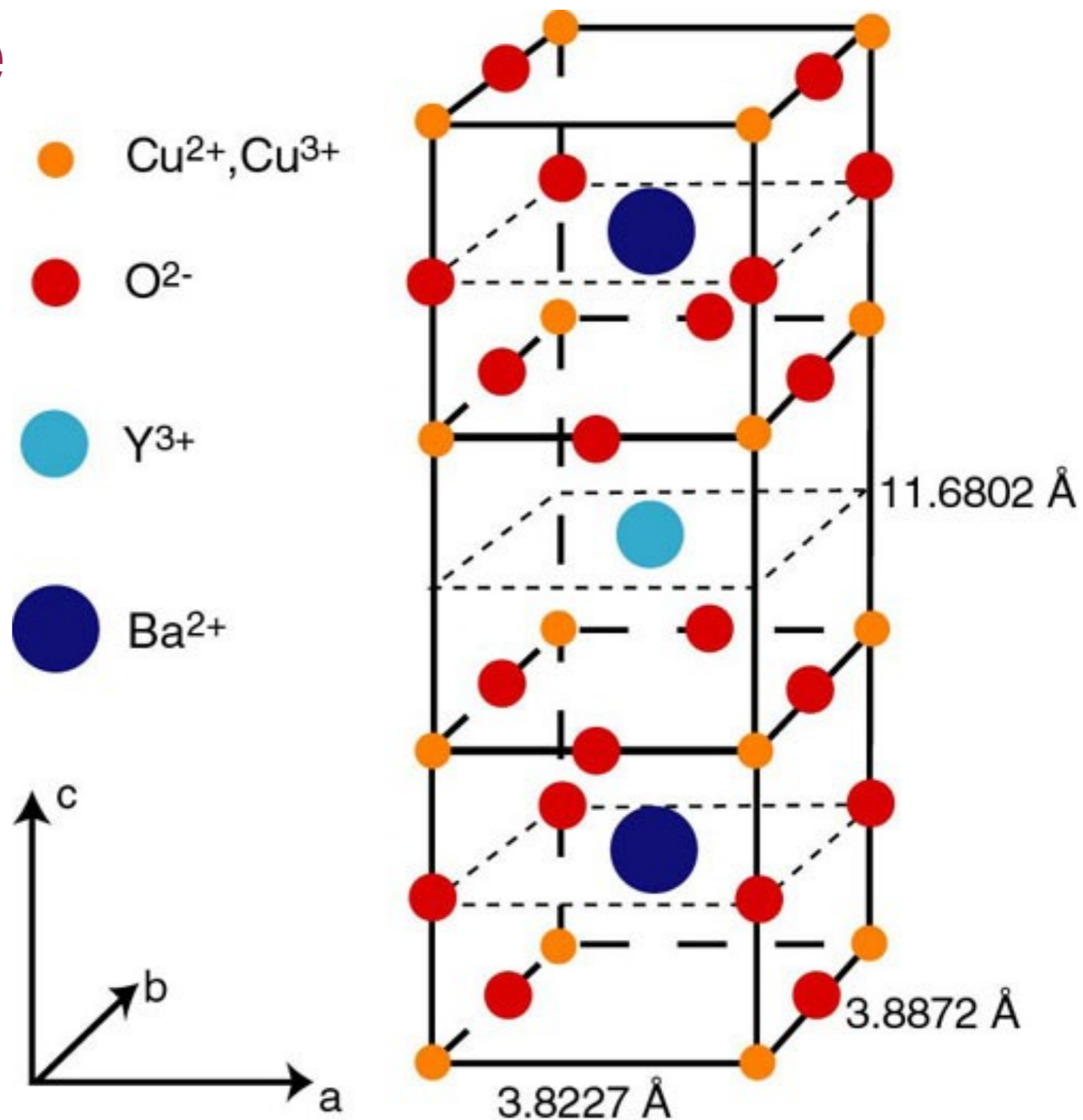


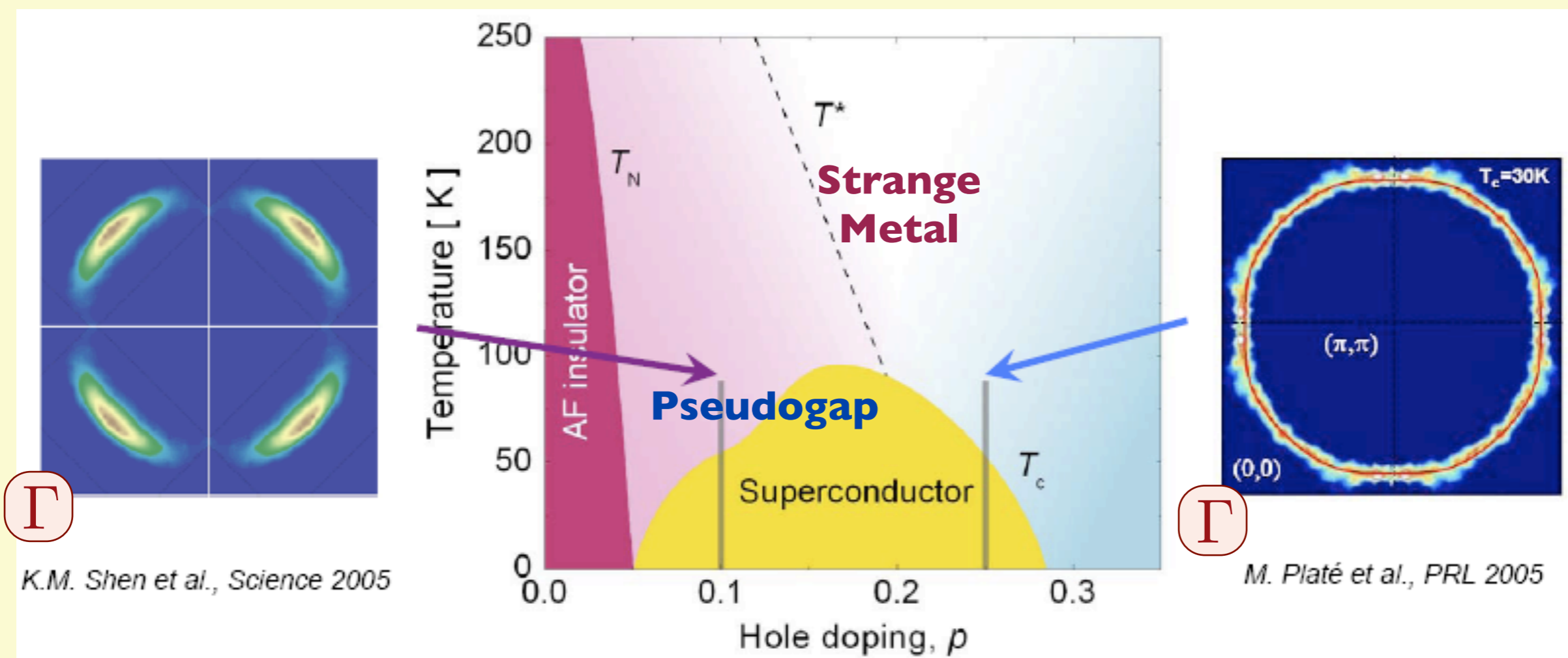
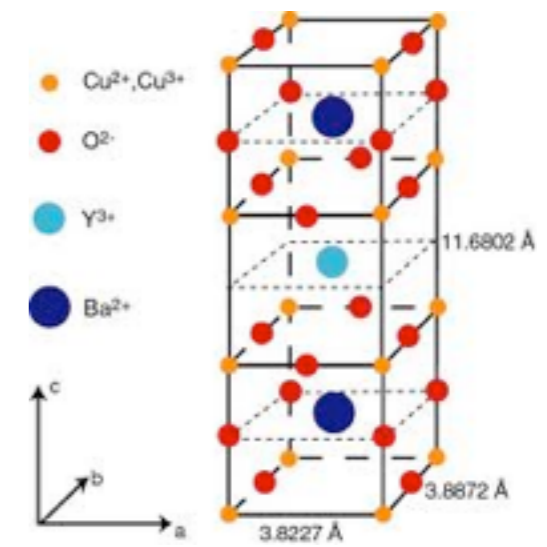
S. Kasahara, T. Shibauchi, K. Hashimoto, K. Ikada, S. Tonegawa, R. Okazaki, H. Shishido,
H. Ikeda, H. Takeya, K. Hirata, T. Terashima, and Y. Matsuda,
Physical Review B **81**, 184519 (2010)

S. Kasahara, H.J. Shi, K. Hashimoto, S. Tonegawa, Y. Mizukami, T. Shibauchi, K. Sugimoto, T. Fukuda, T. Terashima, A.H. Nevidomskyy, and Y. Matsuda, *Nature* **486**, 382 (2012).



High temperature superconductors



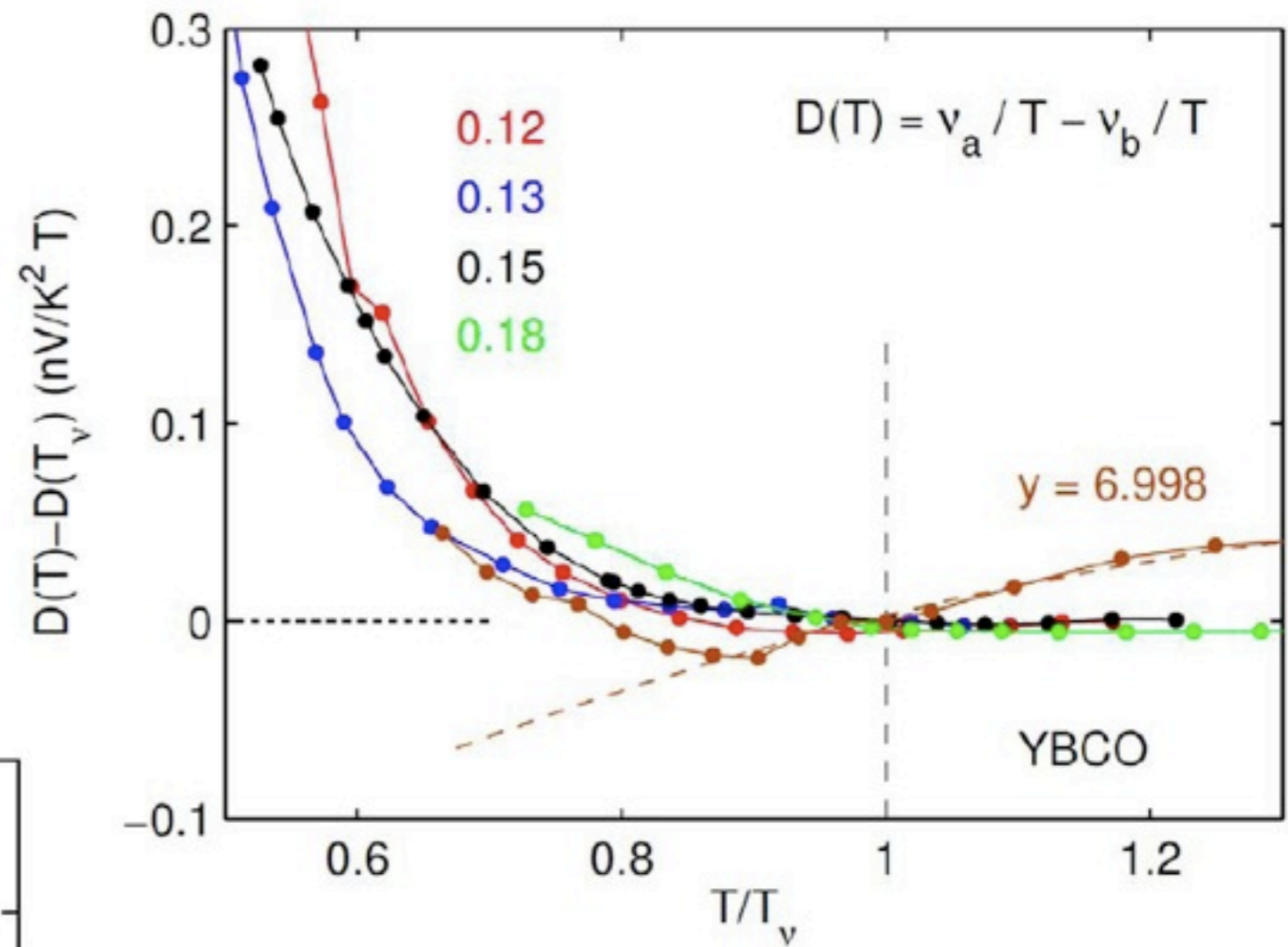
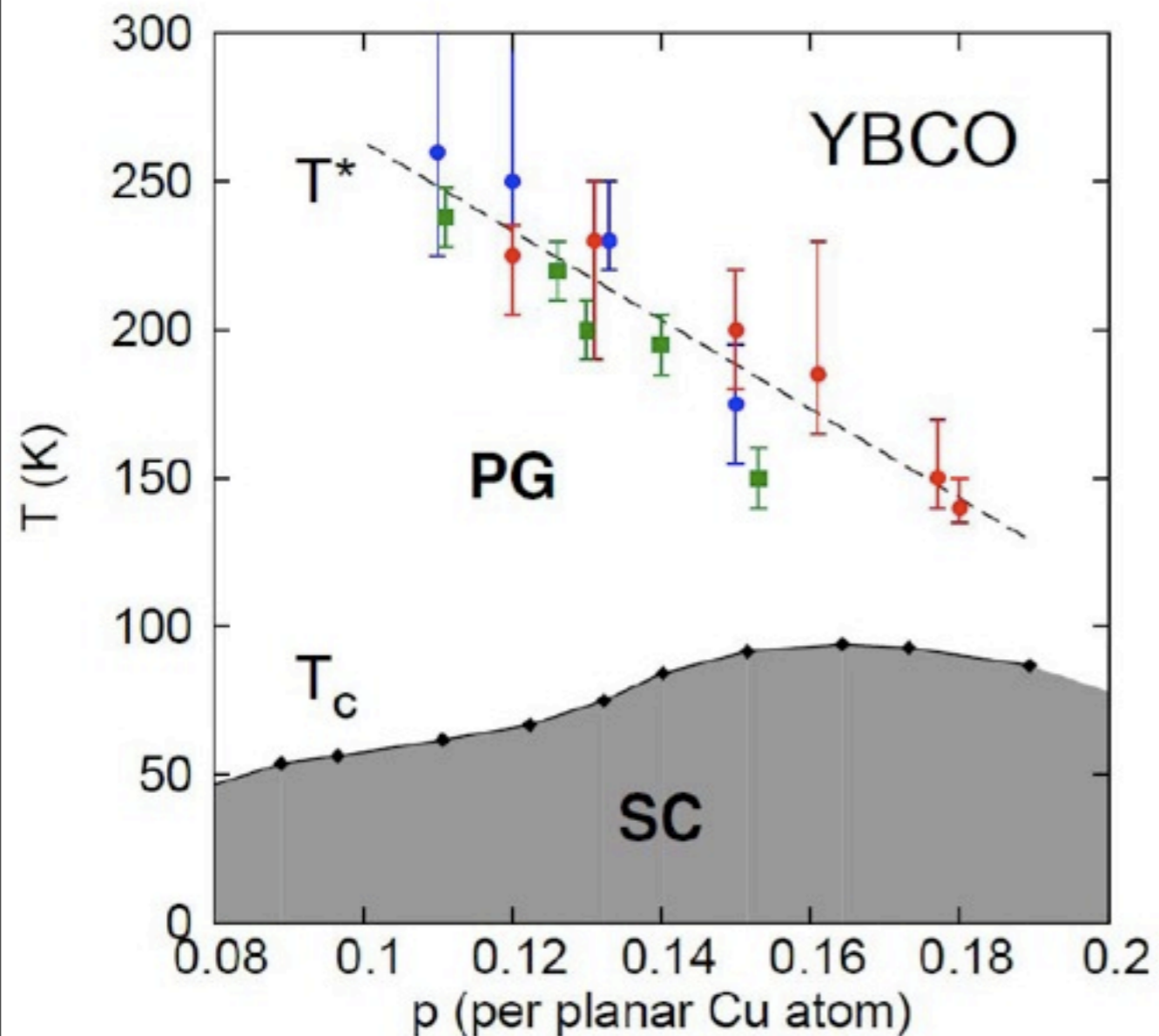


Smaller hole Fermi-pockets

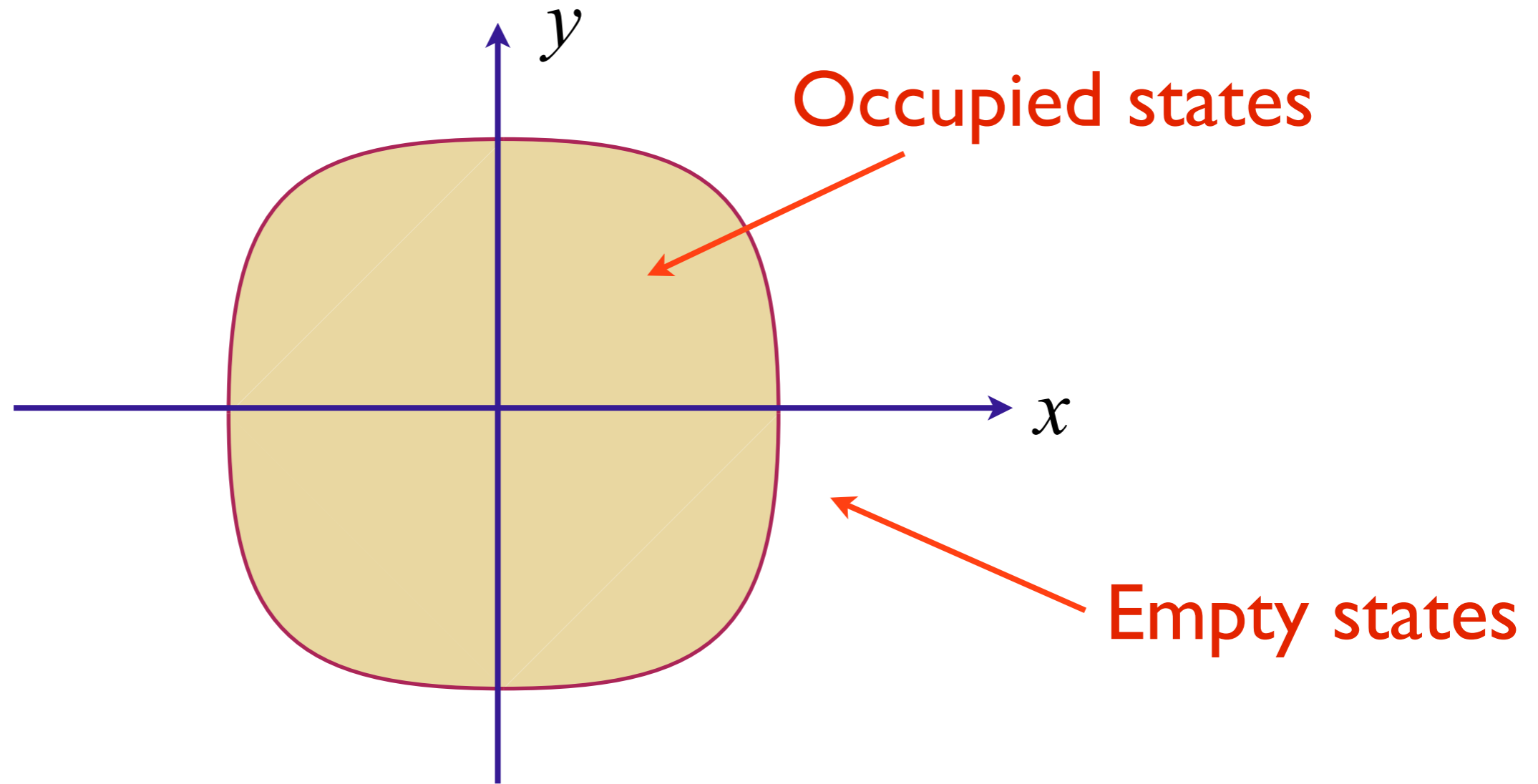
Large hole Fermi surface

Broken rotational symmetry in the pseudogap phase of a high- T_c superconductor

R. Daou, J. Chang, David LeBoeuf, Olivier Cyr-Choiniere, Francis Laliberte, Nicolas Doiron-Leyraud, B. J. Ramshaw, Ruixing Liang, D.A. Bonn, W. N. Hardy, and Louis Taillefer
Nature, **463**, 519 (2010).

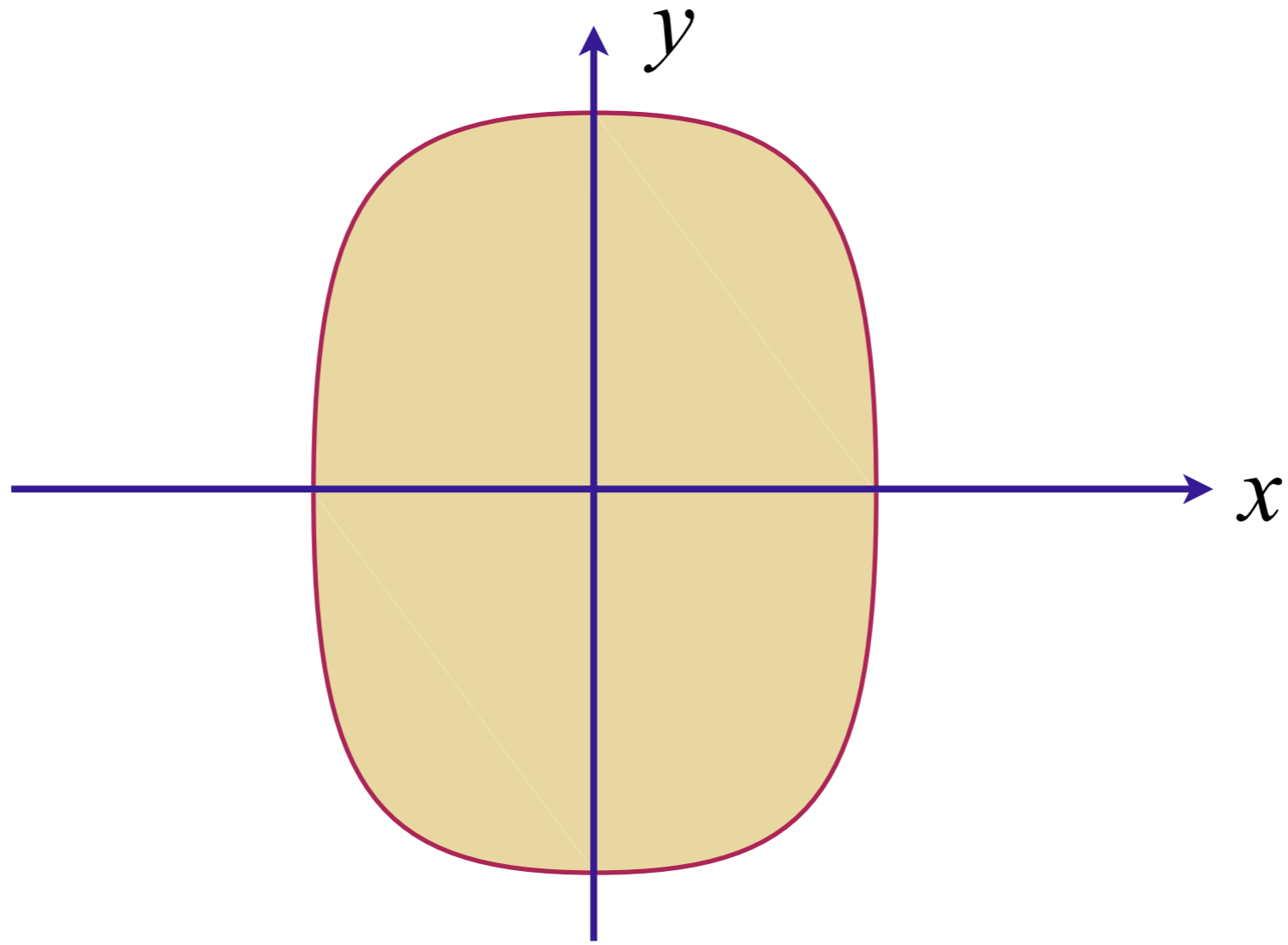


Quantum criticality of Ising-nematic ordering in a metal



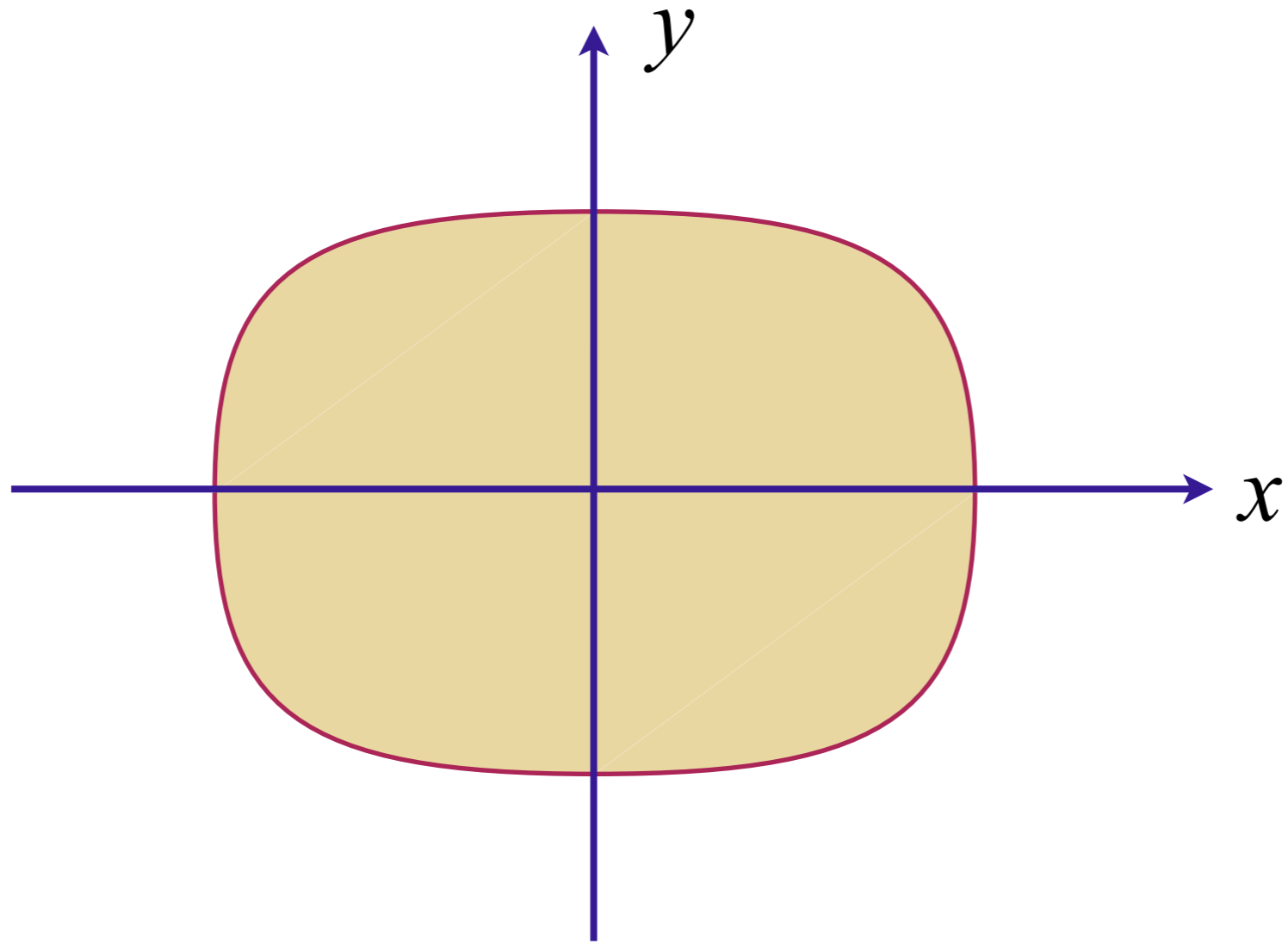
A metal with a Fermi surface
with full square lattice symmetry

Quantum criticality of Ising-nematic ordering in a metal



Spontaneous elongation along y direction:

Quantum criticality of Ising-nematic ordering in a metal



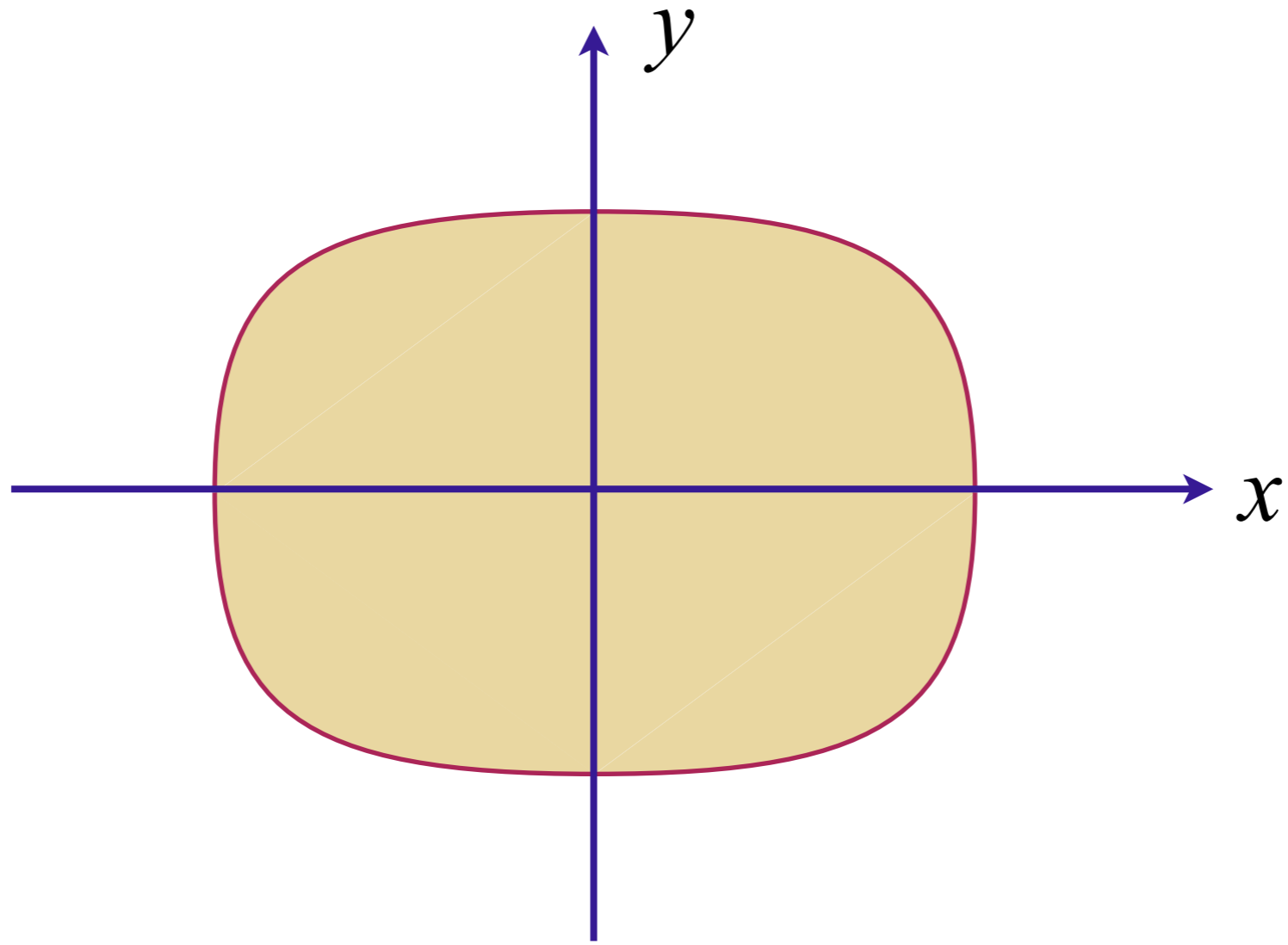
Spontaneous elongation along x direction:

Ising-nematic order parameter

$$\phi \sim \int d^2k (\cos k_x - \cos k_y) c_{\mathbf{k}\sigma}^\dagger c_{\mathbf{k}\sigma}$$

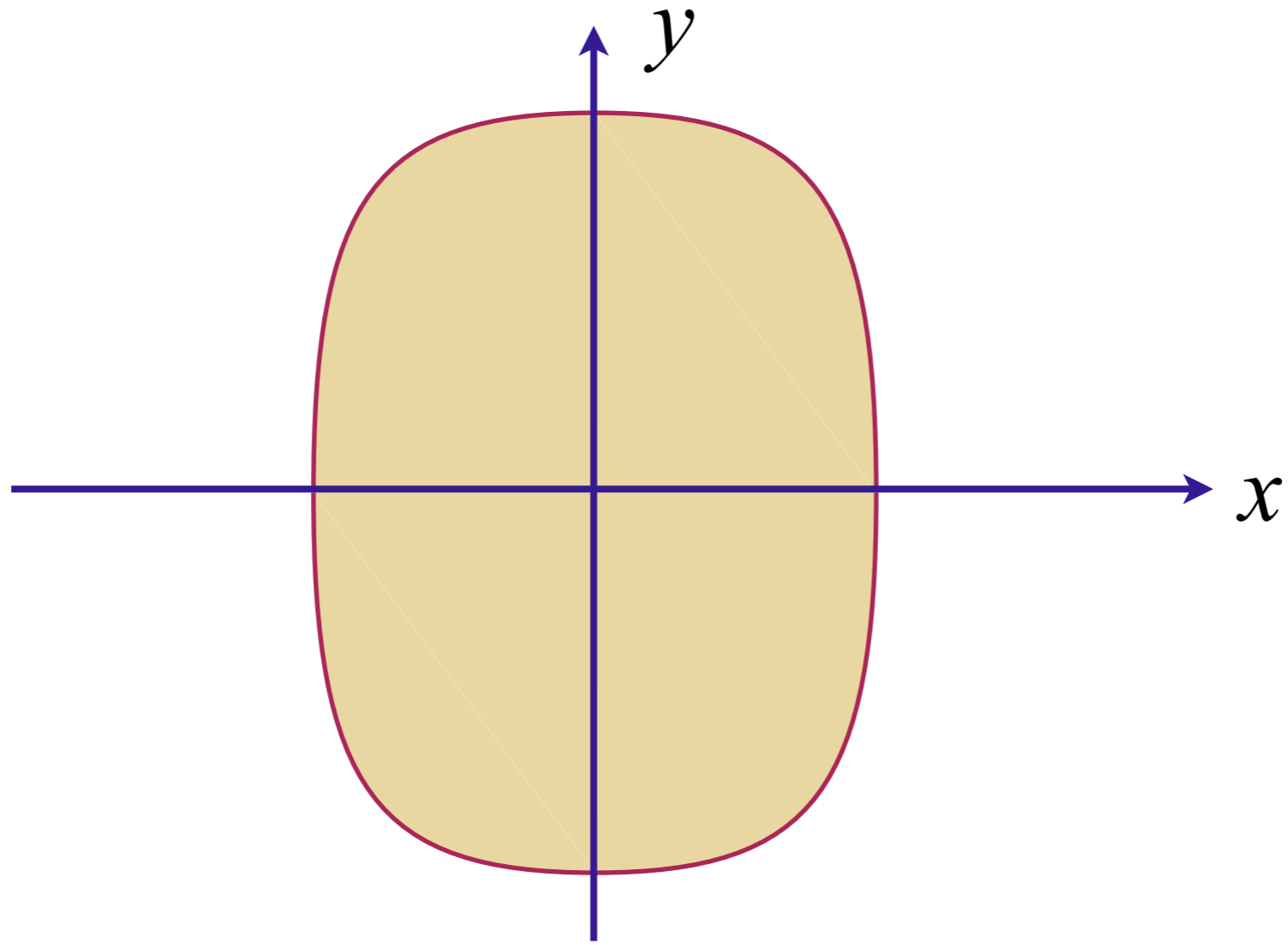
Measures spontaneous breaking of square lattice point-group symmetry of underlying Hamiltonian

Quantum criticality of Ising-nematic ordering in a metal



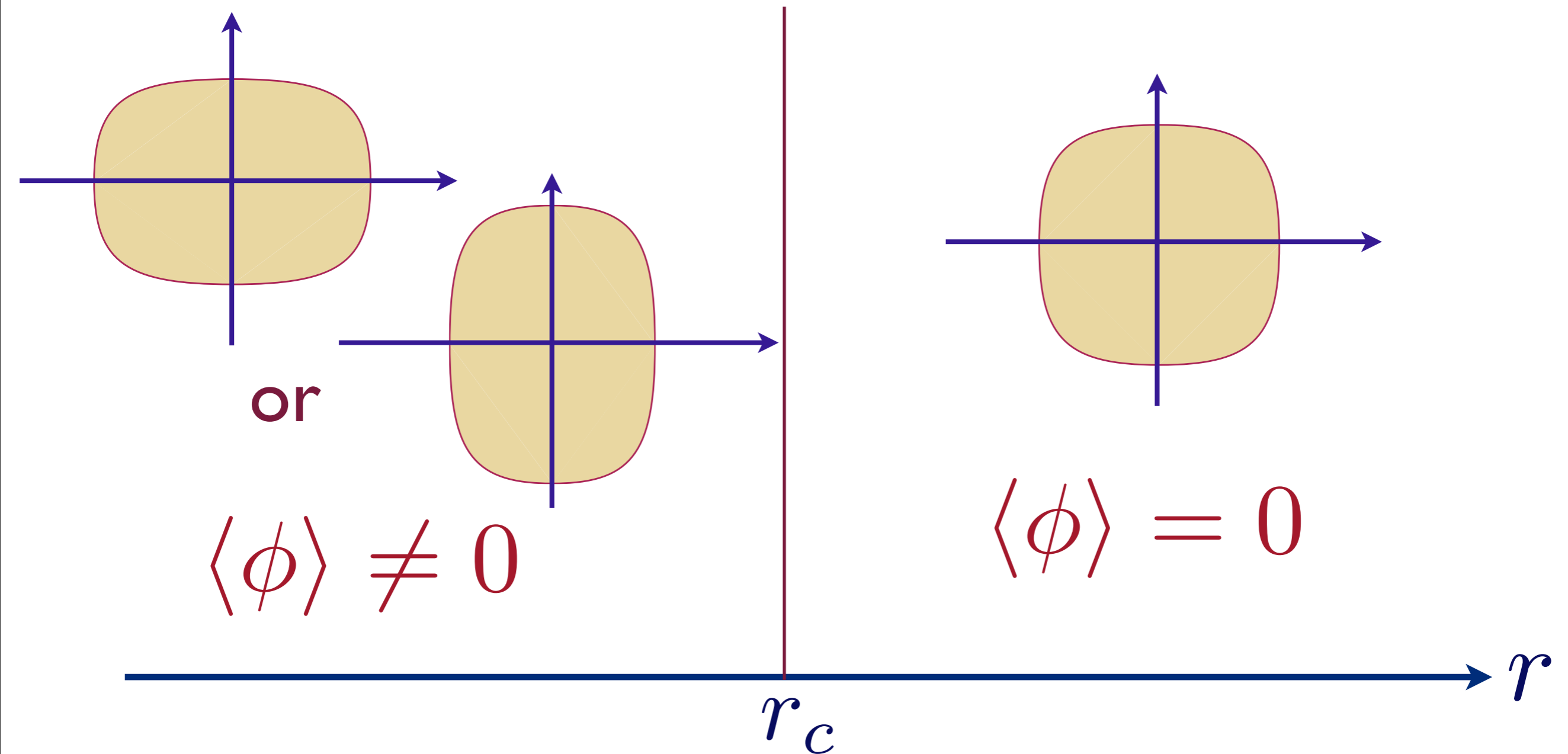
Spontaneous elongation along x direction:
Ising order parameter $\phi > 0$.

Quantum criticality of Ising-nematic ordering in a metal



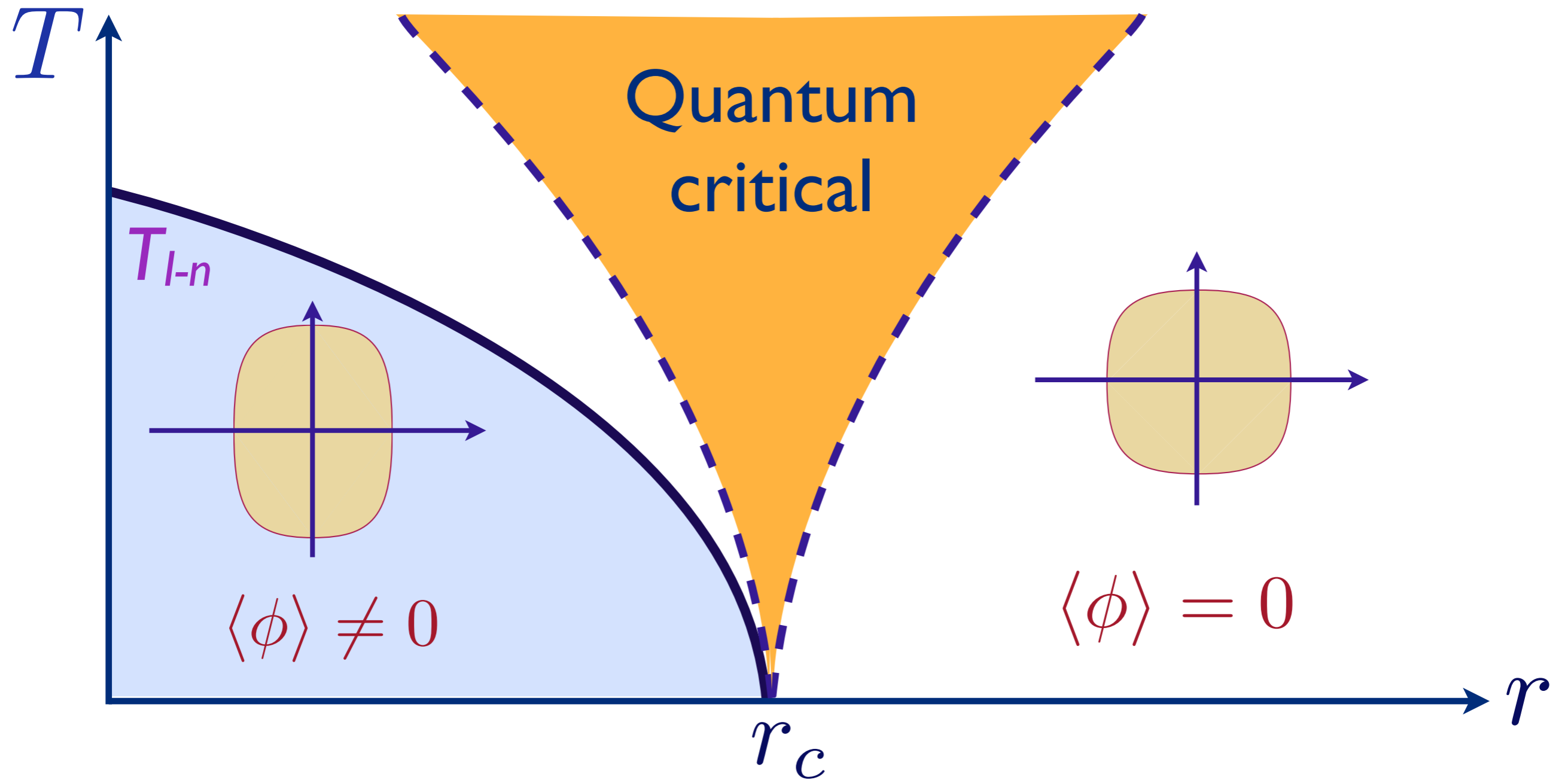
Spontaneous elongation along y direction:
Ising order parameter $\phi < 0$.

Quantum criticality of Ising-nematic ordering in a metal



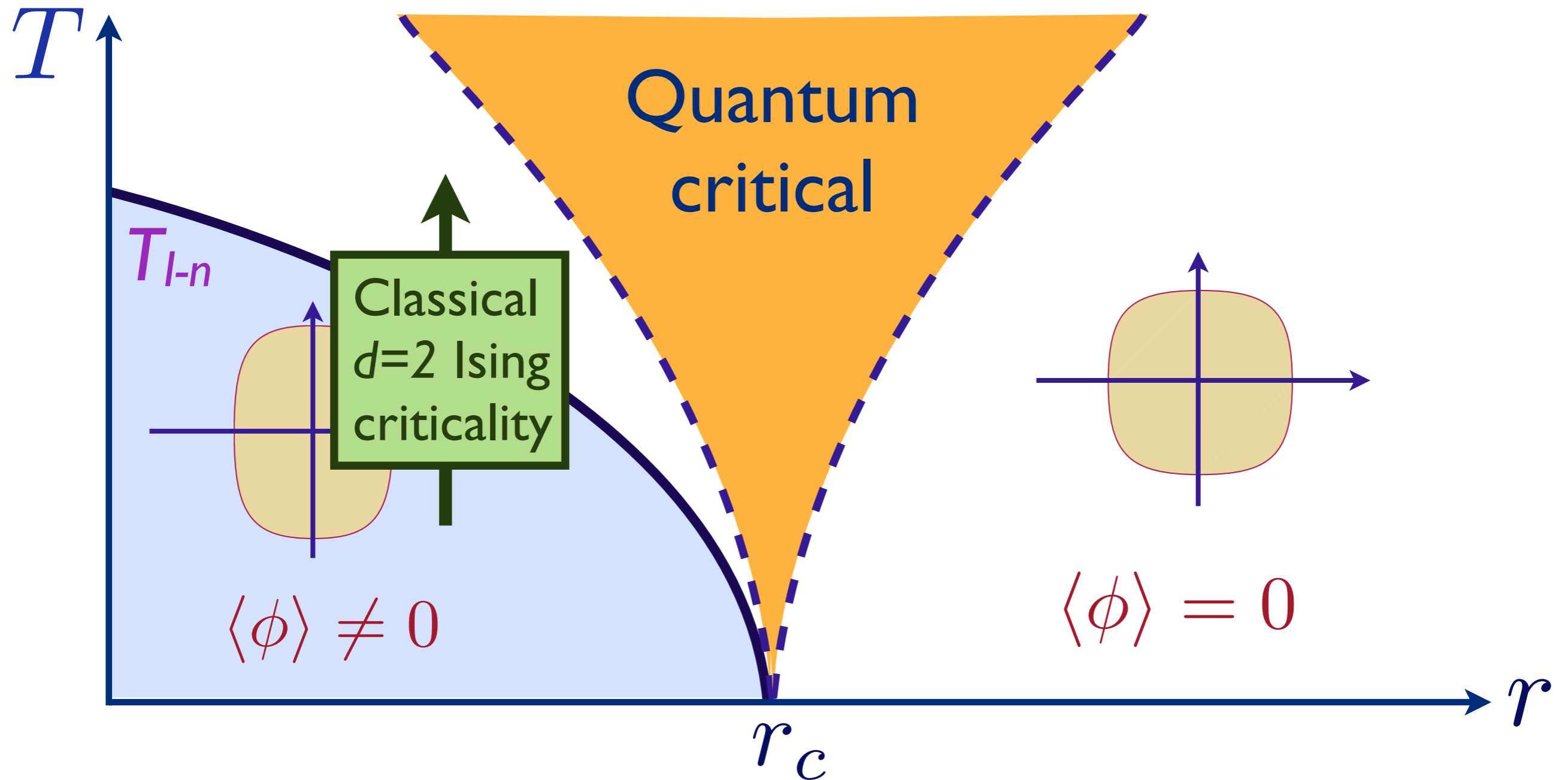
Pomeranchuk instability as a function of coupling r

Quantum criticality of Ising-nematic ordering



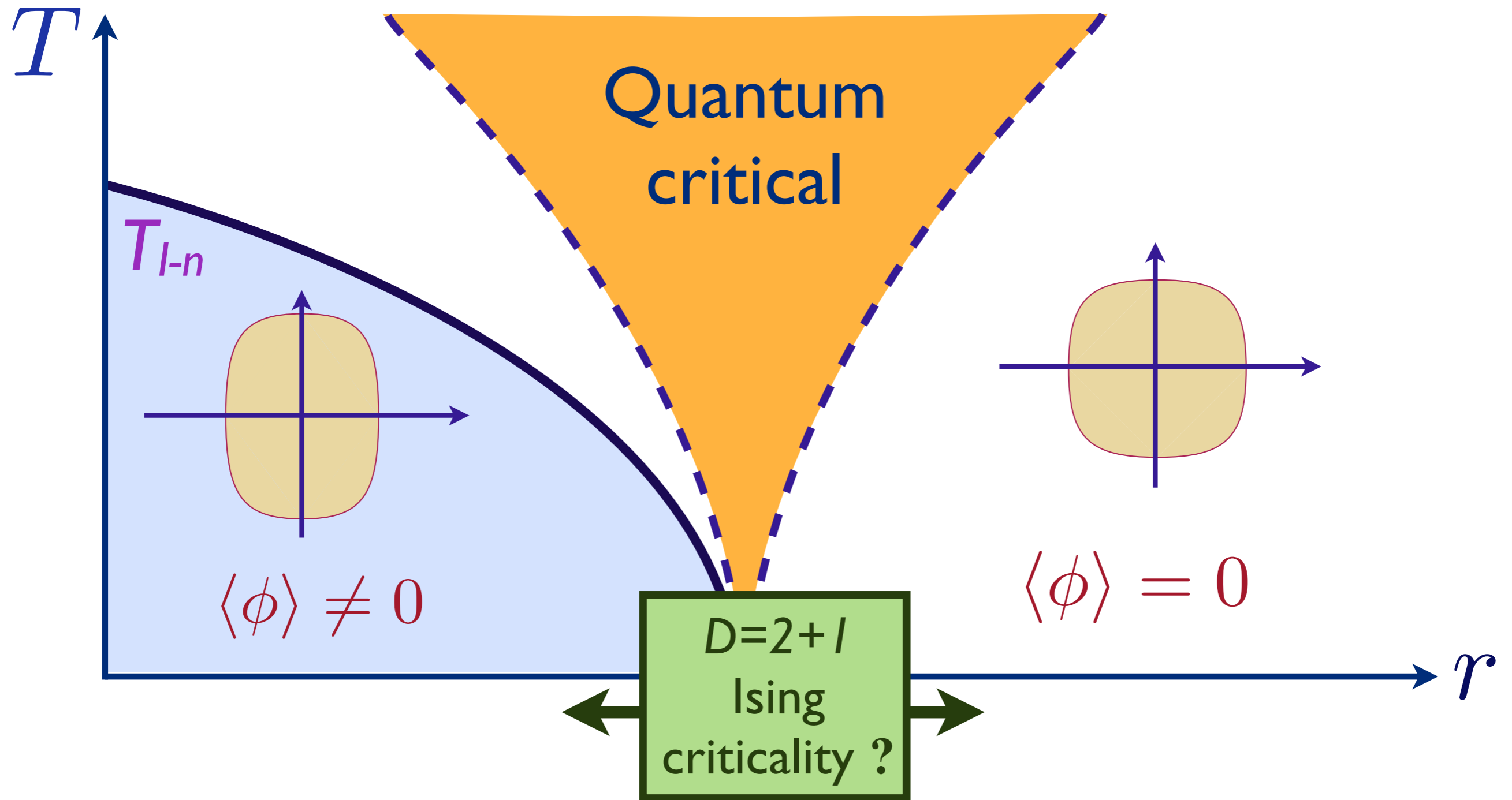
Phase diagram as a function of T and r

Quantum criticality of Ising-nematic ordering in a metal



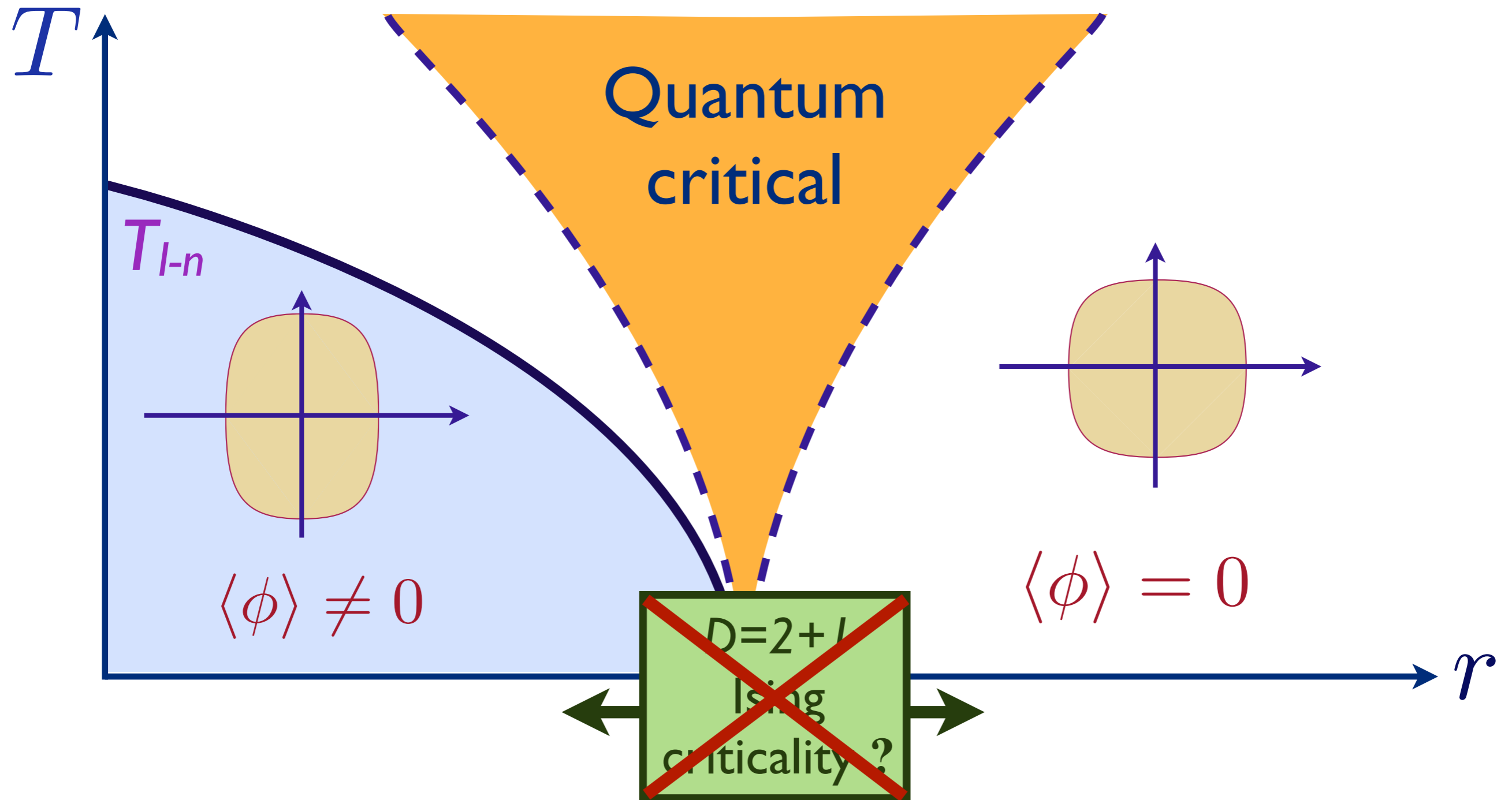
Phase diagram as a function of T and r

Quantum criticality of Ising-nematic ordering in a metal



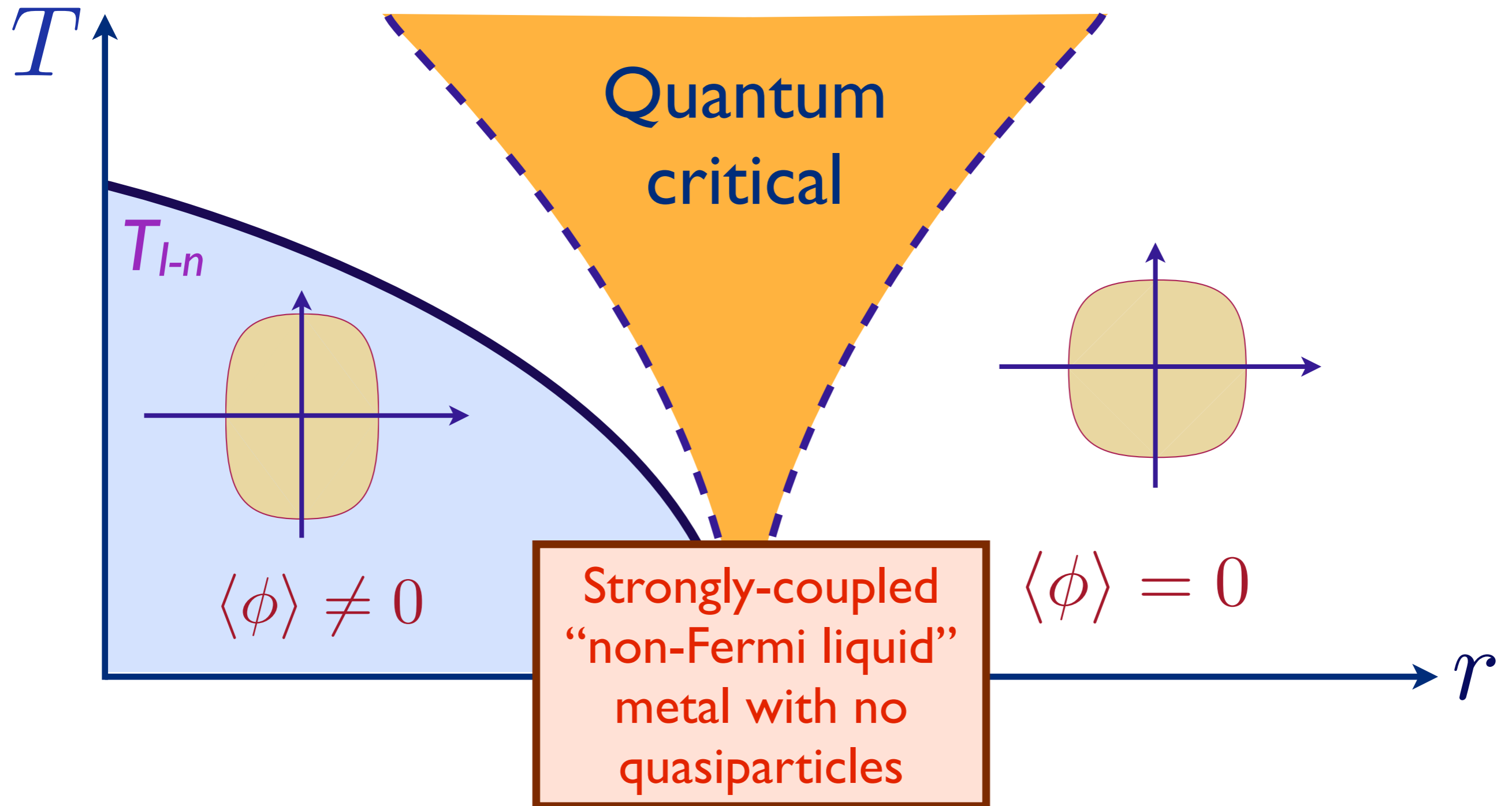
Phase diagram as a function of T and r

Quantum criticality of Ising-nematic ordering in a metal



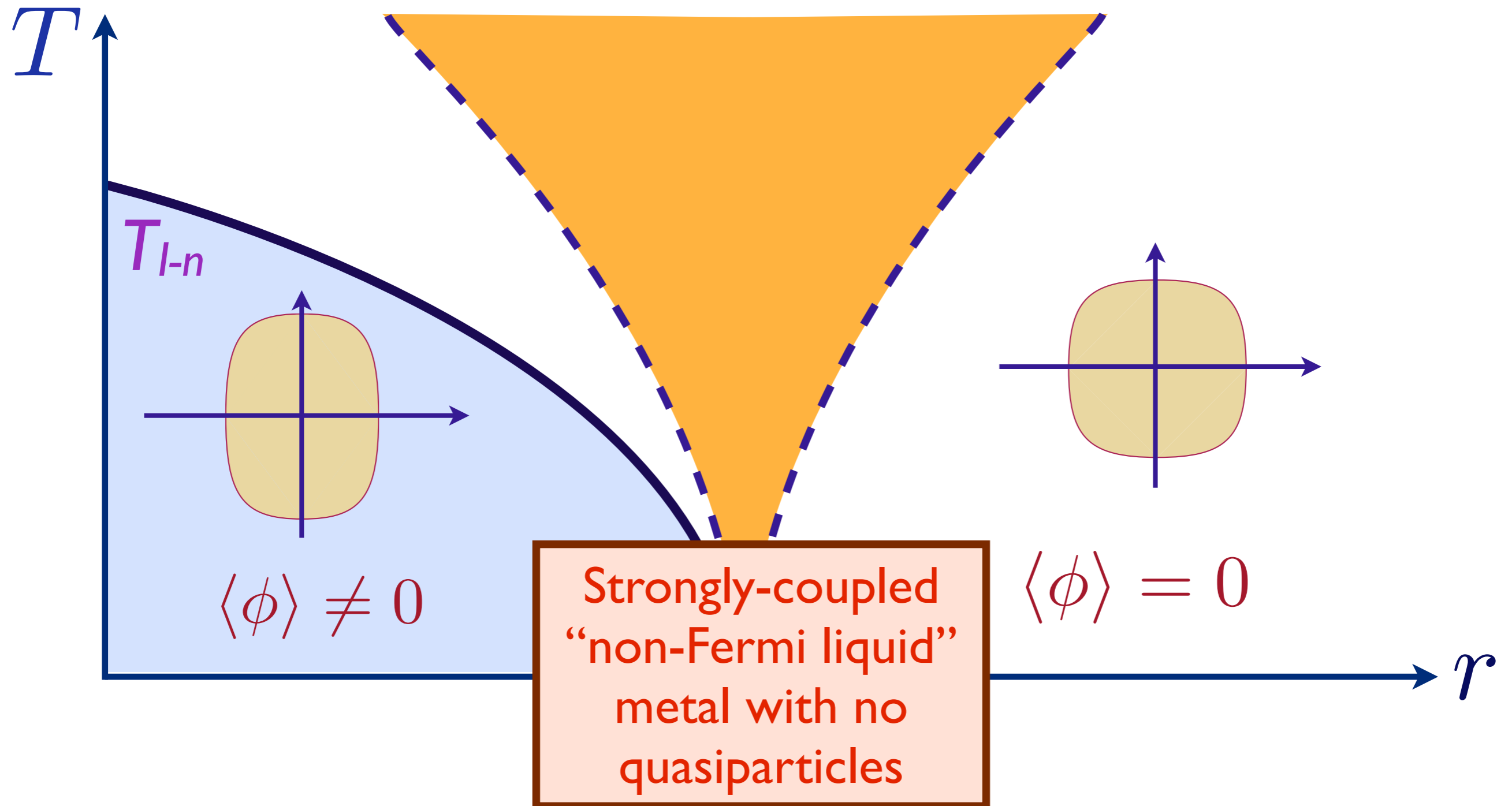
Phase diagram as a function of T and r

Quantum criticality of Ising-nematic ordering in a metal



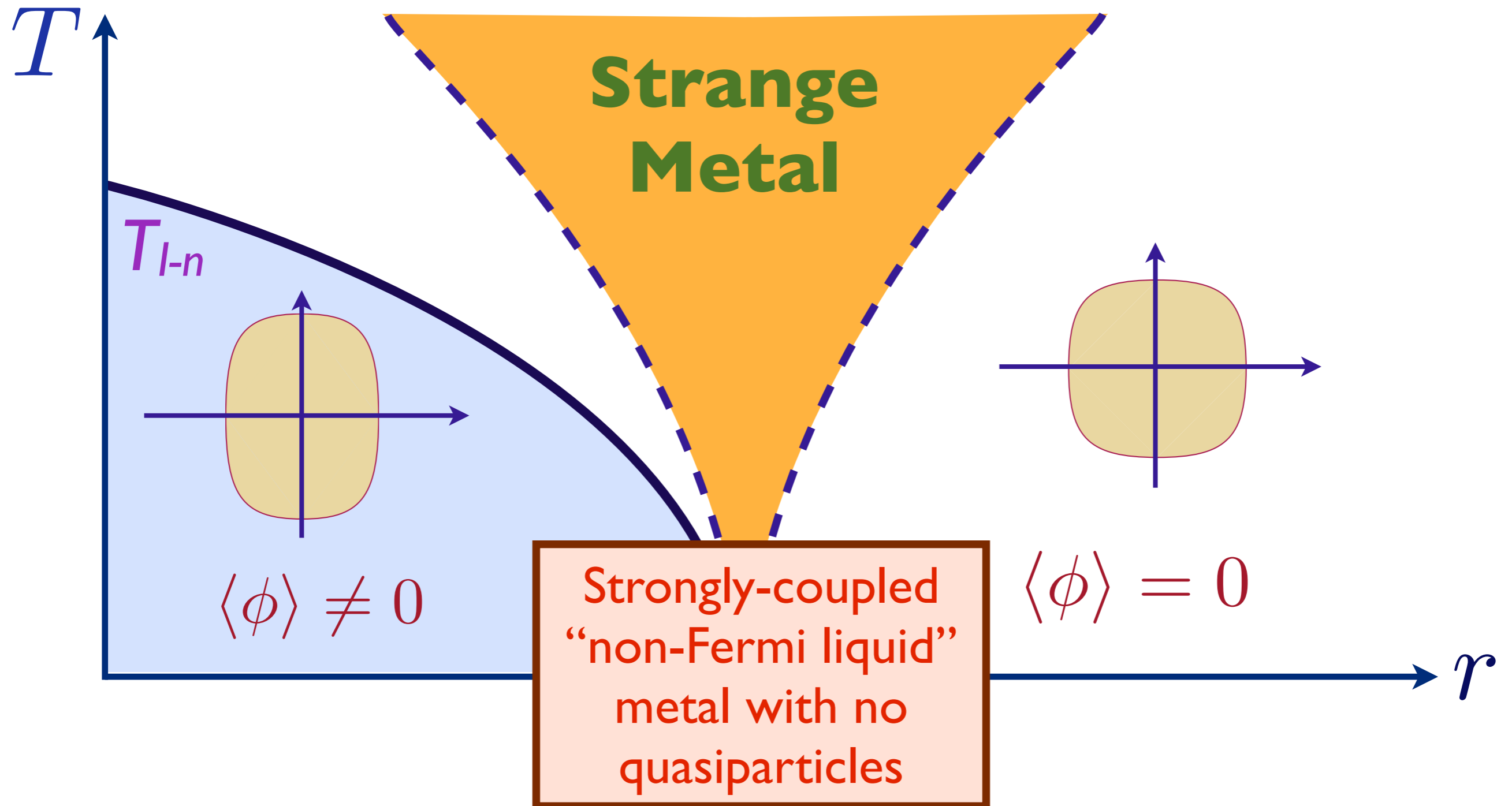
Phase diagram as a function of T and r

Quantum criticality of Ising-nematic ordering in a metal



Phase diagram as a function of T and r

Quantum criticality of Ising-nematic ordering in a metal



Phase diagram as a function of T and r

Quantum criticality of Ising-nematic ordering

Effective action for Ising order parameter

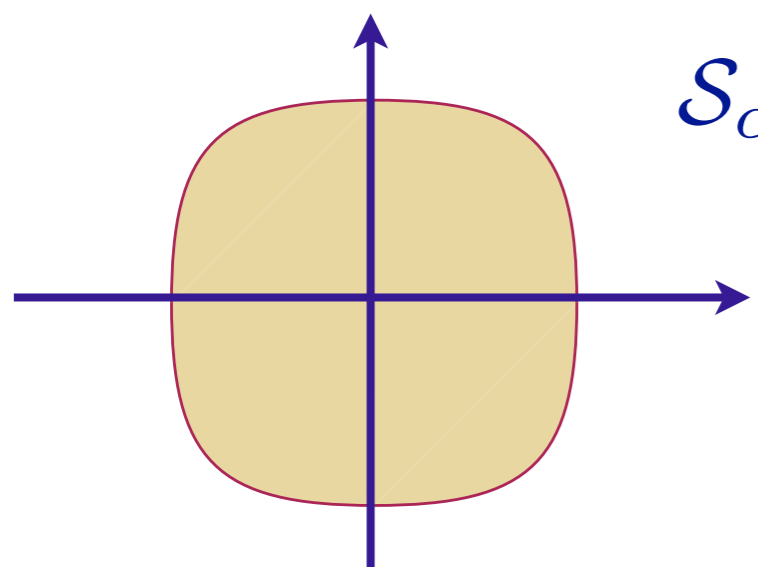
$$\mathcal{S}_\phi = \int d^2r d\tau [(\partial_\tau \phi)^2 + c^2 (\nabla \phi)^2 + (\lambda - \lambda_c) \phi^2 + u \phi^4]$$

Quantum criticality of Ising-nematic ordering

Effective action for Ising order parameter

$$\mathcal{S}_\phi = \int d^2r d\tau [(\partial_\tau \phi)^2 + c^2 (\nabla \phi)^2 + (\lambda - \lambda_c) \phi^2 + u \phi^4]$$

Effective action for electrons:

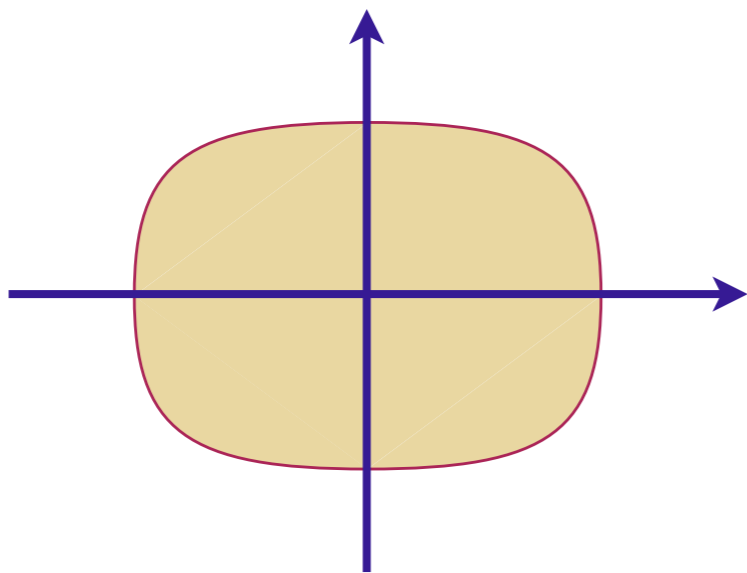

$$\begin{aligned} \mathcal{S}_c &= \int d\tau \sum_{\alpha=1}^{N_f} \left[\sum_i c_{i\alpha}^\dagger \partial_\tau c_{i\alpha} - \sum_{i<j} t_{ij} c_{i\alpha}^\dagger c_{j\alpha} \right] \\ &\equiv \sum_{\alpha=1}^{N_f} \sum_{\mathbf{k}} \int d\tau c_{\mathbf{k}\alpha}^\dagger (\partial_\tau + \varepsilon_{\mathbf{k}}) c_{\mathbf{k}\alpha} \end{aligned}$$

Quantum criticality of Ising-nematic ordering

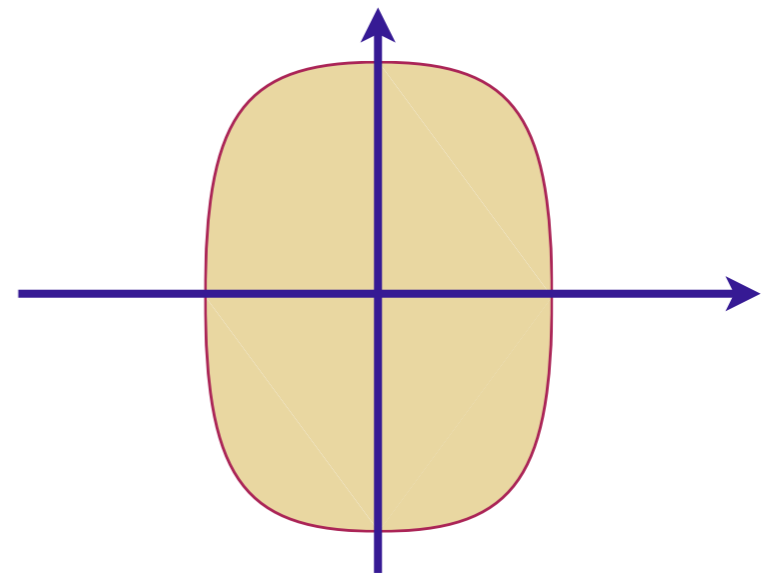
Coupling between Ising order and electrons

$$\mathcal{S}_{\phi c} = -g \int d\tau \sum_{\alpha=1}^{N_f} \sum_{\mathbf{k}, \mathbf{q}} \phi_{\mathbf{q}} (\cos k_x - \cos k_y) c_{\mathbf{k}+\mathbf{q}/2, \alpha}^\dagger c_{\mathbf{k}-\mathbf{q}/2, \alpha}$$

for spatially dependent ϕ



$$\langle \phi \rangle > 0$$



$$\langle \phi \rangle < 0$$

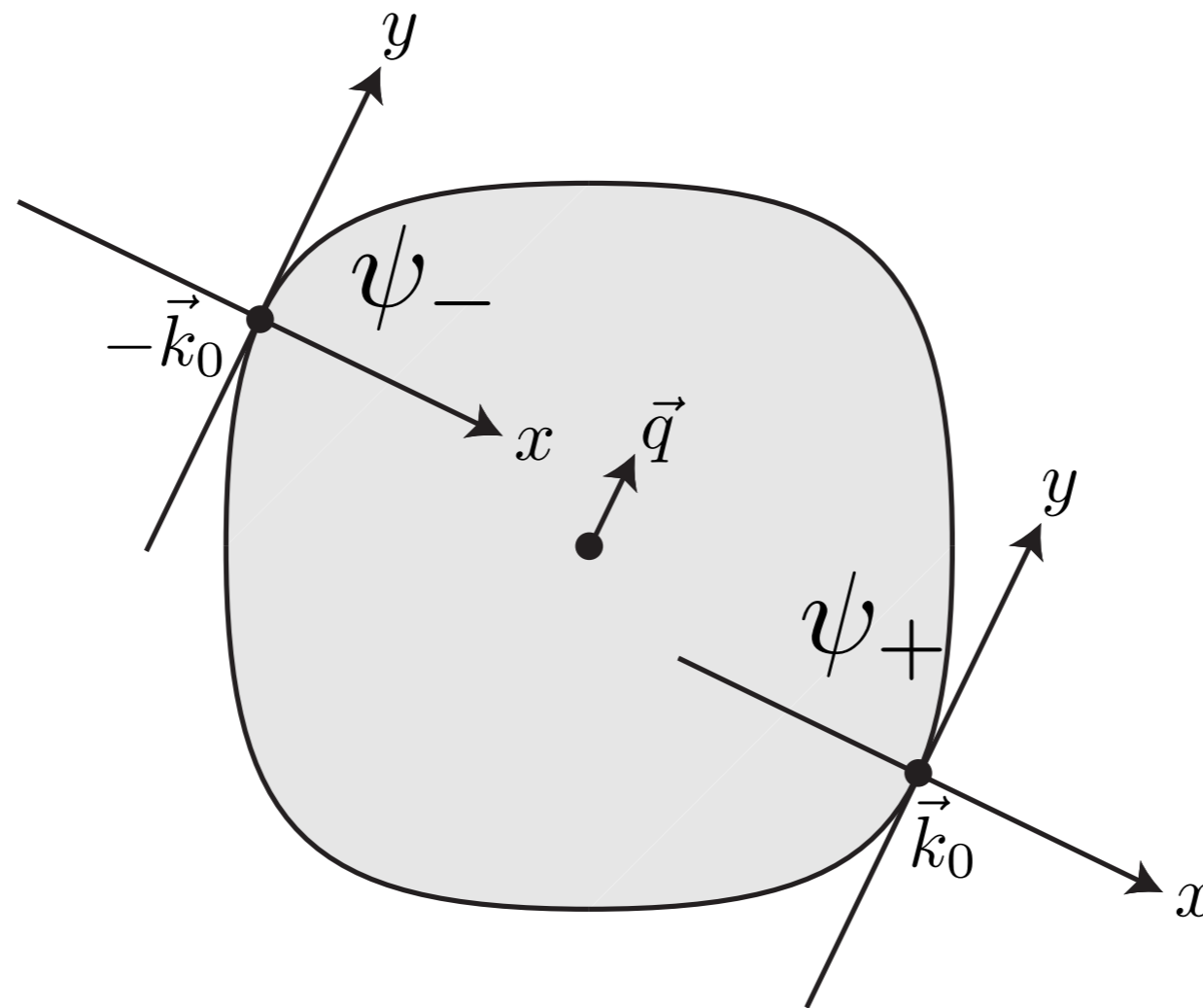
Quantum criticality of Ising-nematic ordering

$$\mathcal{S}_\phi = \int d^2r d\tau [(\partial_\tau \phi)^2 + c^2 (\nabla \phi)^2 + (\lambda - \lambda_c) \phi^2 + u \phi^4]$$

$$\mathcal{S}_c = \sum_{\alpha=1}^{N_f} \sum_{\mathbf{k}} \int d\tau c_{\mathbf{k}\alpha}^\dagger (\partial_\tau + \varepsilon_{\mathbf{k}}) c_{\mathbf{k}\alpha}$$

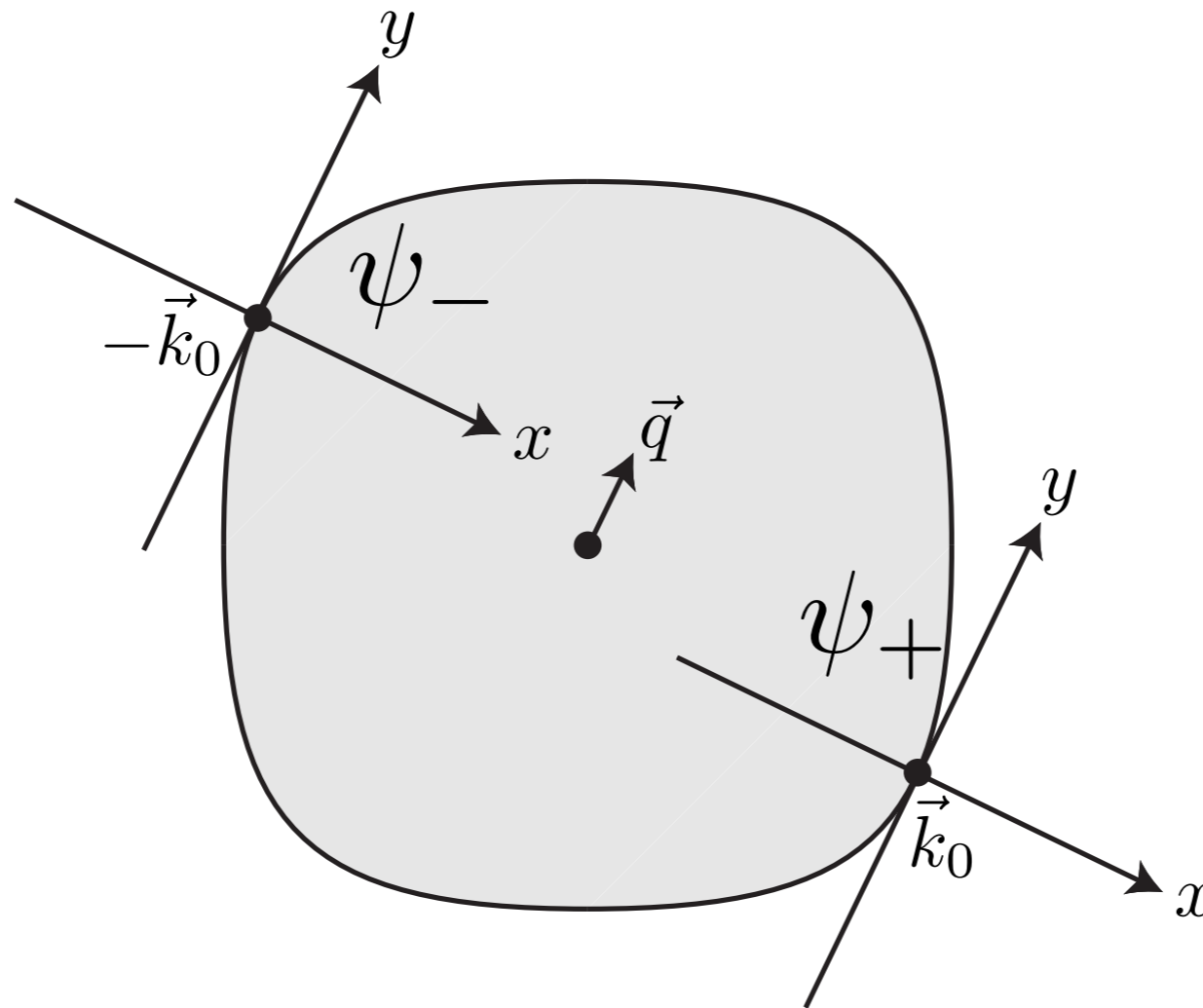
$$\mathcal{S}_{\phi c} = -g \int d\tau \sum_{\alpha=1}^{N_f} \sum_{\mathbf{k}, \mathbf{q}} \phi_{\mathbf{q}} (\cos k_x - \cos k_y) c_{\mathbf{k}+\mathbf{q}/2, \alpha}^\dagger c_{\mathbf{k}-\mathbf{q}/2, \alpha}$$

Quantum criticality of Ising-nematic ordering



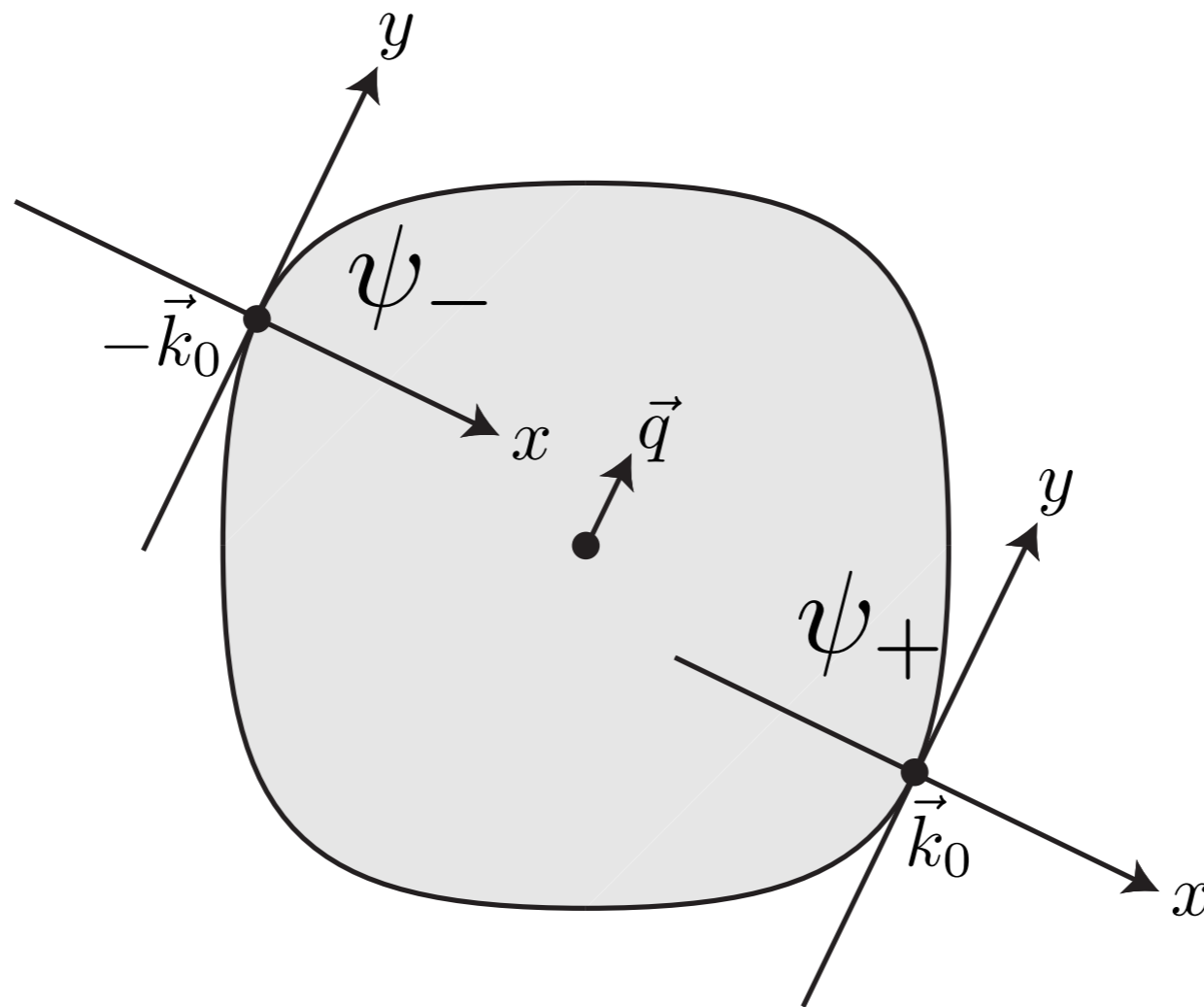
- ϕ fluctuation at wavevector \vec{q} couples most efficiently to fermions near $\pm\vec{k}_0$.

Quantum criticality of Ising-nematic ordering



- ϕ fluctuation at wavevector \vec{q} couples most efficiently to fermions near $\pm\vec{k}_0$.
- Expand fermion kinetic energy at wavevectors about $\pm\vec{k}_0$ and boson (ϕ) kinetic energy about $\vec{q} = 0$.

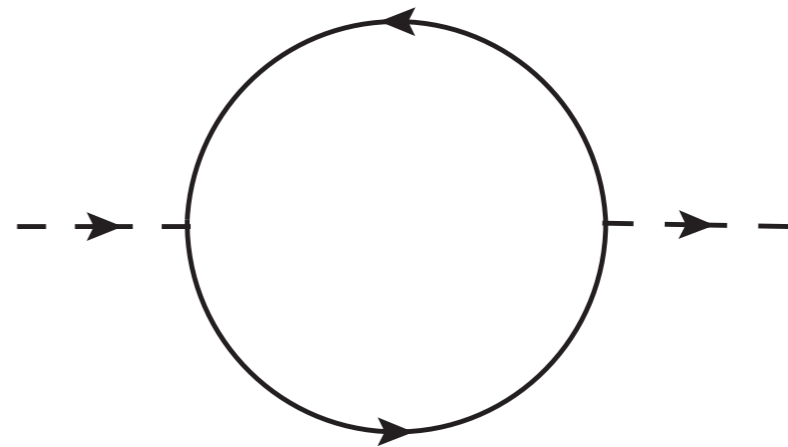
Quantum criticality of Ising-nematic ordering



$$\mathcal{L}[\psi_{\pm}, \phi] = \psi_+^\dagger (\partial_\tau - i\partial_x - \partial_y^2) \psi_+ + \psi_-^\dagger (\partial_\tau + i\partial_x - \partial_y^2) \psi_- - \phi \left(\psi_+^\dagger \psi_+ + \psi_-^\dagger \psi_- \right) + \frac{1}{2g^2} (\partial_y \phi)^2$$

Quantum criticality of Ising-nematic ordering

$$\mathcal{L} = \psi_+^\dagger (\partial_\tau - i\partial_x - \partial_y^2) \psi_+ + \psi_-^\dagger (\partial_\tau + i\partial_x - \partial_y^2) \psi_- - \phi \left(\psi_+^\dagger \psi_+ + \psi_-^\dagger \psi_- \right) + \frac{1}{2g^2} (\partial_y \phi)^2$$



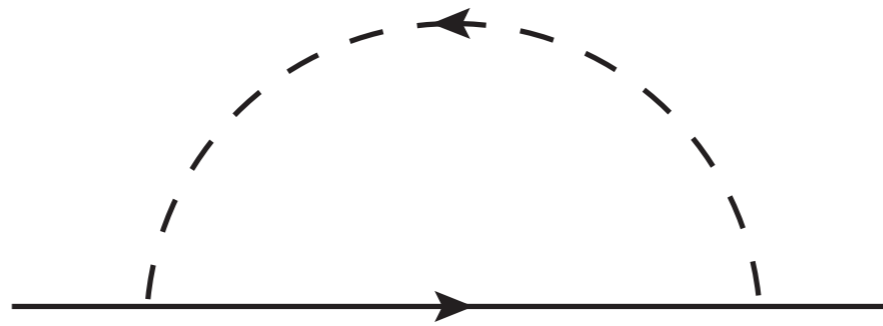
One loop ϕ self-energy with N_f fermion flavors:

$$\begin{aligned} \Sigma_\phi(\vec{q}, \omega) &= N_f \int \frac{d^2 k}{4\pi^2} \frac{d\Omega}{2\pi} \frac{1}{[-i(\Omega + \omega) + k_x + q_x + (k_y + q_y)^2] [-i\Omega - k_x + k_y^2]} \\ &= \frac{N_f}{4\pi} \frac{|\omega|}{|q_y|} \end{aligned}$$

Landau-damping

Quantum criticality of Ising-nematic ordering

$$\mathcal{L} = \psi_+^\dagger (\partial_\tau - i\partial_x - \partial_y^2) \psi_+ + \psi_-^\dagger (\partial_\tau + i\partial_x - \partial_y^2) \psi_- - \phi \left(\psi_+^\dagger \psi_+ + \psi_-^\dagger \psi_- \right) + \frac{1}{2g^2} (\partial_y \phi)^2$$



Electron self-energy at order $1/N_f$:

$$\begin{aligned} \Sigma(\vec{k}, \Omega) &= -\frac{1}{N_f} \int \frac{d^2q}{4\pi^2} \frac{d\omega}{2\pi} \frac{1}{[-i(\omega + \Omega) + k_x + q_x + (k_y + q_y)^2] \left[\frac{q_y^2}{g^2} + \frac{|\omega|}{|q_y|} \right]} \\ &= -i \frac{2}{\sqrt{3}N_f} \left(\frac{g^2}{4\pi} \right)^{2/3} \text{sgn}(\Omega) |\Omega|^{2/3} \end{aligned}$$

$$\Sigma(k, \omega_n) = \lambda^2 \int \frac{d^d q}{(2\pi)^d} \int \frac{d\epsilon_n}{2\pi} \frac{1}{q_y^2 + \gamma|\epsilon_n|/|q_y|} G_0(k + q, \epsilon_n + \omega_n) \quad (45)$$

This can be evaluated by the same methods used for (18). Integrating over q_x we find the analog of (21)

$$\begin{aligned} \Sigma(k, \omega_n) &= i \frac{\lambda^2}{v_F} \int \frac{d^{d-1} q_y}{(2\pi)^{d-1}} \int \frac{d\epsilon_n}{2\pi} \frac{\text{sgn}(\epsilon_n + \omega_n) |q_y|}{|q_y|^3 + \gamma|\epsilon_n|} \\ &= i \frac{\lambda^2}{\pi v_F \gamma} \text{sgn}(\omega_n) \int \frac{d^{d-1} q_y}{(2\pi)^{d-1}} |q_y| \ln \left(\frac{|q_y|^3 + \gamma|\omega_n|}{|q_y|^3} \right). \end{aligned} \quad (46)$$

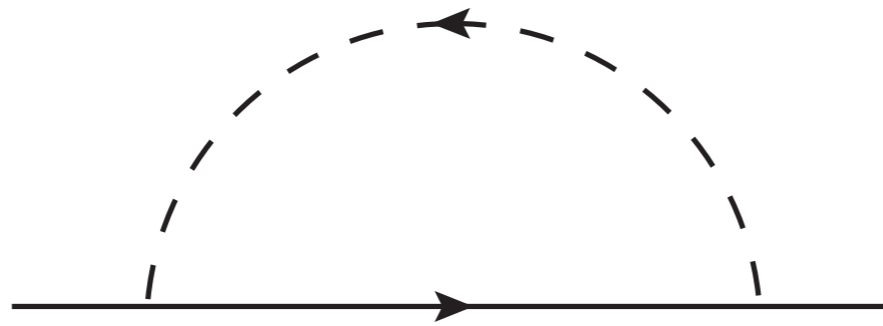
Evaluation of the q_y integral yields a result which agrees with (42) and (43) in $d = 2$, and with the expected logarithmic corrections in $d = 3$. In the physically important case of $d = 2$, the q_y integral evaluates to

$$\Sigma(k, \omega_n) = \frac{\lambda^2}{\pi v_F \gamma^{1/3} \sqrt{3}} \text{sgn}(\omega_n) |\omega_n|^{2/3}, \quad d = 2, \quad (47)$$

in agreement with (43).

Quantum criticality of Ising-nematic ordering

$$\mathcal{L} = \psi_+^\dagger (\partial_\tau - i\partial_x - \partial_y^2) \psi_+ + \psi_-^\dagger (\partial_\tau + i\partial_x - \partial_y^2) \psi_- - \phi \left(\psi_+^\dagger \psi_+ + \psi_-^\dagger \psi_- \right) + \frac{1}{2g^2} (\partial_y \phi)^2$$



Electron self-energy at order $1/N_f$:

$$\begin{aligned} \Sigma(\vec{k}, \Omega) &= -\frac{1}{N_f} \int \frac{d^2q}{4\pi^2} \frac{d\omega}{2\pi} \frac{1}{[-i(\omega + \Omega) + k_x + q_x + (k_y + q_y)^2] \left[\frac{q_y^2}{g^2} + \frac{|\omega|}{|q_y|} \right]} \\ &= -i \frac{2}{\sqrt{3}N_f} \left(\frac{g^2}{4\pi} \right)^{2/3} \text{sgn}(\Omega) |\Omega|^{2/3} \sim |\Omega|^{d/3} \text{ in dimension } d. \end{aligned}$$

Quantum criticality of Ising-nematic ordering

$$\mathcal{L} = \psi_+^\dagger (\partial_\tau - i\partial_x - \partial_y^2) \psi_+ + \psi_-^\dagger (\partial_\tau + i\partial_x - \partial_y^2) \psi_- - \phi \left(\psi_+^\dagger \psi_+ + \psi_-^\dagger \psi_- \right) + \frac{1}{2g^2} (\partial_y \phi)^2$$

Schematic form of ϕ and fermion Green's functions in d dimensions

$$D(\vec{q}, \omega) = \frac{1/N_f}{q_\perp^2 + \frac{|\omega|}{|q_\perp|}}, \quad G_f(\vec{q}, \omega) = \frac{1}{q_x + q_\perp^2 - i \text{sgn}(\omega) |\omega|^{d/3} / N_f}$$

In the boson case, $q_\perp^2 \sim \omega^{1/z_b}$ with $z_b = 3/2$.

In the fermion case, $q_x \sim q_\perp^2 \sim \omega^{1/z_f}$ with $z_f = 3/d$.

Note $z_f < z_b$ for $d > 2 \Rightarrow$ Fermions have *higher* energy than bosons, and perturbation theory in g is OK.

Strongly-coupled theory in $d = 2$.

Quantum criticality of Ising-nematic ordering

$$\mathcal{L} = \psi_+^\dagger (\partial_\tau - i\partial_x - \partial_y^2) \psi_+ + \psi_-^\dagger (\partial_\tau + i\partial_x - \partial_y^2) \psi_- - \phi \left(\psi_+^\dagger \psi_+ + \psi_-^\dagger \psi_- \right) + \frac{1}{2g^2} (\partial_y \phi)^2$$

Schematic form of ϕ and fermion Green's functions in $d = 2$

$$D(\vec{q}, \omega) = \frac{1/N_f}{q_y^2 + \frac{|\omega|}{|q_y|}}, \quad G_f(\vec{q}, \omega) = \frac{1}{q_x + q_y^2 - i \text{sgn}(\omega) |\omega|^{2/3} / N_f}$$

In *both* cases $q_x \sim q_y^2 \sim \omega^{1/z}$, with $z = 3/2$. Note that the bare term $\sim \omega$ in G_f^{-1} is irrelevant.

Strongly-coupled theory without quasiparticles.

Quantum criticality of Ising-nematic ordering

$$\begin{aligned} \mathcal{L} = & \psi_+^\dagger (\partial_\tau - i\partial_x - \partial_y^2) \psi_+ + \psi_-^\dagger (\partial_\tau + i\partial_x - \partial_y^2) \psi_- \\ & - \phi \left(\psi_+^\dagger \psi_+ + \psi_-^\dagger \psi_- \right) + \frac{1}{2g^2} (\partial_y \phi)^2 \end{aligned}$$

Simple scaling argument for $z = 3/2$.

Quantum criticality of Ising-nematic ordering

$$\mathcal{L} = \psi_+^\dagger (\cancel{\partial_\tau} - i\partial_x - \partial_y^2) \psi_+ + \psi_-^\dagger (\cancel{\partial_\tau} + i\partial_x - \partial_y^2) \psi_- \\ - \phi \left(\psi_+^\dagger \psi_+ + \psi_-^\dagger \psi_- \right) + \frac{1}{2g^2} (\partial_y \phi)^2$$

Simple scaling argument for $z = 3/2$.

Quantum criticality of Ising-nematic ordering

$$\mathcal{L} = \psi_+^\dagger (\cancel{\partial_\tau} - i\partial_x - \partial_y^2) \psi_+ + \psi_-^\dagger (\cancel{\partial_\tau} + i\partial_x - \partial_y^2) \psi_- - \phi \left(\psi_+^\dagger \psi_+ + \psi_-^\dagger \psi_- \right) + \frac{1}{2g^2} (\partial_y \phi)^2$$

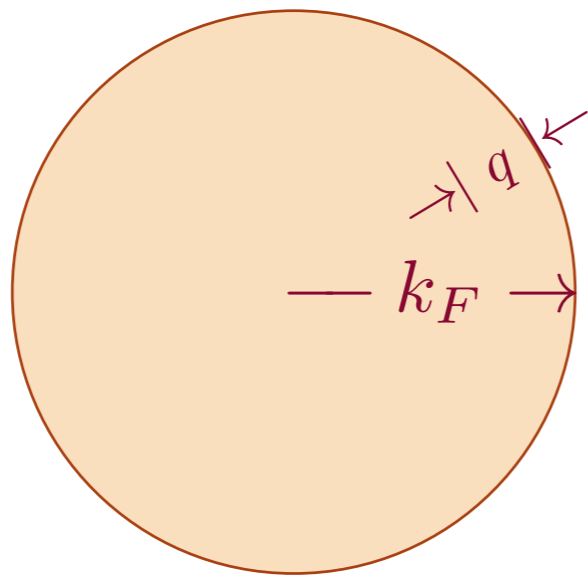
Simple scaling argument for $z = 3/2$.

Under the rescaling $x \rightarrow x/s$, $y \rightarrow y/s^{1/2}$, and $\tau \rightarrow \tau/s^z$, we find invariance provided

$$\begin{aligned} \phi &\rightarrow \phi s \\ \psi &\rightarrow \psi s^{(2z+1)/4} \\ g &\rightarrow g s^{(3-2z)/4} \end{aligned}$$

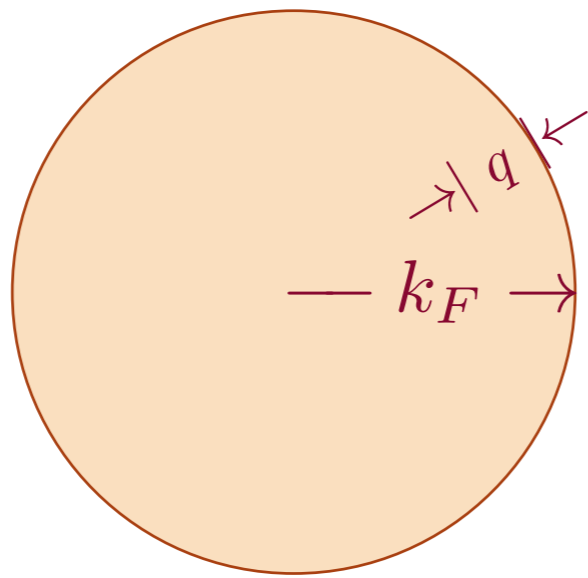
So the action is invariant provided $z = 3/2$.

FL Fermi liquid



- $k_F^d \sim Q$, the fermion density
- Sharp fermionic excitations near Fermi surface with $\omega \sim |q|^z$, and $z = 1$.
- Entropy density $S \sim T^{(d-\theta)/z}$ with violation of hyperscaling exponent $\theta = d - 1$.
- Entanglement entropy $S_E \sim k_F^{d-1} P \ln P$.

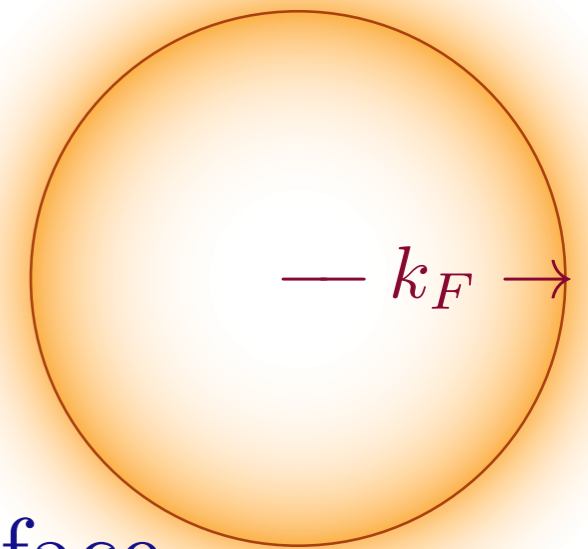
FL Fermi liquid



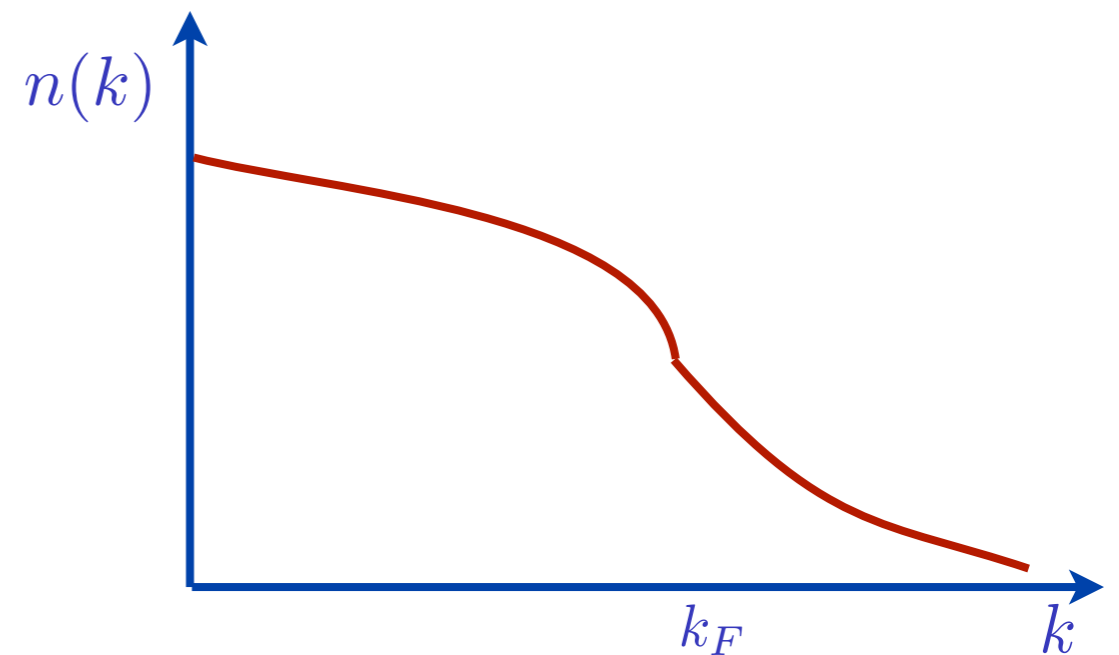
- $k_F^d \sim Q$, the fermion density

- Sharp fermionic excitations near Fermi surface with $\omega \sim |q|^z$, and $z = 1$.
- Entropy density $S \sim T^{(d-\theta)/z}$ with violation of hyperscaling exponent $\theta = d - 1$.
- Entanglement entropy $S_E \sim k_F^{d-1} P \ln P$.

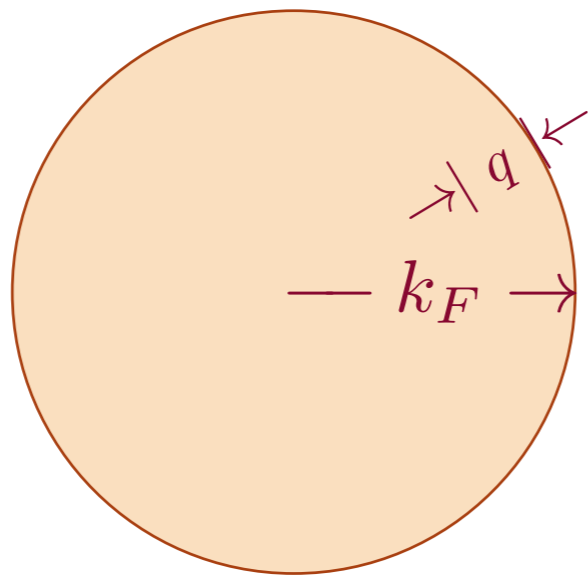
NFL Nematic QCP



- Fermi surface with $k_F^d \sim Q$.



FL Fermi liquid



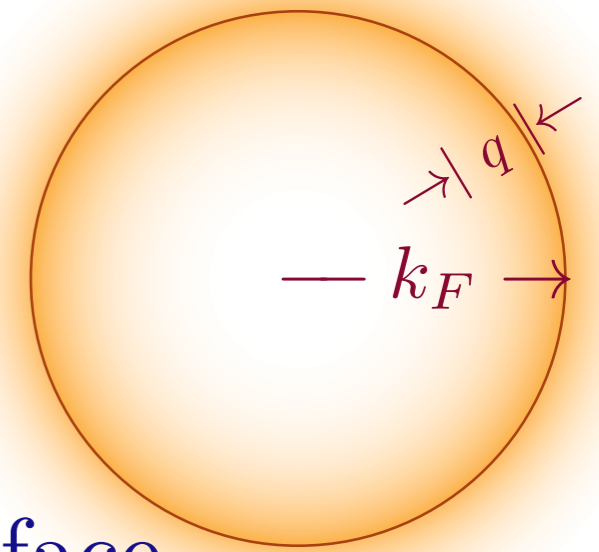
- $k_F^d \sim Q$, the fermion density

- Sharp fermionic excitations near Fermi surface with $\omega \sim |q|^z$, and $z = 1$.

- Entropy density $S \sim T^{(d-\theta)/z}$ with violation of hyperscaling exponent $\theta = d - 1$.

- Entanglement entropy $S_E \sim k_F^{d-1} P \ln P$.

NFL Nematic QCP

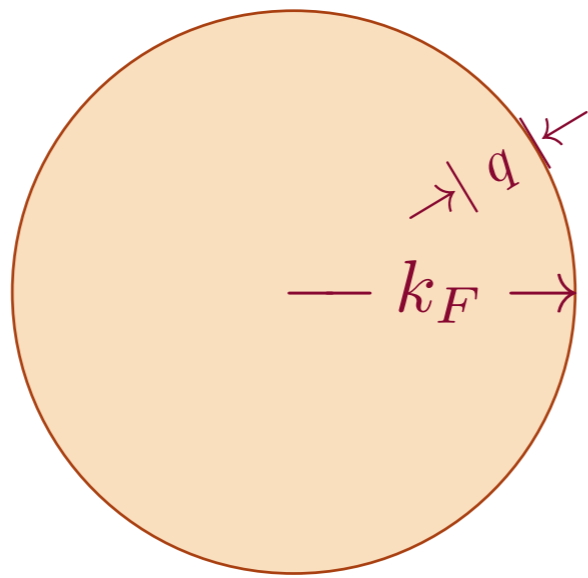


- Fermi surface with $k_F^d \sim Q$.

- Diffuse fermionic excitations with $z = 3/2$ to three loops.

M. A. Metlitski and S. Sachdev,
Phys. Rev. B **82**, 075127 (2010)

FL Fermi liquid



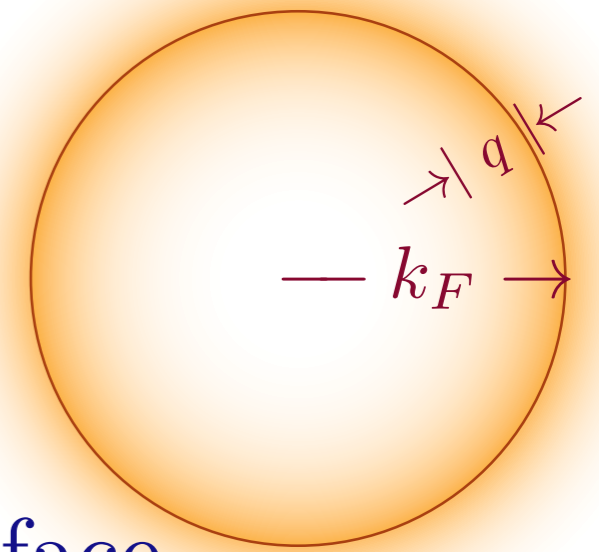
- $k_F^d \sim Q$, the fermion density

- Sharp fermionic excitations near Fermi surface with $\omega \sim |q|^z$, and $z = 1$.

- Entropy density $S \sim T^{(d-\theta)/z}$ with violation of hyperscaling exponent $\theta = d - 1$.

- Entanglement entropy $S_E \sim k_F^{d-1} P \ln P$.

NFL Nematic QCP

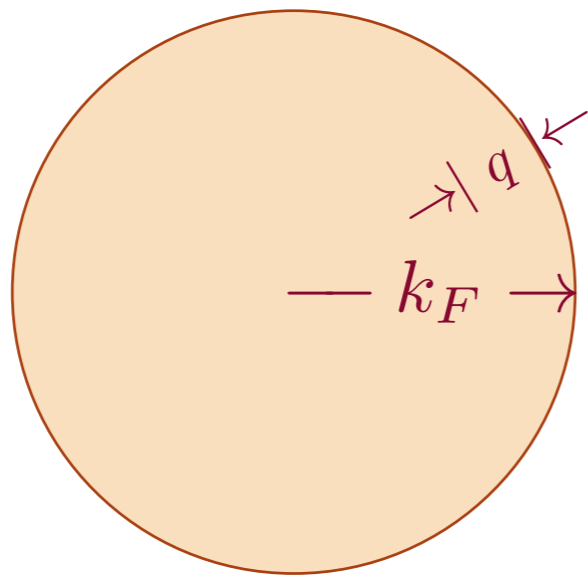


- Fermi surface with $k_F^d \sim Q$.

- Diffuse fermionic excitations with $z = 3/2$ to three loops.

- $S \sim T^{(d-\theta)/z}$ with $\theta = d - 1$.

FL Fermi liquid



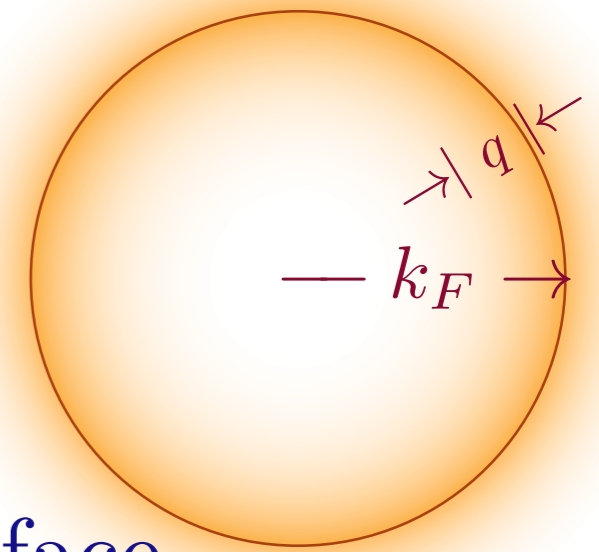
- $k_F^d \sim Q$, the fermion density

- Sharp fermionic excitations near Fermi surface with $\omega \sim |q|^z$, and $z = 1$.

- Entropy density $S \sim T^{(d-\theta)/z}$ with violation of hyperscaling exponent $\theta = d - 1$.

- Entanglement entropy $S_E \sim k_F^{d-1} P \ln P$.

NFL Nematic QCP



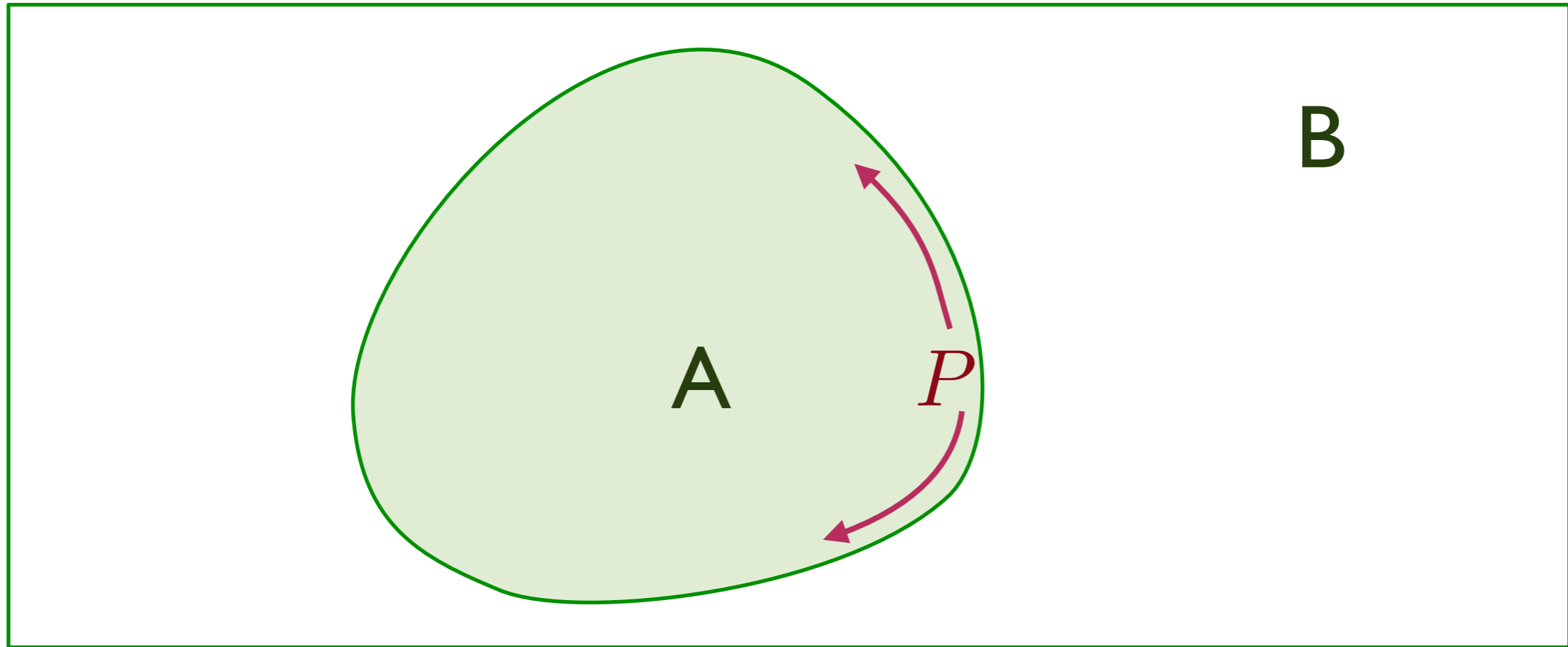
- Fermi surface with $k_F^d \sim Q$.

- Diffuse fermionic excitations with $z = 3/2$ to three loops.

- $S \sim T^{(d-\theta)/z}$ with $\theta = d - 1$.

- $S_E \sim k_F^{d-1} P \ln P$.

Entanglement entropy of the non-Fermi liquid



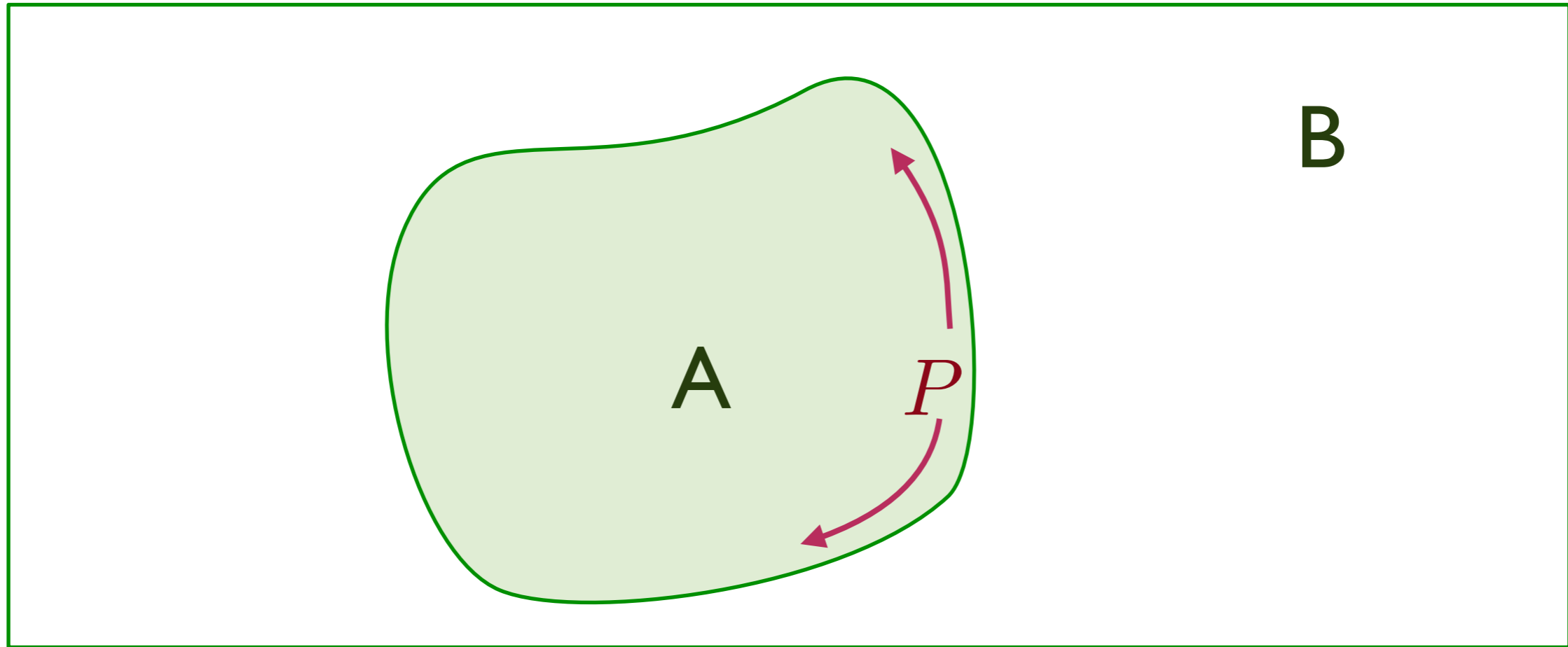
Logarithmic violation of “area law”: $S_E = \mathcal{C}_E k_F P \ln(k_F P)$

for a circular Fermi surface with Fermi momentum k_F , where P is the perimeter of region A with an arbitrary smooth shape.

The prefactor \mathcal{C}_E is expected to be universal but $\neq 1/12$: independent of the shape of the entangling region, and dependent only on IR features of the theory.

B. Swingle, *Physical Review Letters* **105**, 050502 (2010)
Y. Zhang, T. Grover, and A. Vishwanath, *Physical Review Letters* **107**, 067202 (2011)

Entanglement entropy of the non-Fermi liquid



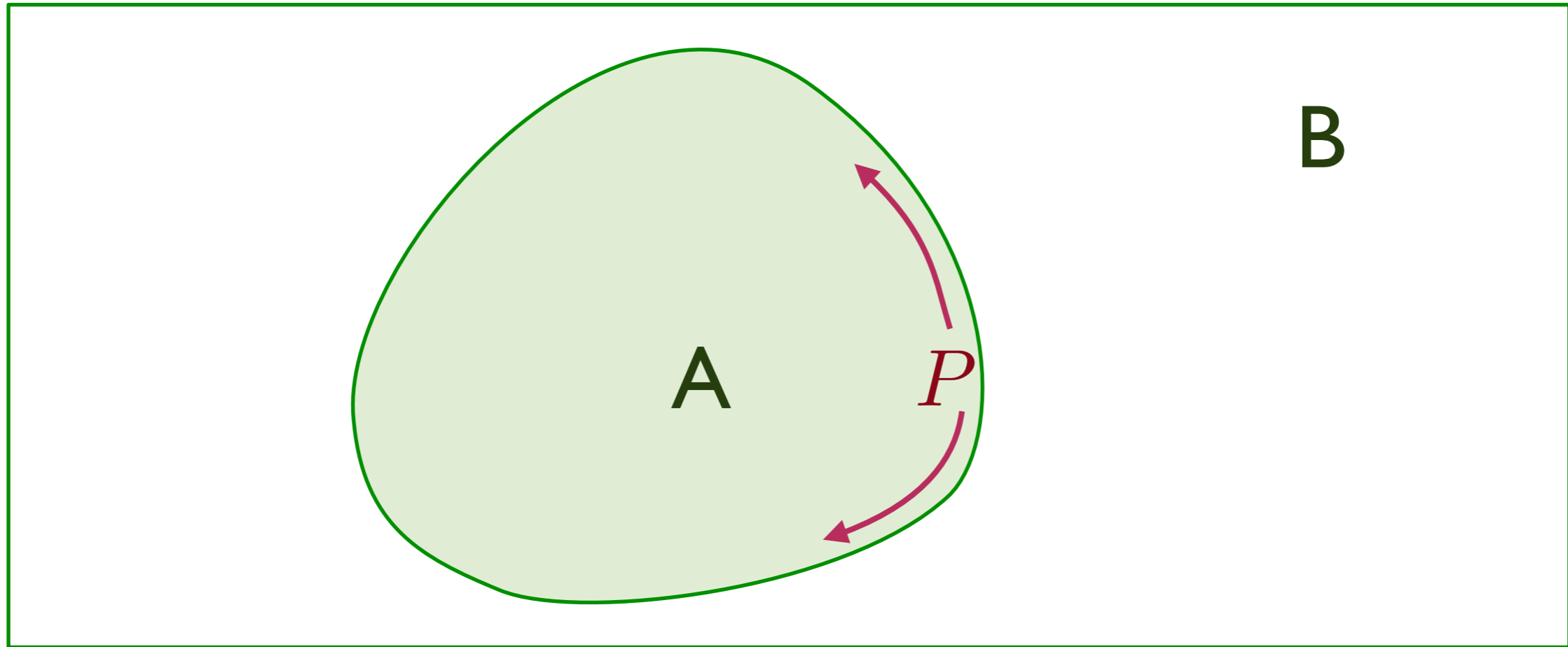
Logarithmic violation of “area law”: $S_E = \mathcal{C}_E k_F P \ln(k_F P)$

for a circular Fermi surface with Fermi momentum k_F , where P is the perimeter of region A with an arbitrary smooth shape.

The prefactor \mathcal{C}_E is expected to be universal but $\neq 1/12$: independent of the shape of the entangling region, and dependent only on IR features of the theory.

B. Swingle, *Physical Review Letters* **105**, 050502 (2010)
Y. Zhang, T. Grover, and A. Vishwanath, *Physical Review Letters* **107**, 067202 (2011)

Entanglement entropy of the non-Fermi liquid



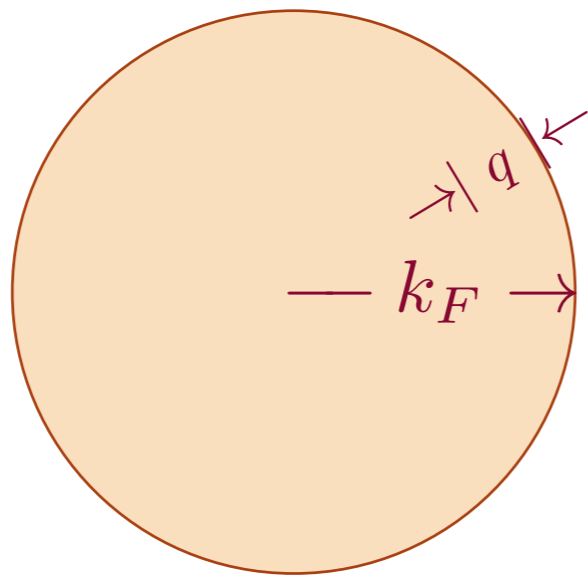
Logarithmic violation of “area law”: $S_E = \mathcal{C}_E k_F P \ln(k_F P)$

for a circular Fermi surface with Fermi momentum k_F , where P is the perimeter of region A with an arbitrary smooth shape.

The prefactor \mathcal{C}_E is expected to be universal but $\neq 1/12$: independent of the shape of the entangling region, and dependent only on IR features of the theory.

B. Swingle, *Physical Review Letters* **105**, 050502 (2010)
Y. Zhang, T. Grover, and A. Vishwanath, *Physical Review Letters* **107**, 067202 (2011)

FL Fermi liquid



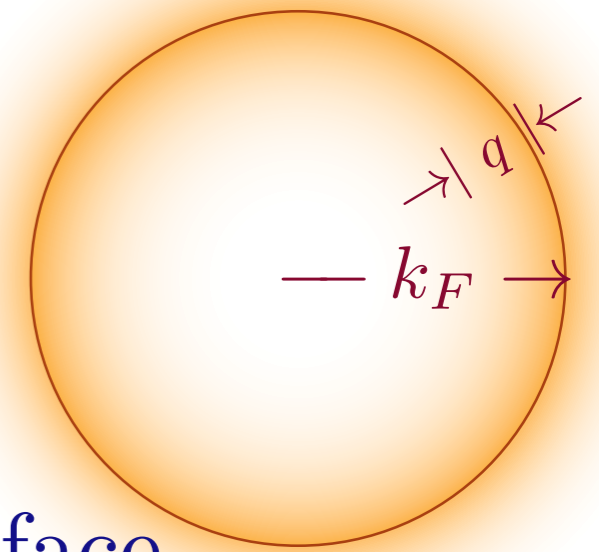
- $k_F^d \sim Q$, the fermion density

- Sharp fermionic excitations near Fermi surface with $\omega \sim |q|^z$, and $z = 1$.

- Entropy density $S \sim T^{(d-\theta)/z}$ with violation of hyperscaling exponent $\theta = d - 1$.

- Entanglement entropy $S_E \sim k_F^{d-1} P \ln P$.

NFL Nematic QCP



- Fermi surface with $k_F^d \sim Q$.

- Diffuse fermionic excitations with $z = 3/2$ to three loops.

- $S \sim T^{(d-\theta)/z}$ with $\theta = d - 1$.

- $S_E \sim k_F^{d-1} P \ln P$.